Universitätsmedizin Essen
Universitätsklinikum
Klinik für Gastroenterologie
und Hepatologie

UNIVERSITÄT
DUISBURG
ESSEN
Open-Minded

Cytokine networks engaging the Jak-Stat-pathway: implications for acute-on-chronic liver failure

Inaugural-Dissertation

zur Erlangung des Doktorgrades

Dr. rer. nat.

der Fakultät für Biologie

an der Universität Duisburg-Essen

vorgelegt von

Stefanie Sichelschmidt

aus Mülheim an der Ruhr

Datum der Abgabe: 06. Oktober 2021

Angaben zur Prüfung

Die der vorliegenden Arbeit zugrunde liegenden Experimente wurden am Institut für Gastroenterologie und Hepatologie am Universitätsklinikum Essen durchgeführt.

1. Gutachter:

Prof. Dr. med. Christian M. Lange

Klinik und Poliklinik für Innere Medizin II

LMU Klinikum München

2. Gutachter:

Prof. Dr. rer. nat. Wiebke Hansen

Institut für Medizinische Mikrobiologie

Universitätsklinikum Essen

Vorsitzender des Prüfungsausschusses: PD Dr. rer. nat. Mark Seifert

Tag der mündlichen Prüfung: 07.12.2021

Table of Contents

1 Introduction

1.1 The immune system – defender of the human body

The human immune system is a complex and highly organised network protecting the human body not only from a variety of exogenous pathogens and microbes but also from endogenous threats such as degenerated host cells or abnormal proteins. Traditionally, the immune system is divided into the innate immune system which provides rapid but rather unspecific responses to a broad range of stimuli, and the adaptive immune system which is able to carry out a more targeted response to distinct immunological triggers [213]. But, with growing knowledge over the last years and further investigation of cells such as innate-like B and T lymphocytes and memory-like NK cells, the conventional classification of the immune system became less rigid [117].

A good coordination and integration of all components of the immune system and the human body is essential to rapidly defend against pathogens and endogenous threats to human health. Among other organs, the liver is a central component of this network as it encounters foreign antigens on a daily basis [167].

1.1.1 The innate immune system

The innate immune system is an evolutionary conserved and approved system to control and eliminate pathogens since it can be found in mammals, insects and also invertebrates [147]. It comprises different strategies to protect the human body from pathogens in a non-specific but quickly acting manner. The first physical barriers that pathogens must cross are the skin and interior epithelial surfaces, the latter often covered with a mucosal layer containing defensins to prevent pathogens from adhering to the cellular structures of the body [4, 71]. The humoral components of the innate immune system comprise the complement system which is a system of soluble, proteolytic plasma proteins that opsonize and kill pathogens or trigger inflammation and soluble cytokines secreted by innate immune cells [213]. The cellular component of the innate immune system includes several subpopulations such as granulocytes, monocytes/macrophages, dendritic cells (DCs) and natural killer cells (NK cells) that either circulate in the periphery of the human body or are tissue-resident populations [50, 197]. These cells are responsible for the recognition of exogenous proteins and structures of microorganisms followed by phagocytosis

and elimination of intruders and finally regulation of the subsequent immune response. Conserved pathogen-associated molecular patterns (PAMPs) like bacterial components or viral nucleic acid are detected via pattern-recognition-receptors (PRRs) [2, 99]. Antigen-presenting cells (APCs) like DCs or macrophages then process antigens and expose these via major histocompatibility complex (MHC) class I and class II molecules on their surface to be recognised by T and B lymphocytes supported by further co-stimulatory surface molecules and stimulatory cytokines [29, 80, 99]. This antigen presentation to lymphocytes happens in the lymph nodes where the adaptive immune reaction is then initiated. Thus, APCs can be called the mediators between the innate and adaptive immune system [193].

NK cells recognize infected or malignant cells by their loss of MHC class I receptors that usually mark a cell as ‘self’. Upon recognition, NK cells secrete cytotoxic granules containing granzymes and perforin followed by lysis of the target cell. Nevertheless, NK cells can identify receptors on cells which are induced by stress and therefore also eliminate cells with a regular expression of MHC I. This reported for tumour and virus-infected cells [34, 44, 52, 126]. Additionally, NK cells release cytokines such as Tumour necrosis factor α (TNFα) and Interferon γ (IFNγ) that trigger other immune cells in their immune response to the threat [28].

Granulocytes are the most abundant cell type in peripheral blood. Their cytoplasmic granules are eponymous and contribute to their designation as polymorphonuclear leukocytes (PMLs or PMNs). The three subtypes of granulocytes are named after their characteristic appearance after histological staining with haematoxylin and eosin which are basophils, eosinophils and neutrophils [108]. They originate and mature in the bone marrow (BM) before being released into the circulation [92].

Basophilic granulocytes are the smallest population with less than 1% of blood leukocytes. Eosinophils are more abundant than basophils and represent 1-10% of the peripheral leukocytes and are involved in defence against parasites and chronic allergic inflammation [142]. Neutrophilic granulocytes convey an important role as phagocytes as part of the innate immune system and are well studied. They act against invading pathogens as one of the first immune cells [92, 135]. They make up 50-70% of the circulating leukocytes in the human body. The maturation process in the BM is regulated by several cytokines giving G-CSF a central function [39, 166]. Mature neutrophils are released to the blood stream where they survive

approximately 8-12 hours but also longer life spans in tissues were reported [24, 155]. Neutrophils react to certain chemokines released during inflammation and infection such as IL-8 or CXCL1 to be attracted by the gradient. Other stimuli like IL-1β, TNFα or IL-17 initiate rolling of the cells once they arrive at the destined location as they induce selectin and integrin expression in neutrophils which facilitates interaction with endothelial cells [24]. After firm adhesion and transepithelial migration, neutrophils chemotax to the site of inflammation and secrete chemokines like CXCL8 (IL-8) or CXCL1 to attract further immune cells. At the site of infection, neutrophils can release toxic molecules like proteinases and antimicrobial peptides via degranulation, rapidly phagocytose pathogens or damaged cells or generate reactive oxygen species (ROS), generated by activation of the NADPH oxygenase [135]. Generation of neutrophil extracellular traps (NETs) is another feature of PMNs that is seen as alternative to apoptosis and necrosis. Neutrophils release decondensed chromatin from the nuclei carrying bactericidal proteins and peptides which help to capture and kill pathogens [26, 72]. However, this process might also cause harm on healthy cells and tissues so NET formation is thought to be involved in certain diseases like thrombosis or lupus erythematosus [73, 211, 231]. On the other hand, investigation of NET formation can predict for instance mortality in intensive care unit patients [1].

1.1.1.1 Cytokines – the humoral component of the innate immune system

As described in the previous chapter, cytokines such as interleukins (ILs) or interferons (IFNs) are an essential part of the humoral branch of the innate immune system. The next chapters give an overview about the cytokines which are most relevant for this project.

1.1.1.1.1 The human interferon system and IFNγ

Interferons are cytokines that were initially described as proteins with anti-viral properties by Isaacs and Lindemann in 1957 [98]. They have the capacity to induce immune responses, promote further cytokine production in the context of inflammation and trigger antigen presentation [137]. In immune therapies, IFNs are considered and discussed as treatment opportunities as part of cancer therapy or anti-viral treatment [66, 151, 216] and even in the context of SARS-CoV-2 infections [238].

They can be divided into three groups namely IFN type I, type II and type III. In humans, type I IFNs include several IFNs: IFNα, IFNβ, IFNε, IFNκ and IFNω that are all structurally related. The alpha IFNs can be further subdivided into 12 subtypes (IFNα1, α2, α4, α5, α6, α7, α8, α10, α14, α16, α17, α21) with IFNα2 mostly used in clinical practice to treat for instance Hepatitis C virus (HCV) or Hepatitis B virus / Hepatitis D virus (HBV/HDV) infections [85, 88, 178]. The central signalling pathway for IFNα is the Janus kinase (Jak) - Signal Transducer and Activator of Transcription (Stat) signalling pathway (further described in 1.1.1.1.2 Interleukin 6 – between inflammation and regeneration) via Stat1 and Stat2 that induces transcription of IFN-stimulated genes such as melanoma differentiation-associated protein 5 (MDA5), retinoic acid inducible gene I (RIG-I) or interferon-stimulated gene 15 (ISG15). The expressed proteins then have direct antiviral effects as they interfere with the viral replication and translation system. Furthermore, indirect effects by modulating the host's innate and adaptive immune response are described, for instance, proliferation and cytotoxicity of NK and $CD8^+$ T cells are enhanced, and MHC molecule expression is upregulated [83, 156].

Primarily acting against viral infections and therefore comparable to type I IFNs are Type III IFNs. They include IL-28A, IL-28B and IL-29, which are also known as IFNλ2, IFNλ3 and IFNλ1 and were described by Pestka et al [83, 153]. Type III IFNs act less globally in the human body but more specific in tissues that are at higher risk of infection and viral exposure [214].

There is only one type II IFN: IFNγ, which is known for its immunomodulatory potential and inflammatory properties. IFNγ production is tightly linked to lymphocytes, namely T cells, NK cells and APCs [182]. It is a stimulus for macrophage activation [96, 105]. Like Type I IFNs, IFNγ also carries out its effects by using mainly the Jak-Stat signalling pathway. A dimer of the cytokine binds to the interferon-gamma receptor 1 (IFNGR1) subunit which then associates with IFNGR2 and leads to phosphorylation of associated Jak1 and Jak2 kinases. That provides a docking site for intracellular Stat1 transcription factors which become in turn phosphorylated. After dissociation from the receptor, Stat1 forms homo- or heterodimers with Stat3 that translocate to the nucleus where it induces transcription of interferon-regulatory factor (IRF)-1 which in turn induces transcription of further IFNγ-responsive genes [21, 153, 179]. IRF-1 is involved in the control of cell growth and cell cycle arrest, apoptosis by upregulation of the Fas receptor. Furthermore, it is

described as tumour suppressor [107, 170]. There is a negative feedback loop to control and regulate the signalling via members of the suppressor of cytokine signalling (SOCS) family [21, 128, 192].

1.1.1.1.2 Interleukin 6 – between inflammation and regeneration

IL-6 is a pleiotropic cytokine which exerts multiple functions in in the body, including responses in immunoglobin production, acute-phase response and cell growth and differentiation [36, 93, 111]. Based on these functions, IL-6 was originally known under different names such as B cell stimulatory factor 2 (BSF-2), hepatocyte-stimulating factor (HSF) or hybridoma growth factor (HGF) until its cDNA was successfully cloned in 1986 [93].

IL-6 is secreted by different cell types like macrophages and monocytes, T cells, fibroblasts and endothelial cells. In the liver, mainly macrophages, monocytes and neutrophils secrete IL-6 to stimulate acute-phase response and IL-6 is strongly involved in mitogenic pathways in liver regeneration and hepatoprotection but also plays a role in carcinogenesis and inflammation [77, 181]. Moreover, IL-6 seems to play a role in liver metabolism as it is linked to the development of type 2 diabetes and obesity [157, 219].

To exert its function on target cells, IL-6 binds to the IL-6 receptor chain (IL-6Rα or CD126). The complex then associates with its second receptor glycoprotein 130 (gp130) which in turn dimerizes to forward the signal. Associated tyrosine kinases (JAK1) autophosphorylate upon dimerization and in turn phosphorylate the intracellular domain of gp130 which initiates downstream signalling pathways such as the PI3 kinase or signal transducer and activator of transcription (Stat) signalling pathway. In case of the Stat pathway, Stat1 or Stat3 signalling molecules are recruited to the receptor and become phosphorylated. After forming dimers, they translocate to the nucleus where they induce transcription of IL-6-responsive genes [77, 91]. Regulation of IL-6 signalling is mediated via members of the suppressor of cytokine signalling (SOCS) family. Especially SOCS3 is described to be induced by IL-6 and forms a negative feedback loop to terminate the signalling cascade [12].

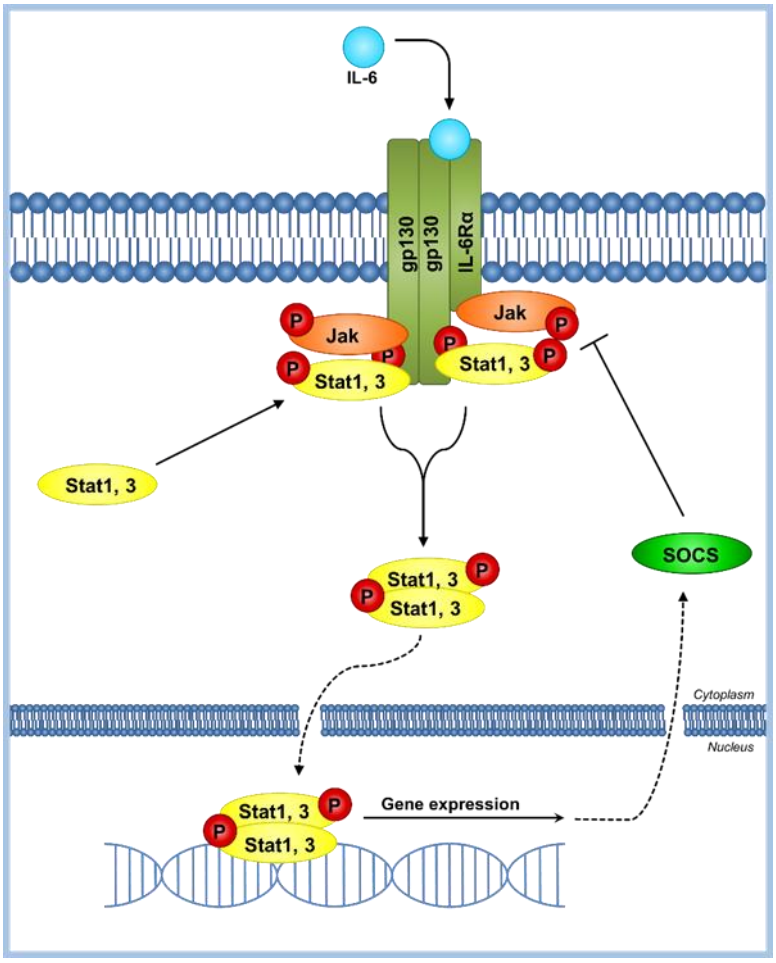

Figure 1: Simplified depiction of classic IL-6 signalling.
Upon cytokine binding to IL-6Rα the complex associates with membrane-bound gp130. After phosphorylation of the receptor and JAK proteins, Stat molecules are recruited which are then also phosphorylated. They form homo- or heterodimers, translocate to the nucleus and initiate gene expression. Besides other proteins, SOCS proteins are generated which function as negative feedback loop to terminate the pathway [12, 77, 91].

While gp130 is expressed ubiquitously, expression of IL-6Rα limits classic IL-6 signalling to a few cell types such as hepatocytes and a few cells of the immune system [91, 201]. Besides the classic pathway described above, there is also the trans-signalling pathway for IL-6 which is conducted by binding of IL-6 to a soluble IL-6 receptor prior to binding to gp130 [55, 171]. Thus, also other cells that express gp130 but not membrane-bound IL-6Rα can react to IL-6. While the classic IL-6 signalling pathway is more associated with anti-inflammatory effects and regenerative properties, IL-6 trans-signalling is thought to mediate pro-inflammatory effects and contributes to cancer development [94, 210, 228]. Nevertheless, there are also further studies that suggest an important role of IL-6 trans-signalling in liver damage response [82].

1.1.1.1.3 Interleukin 22 – a protective player with unknown side-effects

IL-22 was originally known under the name T cell-derived inducible factor (TIF) [57]. This cytokine is produced by several immune cell types including subsets of CD4+ T cells, NKT cells but also macrophages, neutrophils and fibroblasts are attributed with this [40, 59, 148, 225]. It has his main impact on fibroblasts and non-haematopoietic cells [57]. IL-22 is described to contribute to innate immunity of different tissues but is not used to communicate between immune cells or is required for their differentiation [40, 57, 224]. It stimulates epithelial cell proliferation, regeneration and strengthens transepithelial resistance in several tissues such as liver, lung and kidney [11, 57]. However, IL-22 also induces acute-phase protein expression like the LPS binding protein (LBP) and pro-inflammatory molecules like IL-6 and IL-8 [6, 123].

IL-22 is a member of the IL-10 cytokine family and uses the IL-10R2 and IL-22R1 as receptor subunits with high affinity to the latter one [22, 103, 114, 125]. After binding of IL-22 to IL-22R1 it associates with IL-10R2. The receptor-associated kinases Jak1/Tyk2 become phosphorylated and in turn recruit Stat proteins to become phosphorylated. In this case, this is mainly Stat3 but also Stat1 and Stat5 are reported to be part of the signalling pathway [121]. Those phosphorylated Stat molecules dimerize and translocate to the nucleus where they initiate gene expression. However, also the MAP kinase pathway and the Akt pathway were described to be involved in IL-22 signalling [6, 141]. Besides other cytokines, one of the key regulators of IL-22 signalling is the IL-22 binding protein (IL-22BP) which is a soluble form of the IL-22 receptor chain with higher affinity to the cytokine than its membrane-bound counterpart [103].

1.1.2 The adaptive immune system

The adaptive or acquired branch of the immune system includes two populations of lymphocytes, namely the B and T lymphocytes, besides circulating antibodies. It provides a targeted immune response to distinct pathogens or antigens and it can establish an immunologic memory. This memory is essential to create a rapid immune response to encounter recurring pathogens [4].

B lymphocytes develop in the bone marrow. After maturation, B cells are encountered in secondary lymphoid organs such as the spleen and the lymph nodes. Before B cells encounter their first antigen they are termed naïve B cells. Upon

binding of the specific antigen to the B cell receptor and a co-stimulatory signal, either dependent or independent of T lymphocytes, the B cells become activated and are triggered to increase proliferations or differentiation into memory cells or antibody-secreting plasma cells [132]. By antibody secretion, the cells build up the humoral branch of the adaptive immune system. Due to class switching mechanism in the germinal centres of the lymph nodes, they produce an enormous variety of different immunoglobulins and work as APCs [4, 120].

T lymphocytes originate from pluripotent hematopoietic stem cells in the BM and mature in the thymus. These cells are effectors and regulators of the adaptive immune response and express defined surface molecules that can be used for differentiation. The CD (cluster of differentiation) nomenclature uses these surface molecules on immune cells as markers for characterization and identification of different cellular subsets [64] but also non-CD markers are used for classification, for instance HLA-DR which is a marker for T cell activation [129]. T lymphocytes have to interact tightly with APCs in order to initiate a successful immune response. This interaction is termed the immunological synapse [60]. Three major steps need to be performed to induce an immune response. First, the T cell receptor (TCR) interacts with the antigen-loaded MHC molecule on an APC. Co-receptors like CD4 and CD8 are indispensable to ensure a T cell response. Adhesion molecules like lymphocyte function–associated antigen-1 (LFA1) on T cells and intercellular adhesion molecule-1 (ICAM1) on APCs are part of the synapse as well as essential co-stimulatory molecules like CD28 and CD80/86 [60, 97].

T cells can be divided in $CD3^+CD4^+$ double positive T helper cells and $CD3^+CD8^+$ double positive cytotoxic T cells; upon further differentiation several important T cell subsets develop for instance natural killer T cells (NKT), memory, effector and regulatory T cells to name only a few. T helper cells recognize antigens presented by APCs via MHC class II molecules and usually use CD4 as co-receptor for the TCR [112]. They activate and regulate other immune cells like macrophages, B cells and cytotoxic T cells. Additionally, they secrete a variety of cytokines [4, 187, 194]. Cytotoxic T lymphocytes (CTL) help to effectively kill degenerated or infected host cells. Foreign antigens need to be presented via MHC class I molecules to be recognized by CTLs. They use CD8 as a co-receptor that interacts specifically with the MHC class I molecule [48]. Additionally, they secrete cytokines and chemokines to attract further immune cells to the side of infection [4, 158]. Both, $CD4^+$ and $CD8^+$

T cells can be further defined by the expression of CCR7 and CD45RA to distinguish naïve, central memory, effector ad effector memory T cells [129].

1.1.2.1 T helper cells

T helper cells react to antigens presented by MHC class II molecules on APCs like DCs, macrophages or B cells. These antigens derive from extracellular pathogens that were phagocytosed or internalised by the APCs and degraded in intracellular vesicles such as lysosomes or endosomes by proteolytic enzymes at a low pH [168]. Hereafter, MHC class II molecules bind the processed antigenic peptides and are transported to the surface of the APC to present the antigen to T helper cells. The expression of the surface marker CD3 and CD4 (negative for CD8) are characteristic for T helper cells. CD4 is acting as co-receptor in the described process by binding to an invariant portion of MHC class II [112]. Additionally, co-stimulatory signals like the interaction of CD28 from the T cell with the receptor B7.1/7.2 (CD80/86) expressed by the APC are essential for a successful activation of the T cell and induction of a T cell response. There are different subsets of T helper cells, all defined by individual constellations of surface markers as described elsewhere [129]. In 1986, type 1 T helper cells (T_H1) and type 2 T helper cells (T_H2) cells were classified by their different profile of cytokine secretion [145]. T_H1 cells primarily produce IL-2, IFNγ or Granulocyte-macrophage colony-stimulating factor (GM-CSF) besides others. These cytokines activate regulatory T cells and $CD25^+$ effector T cells [25], activate and attract macrophages and other leukocytes [182] and promote hematopoietic growth [61]. In reaction to a presented antigen, T_H2 are known to release IL-4, IL-5 and IL-13 that are crucial in the immunological response to extracellular pathogens such as helminths [177] and support anti-inflammatory macrophage functions [215]. These cytokines also drive B cell proliferation and support class switching. Beside these two popular subsets of T helper cells, there are further populations such as T_H17 cells, regulating the gut microbiota and crucial for fighting fungal or bacterial infections, regulatory T cells (T_{reg}, $CD3^+CD25^+FoxP3^+$) that are known for their immunosuppressive properties or T follicular helper cells (T_{FH}) supporting the humoral immune response [177] to name only a few. Native T cells or antigen-inexperienced T cells express the marker CD45RA. Upon differentiation this surface marker becomes downregulated [129, 130].

1.1.2.2 Cytotoxic T cells

Cytotoxic T cells recognize peptides presented by MHC class I molecules with the help of their specific co-receptor CD8. MHC class I molecules are widely expressed by all nucleated cell types in the human body. Antigens presented by this class derive from cytosolic pathogens like viruses or endogenous structures and are directly degraded in the cytosol. By this mechanism, $CD8^+$ T cells can recognize and effectively eliminate virus or bacteria infected or altered cells. Due to T cell maturation and selection in the thymus, CTLs usually do not recognize endogenous proteins as threatening. One way to achieve this is to release cytotoxic granules containing perforin and granzymes (proteases) that lead to lysis and degradation of the infected or altered cell. In addition, some professional APCs like dendritic cells are able to endocytose, process and present extracellular antigens on MHC class I molecules which in turn leads to cross-priming, the activation of naïve cytotoxic $CD8^+$ T cells [63, 102].

Moreover, CTLs can induce apoptosis via Fas/FasL interactions with the infected host cell and activation of the intracellular caspases [27]. Cytotoxic T cells primarily secrete TNFα and IFNγ to support anti-microbial functions. Furthermore, they are a source of a variety of chemokines such as RANTES (Regulated on Activation, Normal T-cell Expressed and Secreted) or MIP-1α/β (Macrophage Inflammatory Protein-1) that attract further lymphocytes and APCs [158].

1.2 The liver as central metabolic organ and its immunological role in the human body

The liver is the largest metabolic organ in the human body and the place for a variety of physiological processes. Metabolism and storage of nutrients, which are transported from the intestines via the portal vein is just one out of many. The liver functions as a regulator of the blood glucose level, thus provides storage of glucose in form of glycogen. It also ensures a regulated protein and amino acid metabolism via the two central enzymes aspartate aminotransferase (AST) and alanine aminotransferase (ALT). Both enzymes catalyse transfer of amino groups and are released into the blood stream upon liver damage, which makes them central unspecific markers in in the diagnostic process of liver damage [49, 58, 206]. Besides bile fluid, a large number of blood proteins like albumin, coagulation factors and

immune related proteins such as acute-phase-proteins are secreted. Additionally, the liver is the side of biotransformation and detoxification of endogenous and exogenous compounds like bilirubin, alcohol, medicine and other xenobiotics [18].

Besides its metabolic and detoxification properties, the liver is also a central immunological organ with several unique characteristics. Most importantly, the liver creates a state of immune tolerance for self- and foreign antigens. As the liver is continuously exposed to immunogenic molecules such as bacterial Lipopolysaccharide (LPS) via its dual blood supply from the portal vein and the hepatic artery, it is critical to maintain a balance between reaction and tolerance to certain antigens[167]. All cells residing in the liver contribute to a coordinated immune response [101, 131].

1.2.1 The liver – cellular composition

Hepatocytes are the most abundant cell population in the liver and fulfil most of the physiological liver functions. The most prominent roles are protein synthesis (including complement proteins and secreted PRRs) and biotransformation [78]. They have great regenerative potential upon liver damage when liver tissue is replaced by replication of already existing hepatocytes and not necessarily by activation of progenitor cells which was investigated in several models of partial hepatectomy [84, 139, 140]. Hepatocytes are equipped with different transporter molecules for uptake and release of biomolecules, anions, etc. [58, 184]. Through the fenestrated epithelial layer of the liver, hepatocytes can interact with circulating lymphocytes and function as antigen-presenting cells (APCs) [131]. In general, low levels of MHC class I and II molecules are expressed but under inflammatory conditions MHC class II is upregulated. This mainly induces Th2 response in order to regulate and impair CD8+ T cell responses, thus supporting tolerance to potential inflammatory triggers [222].

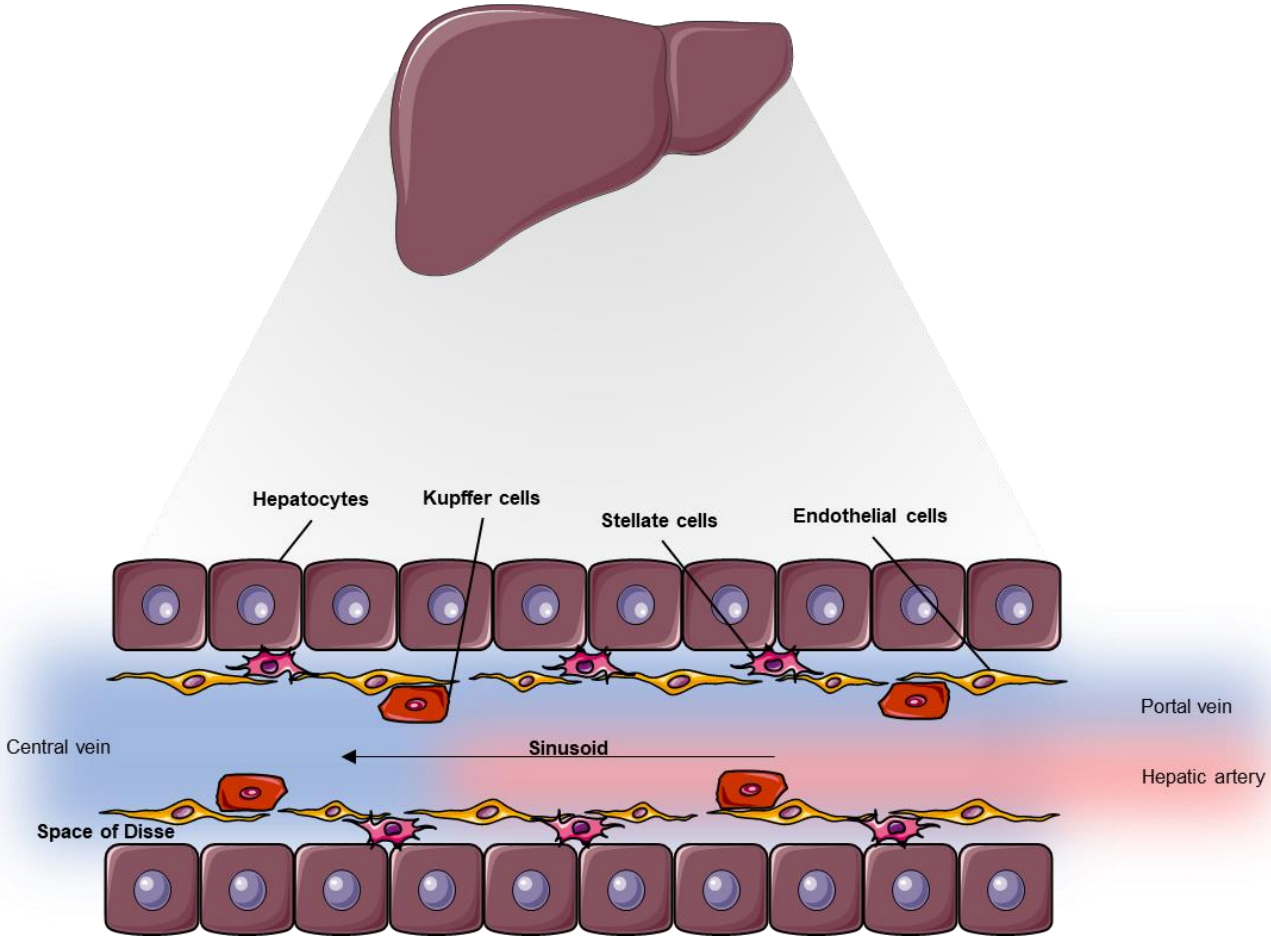

Figure 2: Simplified depiction of the liver's cellular structure.
The liver's dual blood supply comes mainly from the portal vein and the hepatic artery. Through the liver sinusoids it is transported to the central vein. Hepatocytes are the most abundant cell type in the liver. Endothelial cells with fenestrae and hepatic stellate cells (HSC), which reside in the space of Disse, next to liver resident macrophages (Kupffer cells (KC)) belong to the non-parenchymal liver cells [30].

Hepatic stellate cells (HSCs), also known as Ito cells, are located in the Space of Disse and are in close contact to hepatocytes and sinusoidal epithelial cells (see Figure 2). Cytoplasmic lipid droplets as structural feature support the HSC's function of storage and metabolism of vitamin A [58]. Upon activation during inflammation, they differentiate into myofibroblasts that produce extracellular matrix (ECM) proteins and therefore contribute to fibrotic alterations in the liver [131, 183, 208]. Aside from that, HSCs function as liver-resident APCs to contribute to activation of T cells and NKT cells. On the other hand, expression of PD-L1 mediating T cell inhibition, TGF-β secretion and Treg expansion contribute to immune tolerance mechanisms [131, 233].

Kupffer cells (KCs) are liver resident macrophages in the sinusoids, predominantly located in the periportal area [131]. Their function is to phagocyte for instance exogenous pathogens or bacterial lipopolysaccharide (LPS) coming to the liver via

the portal vein. They also clear apoptotic hepatocytes or red blood cells. KCs have limited expression of MHC class I and II or T cell co-stimulatory molecules (CD80, CD86, CD40) under steady-state conditions and T cell proliferation becomes inhibited [116, 235]. Nevertheless, upon stimulation by toll-like receptor (TLR) ligands during infection, Kupffer cells can induce T cell proliferation [17]. KCs secrete cytokines like TNFα or IL-6. The production of inflammatory mediators is their main function in order to clear pathogens and bacterial products. These pattern-associated molecular patterns (PAMPs) are sensed primarily via toll-like receptors (TLRs). As the liver is continuously exposed to food-ingested antigens and other triggers of inflammation the immunological response is highly controlled and the endotoxin tolerance (ET) of Kupffer cells is essential to prevent uncontrolled and strong immune responses. This comprises downregulation of proinflammatory cytokines, upregulation of anti-inflammatory cytokines such as IL-10 and low expression of costimulatory molecules that contribute to antigen presentation [58, 62].

Another cell type found in the liver is the population of liver sinusoidal endothelial cells (LSECs) which show a unique structure compared to other endothelial cells as they comprise fenestrae and do not have a basal membrane. With these properties they contribute to liver homeostasis by facilitating the transfer of different molecules from the blood stream to the hepatocytes. Additionally, leukocyte transmigration through this discontinuous epithelial barrier is facilitated so that leukocytes reach the inflamed destination within the liver more easily. LSECs also express a variety of pattern recognition receptors (PRRs) [227] and can take up macromolecules via endocytosis. Those become processed and presented to T cells which in turn release pro- and anti-inflammatory molecules [58, 131].

1.3 Chronic liver diseases: Liver cirrhosis and acute-on-chronic liver failure (ACLF)

Liver cirrhosis (LC) is the worldwide leading cause for liver-related death [43] and the 11th leading cause of globally deaths [10, 143]. Therefore, there is the urgent need for a better understanding of the disease and its underlying mechanisms.

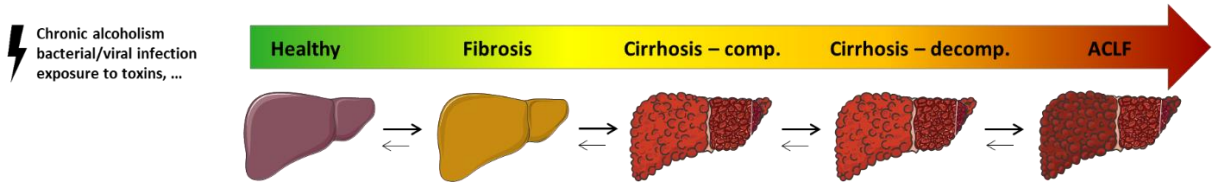

Figure 3: Stages of liver disease.
Initial triggers like chronic alcoholism or hepatic infections cause scarring events and lead to fibrotic restructuring of the organ. With further progression and without elimination of the disease cause, development to end-stage liver disease such as cirrhosis and ACLF is highly likely.

Development of chronic liver disease and LC starts with the development of progressive liver fibrosis which is the accumulation of ECM proteins like collagen in the liver due to a chronic trigger or inflammation such as chronic alcoholism, bacterial or viral infections (e.g. HCV) or exposure to toxins (Figure 3). Inflammation leads to scar tissue formation in the liver, to deformation of the liver's cellular architecture and therefore its dysfunction [7, 15, 188]. Reaching the state of late stage fibrosis termed liver cirrhosis, it is initially asymptomatic, so mostly undetected, and designated compensated cirrhosis. Further aggravation of the disease state and when the trigger is not abrogated decompensated cirrhosis is the next stage. It is then identified by emerging symptoms like gastrointestinal haemorrhage, development of ascites, hepatic encephalopathy (HE) and jaundice [87, 144]. Acute-on-chronic liver failure (ACLF) is a defined syndrome resulting from the CANONIC study's outcomes which was designed to identify patients with severe courses of disease and a high short-term mortality [144]. The definition includes acute decompensation (AD) with organ failure (defined by the CLIF-SOFA score) and a high short-term mortality (32-76% in 28 days), dependent on the number of organ failures [9, 144].

In the context of liver cirrhosis and ACLF, there are several score systems to evaluate the patient's state of disease. First to name is the Child-Pugh score, also known as the Child-Turcotte-Pugh score which possesses prognostic potential in the evaluation of liver cirrhosis. This score includes several parameters such as total bilirubin and serum albumin of the patients but also the international normalized ratio (INR) which is a method to determine blood coagulation, ascites development and presence of HE [37]. Alternatively, in the context of potential transplantations, the Model of end stage liver disease (MELD) score is used for evaluation of the severity of liver disease. Parameters that contribute to the score are the total bilirubin, INR and the serum creatinine and sodium levels [87]. Furthermore, the chronic liver failure-sequential organ failure assessment (CLIF-SOFA) score is used

as a prognostic factor to determine organ failure. It combines subscores from zero to four from six different organ systems (lungs, liver, kidneys, brain, coagulation and circulation) depending on lab parameters and functional tests [144]. The higher the CLIF-SOFA score, the higher is the organ impairment of the respective patient. This score is based on the original SOFA score from Vincent et al. [212].

Both cirrhosis and ACLF are strongly associated with immune dysregulation and dysfunction which comprises both immunodeficiency and systemic inflammation (SI) [5, 118, 119, 205]. The CANONIC study reported elevated white blood cell counts and increased levels of C-reactive protein (CRP), which are considered markers for SI, both further elevated with ACLF severity [144]. Additionally, bacterial infections or other precipitating events associated with SI were related to ACLF development. Moreover, dysregulation of blood immune cells in ACLF patients are thought to contribute to immunosuppression [218].

Several studies report that pro- and anti-inflammatory cytokine levels in the patients' sera strongly increased with the course of disease from cirrhosis to later stages of ACLF (e.g. IL-6, TNFα, IL-8, G-CSF, IL-10, IL-22) and therefore contribute to organ failure and worse outcome [42, 185]. IL-6 is a central mediator of the liver's acute-phase response and stimulates synthesis of hepatic acute-phase proteins such as CRP, fibrinogen or α1-antichymotrypsin [33, 89] which were shown to be elevated in ACLF patients [144]. IL-8 is a chemokine which efficiently recruits neutrophils to the site of inflammation [13] and is upregulated in ACLF patients besides other cytokines related to migration and chemotaxis of leukocytes [191]. Additionally, also G-CSF is known to activate neutrophils and to force haematopoiesis which is in line with the higher white blood cell count in ACLF patients [19, 41, 47]. This cytokine is already evaluated for therapeutic treatment. However, the success of G-CSF treatment and study design is currently debated as studies associate either an improved survival or nor therapeutic effect at all [65, 180, 189].

The current strategy to treat patients that suffer from decompensated cirrhosis and ACLF is to suppress the etiological factors, counteract the symptoms and address the central factors of disease progression such as portal hypertension or treating inflammation. As example, chronic alcoholism can be avoided and chronic viral infections such as Hepatitis B and C can be specifically targeted. Due to the severity of the potential course of disease, there are several guidelines that give orientation in

diagnosis and treatment options [87]. Besides the option of liver transplantation, there are strategies that address the immune system itself. Several cytokines like IL-22 or G-CSF are currently involved in *in vivo* and clinical studies that assume a positive outcome for patients with LC and ACLF [35, 56, 79, 229]. But it is important to note that the first multicentre study trying to prove the safety and efficacy of G-CSF in patients with ACLF failed to show improved survival in those patients [65]. Furthermore, long-term albumin administration prolonged patients' survival by a 38% reduction in the mortality ratio [32] and patients benefit from surgical options like the transjugular intrahepatic portosystemic shunt (TIPS) [90].

1.4 Cytokines and their important role in liver diseases

As mentioned in the previous chapters, several cytokine levels are altered in patients with liver cirrhosis and ACLF compared to healthy controls. The following part will introduce three of those cytokines in detail, namely IL-6, IL-22 and IFNγ which are of central interest for this project.

1.4.1 Interleukin 6 – a balancing act between inflammation and regeneration

In the liver, IL-6 fulfils several functions. Stimulated hepatocytes produce acute-phase proteins (e.g. C-reactive protein (CRP), fibrinogen, serum amyloid A) [81] which is diminished in IL-6 knock-out mice [113]. Throughout many studies, IL-6 has a central role in liver regeneration and IL-6 knock-out mice show impaired liver regeneration [23, 46, 67, 100, 154]. Among other functions, IL-6 is involved in cell cycle arrest and activation of DNA repair enzymes in this context to ensure accurate restoration of the organ [200]. Nevertheless, elevated IL-6 levels are associated with systemic inflammation (SI), worse outcome of LC patients and ACLF development [45, 205].

IL-6 is a promising target for therapy. A study from Lu et al. showed that IL-6 contributes in the process of *ex vivo* expansion of liver progenitor cells (LPCs) and liver regeneration [127]. Overall, there is a lot of evidence that IL-6 activity is beneficial to the liver [115, 181, 232]. Clinical practice that targets IL-6 signalling with focus on signalling blockade (e.g. Tocilizumab, Sarilumab) have shown to be advantageous against inflammatory conditions but might cause hepatocellular

damage [74, 106]. Thus, there is the urgent need to further evaluate IL-6 functions in the context of liver therapy options.

1.4.2 Interleukin 22 – importance in liver disease

In the liver, IL-22 targets mainly hepatocytes and induces expression of acute-phase proteins [123, 226]. It is also a mediator of inflammatory response in HBV infection. However, it promotes proliferation of liver stem and progenitor cells and improves liver pathology [68, 152, 237]. Still, it is reported that high IL-22 levels and a low IL-22BP/IL-22 ratio are associated with an elevated mortality in LC patients and ACLF [185]. IL-22 ameliorates alcoholic liver injury in murine models via Stat3 signalling in an antiapoptotic, antimicrobial and hepatoprotective manner [110]. It supports liver regeneration after partial hepatectomy [165]. Due to its regenerative properties, especially in the context of ACLF, IL-22 is currently evaluated for its therapeutic potential [180]. Xiang et al. could show that IL-22 administration and therefore supporting Stat3 pathway counteracts bacterial infection and improved liver regeneration and survival in ACLF mice [229].

1.4.3 IFNγ in the liver

In the liver, increased expression of the IFNγ receptor was described in the context of liver injury and inflammation [209]. As IFNγ has an impact on hepatocyte apoptosis via p21, it might contribute to the development of hepatitis [136]. Additionally, NK cell secreted IFNγ inhibits DNA synthesis and therefore hepatocyte proliferation during liver regeneration probably in a Stat1-dependend way [198, 199, 202, 204]. Furthermore, IFNγ was recently described to induce IL-7 expression in hepatocytes in an IRF-1-dependent manner. IL-7 is important for adaptive immune cell proliferation and was found to be reduced in patients suffering from liver cirrhosis suggesting a link to their described LPS tolerance and cirrhosis-associated immune dysfunction [173].

Of note, IFNγ is additionally attributed with antifibrogenic properties for instance inhibition of hepatic stellate cell (HSC) activation in rodent models [14, 169] and HCV infected patients [146].

2 Aim of the project

Patients suffering from different stages of liver cirrhosis and acute-on-chronic liver failure (ACLF) show systemic inflammation and high levels of pro- and anti-inflammatory cytokines. The impact of this cytokines and especially their combination is yet not fully understood. Therefore, the present work aims to investigate the influence of combined cytokine stimulation on hepatocytes and on immune cells of healthy donors and patients suffering from different stages of liver cirrhosis and ACLF. Further insight into the interplay of cytokines and their influence on the liver and on immune cells will help to assess options to support potential future immunotherapy and to enhance beneficial effects of the cytokines' signalling for the patients.

To address these questions, ideal cytokine concentrations and stimulation conditions for different cytokines such as IL-6 were assessed first. All used cytokines share the Jak-Stat signalling pathway to convey their function. Using Western Blot analysis, hepatocarcinoma cell lines and primary human hepatocytes were stimulated with different cytokines either as single dose or as combination to investigate whether there are synergistic or antagonistic effects in terms of Jak-Stat signalling pathway activation. Phosphorylated Stat proteins were detected to evaluate pathway activation. Effects on described target genes due to cytokine stimulation were determined via quantitative Real-Time PCR. Furthermore, repeated cytokine stimulations and viability assays were performed. Finally, the influence of IL-6 and IFNγ on peripheral immune cells from healthy donors, liver cirrhosis and ACLF patients in terms of Stat phosphorylation was examined using multicolour (phospho-) flow cytometry.

3 Material and Methods

3.1 Material

Table 1: Laboratory equipment and devices.

Device	Name/Detail	Supplier
Centrifuge	5810R, Rotor A-4-81	Eppendorf
Centrifuge	5424, Rotor FA-45-24-11	Eppendorf
Centrifuge	4524R, Rotor FA-45-24-11	Eppendorf
Centrifuge	Megafuge 40R, Rotor Thermo 75003607	Heraeus
CO_2 Incubator	BB15	Thermo Scientific
Counting chamber	Neubauer improved	BRAND
Flow Cytometer	Cyto Flex S	Beckman Coulter
Fluorescence Imager	ChemoStar ECL	Intas
Freezer	Comfort, -20°C	Liebherr
Freezer	Medline, -20°C	Liebherr
Fridge	Medline, 4°C	Liebherr
Microscope	Primo Vert	Zeiss
Orbital shaker	Rocky 3D	Oehmen
Overhead-shaker	REAX 2	Heidolph
Pipette	Eppendorf Research/Research Plus, 2,5 µl	Eppendorf
Pipette	Eppendorf Research & Research Plus,10 µl	Eppendorf
Pipette	Eppendorf Research/Research Plus, 20 µl	Eppendorf
Pipette	Eppendorf Research/Research Plus, 100 µl	Eppendorf
Pipette	Eppendorf Research/Research Plus, 200 µl	Eppendorf
Pipette	Eppendorf Research/Research Plus 10000 µl	Eppendorf
Pipette	1000 µl	Gilson
Pipette	200 µl	Gilson
Pipette	100 µl	Gilson
Pipette	20 µl	Gilson
Pipette	10 µl	Gilson
Pipetus		Hirschmann Laborgeräte
Plate Reader	FluoStar Omega	BMG Labtech
Power Supply	Power Pack HC	Bio Rad
Sterile bench	Safe 2020	Oehmen/Thermo Scientific
Trans-Blot Turbo Transfer System		Bio Rad
Ultrasonic bath	Emmi-D21	EMAG Technologies
Vortexer	RS-VA10	Phoenix Instruments
Water bath	TW12	Oehmen

Table 2: Consumables

Name	Supplier	Cat-No.
Cell Culture Flasks, 175 cm^2	Cell Star	658170
Cell Culture Flasks, 75 cm^2	Cell Star	660160
Cell culture plate, 24-well	Greiner Bio-One	662160
Cell culture plate, 6-well	Falcon	353502
Cell culture plate, 96-well	Greiner Bio-One	655180
Cell Scraper	TPP	99002
Cryo vials, 1 ml	Greiner Bio-One	123263
Cryo vials, 1.8 ml	Thermo	377267
Electrode Paper	GE Healthcare	80110619
Filter tips, TipOne, 10/20 µl	Star Lab	S11203810
Filter tips, TipOne, 100 µl	Star Lab	S11201840
Filter tips, TipOne, 1000 µl	Star Lab	S11267810
Filter tips, TipOne, 20 µl	Star Lab	S11201810
Filter tips, TipOne, 200 µl	Star Lab	S1120-8810
Gloves, nitril, Dermagrip	WPR	
Nitrocellulose Blotting Membrane (Amersham Protran 0,2 µm NC)	GE Healthcare	1060301
Safe-lock Tubes, 0.5 ml	Eppendorf	30121023
Safe-lock Tubes, 1.5 ml	Eppendorf	30120086
Safe-lock Tubes, 2 ml	Eppendorf	30120094
Serological pipettes, 10 ml	Greiner Bio-One	607180
Serological pipettes, 25 ml	Greiner Bio-One	760180
Serological pipettes, 5 ml	Greiner Bio-One	606180
Serological pipettes, 50 ml	Greiner Bio-One	768180
Tubes, 15 ml	Cell Star	188271
Tubes, 5 ml	Eppendorf	30119401
Tubes, 50 ml	Cell Star	227261

Table 3: Chemicals

Device	Supplier	Cat-No.	CAS-No.
2-propanol	Applichem	A3928	67-63-0
Ammonium Persulfate (APS)	Sigma	A3678	7727-54-0
Ampicillin	Gibco	11593027	
APS (Ammonium Persulfate)	Sigma	A3678	
APS (Ammonium Persulfate)	Bio Rad	1610700	
Cyto Flex Sheath Fluid	Beckman Coulter	B51503	
Dimethylsulfoxid (DMSO)	Sigma	D2650	67-68-5
Ethanol absolute	AppliChem	A3678	64-17-5
Flow Clean Cleaning Agent	Beckman Coulter	A64669	
Glycerol	Sigma		56-81-5
Human Fc-Block	Miltenyi	130-059-901	
Immobilon Forte Western HRP Substrate	Millipore	WBLUF0100	
Methanol	JT Baker	10037550	67-56-1
Milk powder	Roth	T145.1	
Pancoll human	Pan Biotech	P04-601000	
Phenol red	Sigma	P5530	34487-61-1
Re-Blot Strong solution, 10X	Millipore	2504	

Sodium chloride	PanREAC AppliChem	APPC141659.1214	7647-14-5
TEMED (Tetramethylethylenediamine)	Sigma	T9281	110-18-9
TEMED (Tetramethylethylenediamine)	Bio Rad	1610800	
Trizma ® base	Sigma	77-86-1	77-86-1
Sodium dodecyl sulfate	MP	04811033-CF	151-21-3

Table 4: Buffers

Product	**Containing**	**Supplier**	**Cat-No.**
ACK Lysing Buffer		Gibco	A1049201
DPBS		Gibco	14190136
Fixation Buffer		BioLegend	420801
Resolving Gel Buffer		Bio Rad	1610798
RIPA buffer, 10X		Cell Signaling Technology	9806S
SDS sample buffer (Laemmli buffer)		Sigma	S3401
Semi Dry Blot Transfer Buffer (10x), stock		Alfa Aesar	J63664
Semi Dry Blot Transfer Buffer, working solution	1X Semi Dry Blot Transfer Buffer, stock 20% Methanol Fill up with Millipore water		
Stacking Gel Buffer		Bio Rad	1610799
TBS washing buffer	200 mM Tris 1.5 M NaCl pH 7.6 Fill up with Millipore water	selfmade	
TGS running buffer	250 mM Tris 130 mM Glycine 1% SDS Millipore water	selfmade	
Ultra Pure Distilled Water		Invitrogen	10977035

Table 5: Media and supplements

Product	**Supplier**	**Cat-No.**
ACK Lysing Buffer	Gibco	A1049201
FBS (Fetal Bovine Serum) Superior	Millipore	S06150114G
RPMI 1640 (Roswell Park Memorial Institute)	Gibco	11875093
DMEM (Dulbecco's Modified Eagle Medium)	Gibco	41966029
EMEM (Eagle's Minimum Essential Medium)	ATCC	30-2003
Penicillin-Streptomycin (P/S)	Gibco	15140122
0.05% Trypsin/EDTA	Gibco	25300054

Table 6: Cells and bacteria

Product	Details	Supplier	Cat-No.
HepG2	Hepatocacinoma cell line	ATCC	HB-8065
Huh7	Hepatocarcinome cell line	JCRB cell bank	JCRB0403

Table 7: Marker

Product	Supplier	Cat-No.
Page Ruler™Plus prestained Protein Ladder	Thermo Scientific	26619
Prescision Plus Protein™ Kaleidoscope™	BioRad	161-0375

Table 8: Cytokines, stimuli and inhibitors

Product	Supplier	Cat-No.
Human G-CSF	PeproTech	300-23
Human IFNα	Gift from Roche	
Human IFNγ	PeproTech	300-02
Human IL-22	PeproTech	200-22
Human IL-26	R&D	1375-IL-025
Human IL-6	PeproTech	200-06
Phosphatase Inhibitor	Roche	4906837001
Protease Inhibitor	Roche	4693159001

Table 9: Antibodies

Product	Supplier	Clone	Cat-No.	Purpose	Dilution
anti-hLBP goat IgG	AF870		R&D Systems	Western Blot, primary antibody	1:2000; in 5% BSA in TBS+0.1% Tween-20
Anti-β-Actin antibody, Mouse mAB	A1978		Sigma Aldrich	Western Blot, primary antibody	1:5000; in 5% Milch in TBS+0.1% Tween-20
CD126 PE-Cy7	352810	UV4	BioLegend	Flow cytometry	
CD130 BV650	564154	AM64	BD Biosciences	Flow cytometry	
CD14 PerCP-Cy5.5	325622	HCD14	BioLegend	Flow cytometry	
CD3 Alexa700	300424	UCHT1	BioLegend	Flow cytometry	
CD4 BV605	317438	Okt 04	BioLegend	Flow cytometry	
CD45RA PE-Dazzle594	304146	HI100	BioLegend	Flow cytometry	
CD8 APF/Fire 750	301066	RPA-T8	BioLegend	Flow cytometry	
HRP-goat anti-mouse IgG antibody	405306		BioLegend	Western Blot, secondary antibody	1:10.000; in 5% Milch in TBS+0.1% Tween-20
mouse anti-goat	sc-2354		Santa Cruz	Western	1:10.000; in

IgG-HRP			Biotechnology	Blot, secondary antibody	5% Milch in TBS+0.1% Tween-20
mouse anti-rabbit IgG-HRP	sc-2357		Santa Cruz Biotechnology	Western Blot, secondary antibody	1:10.000; in 5% Milch in TBS+0.1% Tween-20
Phospho-Stat1 (Tyr701) (D4A7) Rabbit mAb	7649S		Cell Signaling Technology	Western Blot, primary antibody	1:1000; in 5% BSA in TBS+0.1% Tween-20
Phospho-Stat3 (Tyr705) (D3A7) XP® Rabbit mAb	9145S		Cell Signaling Technology	Western Blot, primary antibody	1:1000; in 5% BSA in TBS+0.1% Tween-20
pStat3 FITC	557814	4/P-STAT3	BD Biosciences	Flow cytometry	
Stat1 p84/p91 Antikörper (E-23), rabbit	sc-346		Santa Cruz Biotechnology	Western Blot, primary antibody	1:1000; in 5% Milch/BSA in TBS+0.1% Tween-20
Stat3 (124H6) Mouse mAb	9139S		Cell Signaling Technology	Western Blot, primary antibody	1:1000; in 5% BSA in TBS+0.1% Tween-20
Stat3 PE	560391	M59-50	BD Biosciences	Flow cytometry	
Zombie Aqua BV510	77143		BioLegend	Flow cytometry	

Table 10: Primer

Name	**Sequence**	**Annealing temperature**
BCL-2 forward	TCT CAT GCC AAG GGG GAA AC	61.5 °C
BCL-2 reverse	CCG GTT ATC GTA CCC CGT TC	61.5 °C
GAPDH forward	GAA GAT GGT GAT GGG ATT TC	58 °C
GAPDH reverse	GAA GGT GAA GGT CGG AGT C	58 °C
IRF forward	CCA CTC TGC CTG ATG ACC AC	62.5 °C
IRF reverse	GGT GCT GTC CGG CAC AAC TT	62.5 °C
LPS-binding-protein forward	TTC GGT CAA CCT CCT GTT GG	60.5 °C
LPS-binding-protein reverse	CGC AAA TCC TGC TCT CCA GT	60.5 °C
TIMP1 forward	TCT GCA ATT CCG ACC TCG TCA TCA	62.5 °C
TIMP1 reverse	AAG GTG GTC TGG TTG ACT TCT GGT	62.5 °C

TNFα forward	GGC AGT CAG ATC ATC TTC TCG AA	63.5 °C
TNFα reverse	GAA GGC CTA AGG TCC ACT TGT GT	63.5 °C
α-1-antichymotrypsin forward	TGC CAG CGC ACT CTT CAT C	61 °C
α-1-antichymotrypsin reverse	TGT CGT TCA GGT TAT AGT CCC TC	61 °C

Table 11: Commercial Kits

Product	**Supplier**	**Cat-No.**	**Purpose**
Cyto Flex Daily QC Fluorophores	Beckman Coulter	B53230	Quality control for flow cytometric analysis
Pierce BCA Protein assay Kit	Thermo Fisher	23225	Protein quantification
PrimeScript RT Reagent Kit	Takara	RR037A	Reverse Transcription of RNA to cDNA
TB Green Premix Ex Taq	Takara	RR42LR	Premix for SYBR Green PCR
Versa Comp Antibody Capture Bead Kit	Beckman Coulter	B22804	Compensation for flow cytometric analysis

Table 12: Software

Product	**Version**	**Supplier**
Endnote	X9.2	Clarivate Analytics
FIJI (ImageJ)	1.52p	
FlowJo	10.6.1	FlowJo, LLC.
GraphPad Prism ®	8	GraphPad Software, Inc.
Microsoft Office	2010	Microsoft

3.2 Methods

3.2.1 Cultivation of mammalian cell lines

Different hepatoma cell lines were cultured in cell culture medium (see Table 13) supplemented with 10% fetal calf serum (FCS) and 1% Penicillin/Streptomycin in cell culture flasks in an incubator with a humidified 5% CO_2 atmosphere at 37 °C. Cells were maintained in the logarithmic growth phase by splitting them at a confluency of 70-80%. Cells were passaged twice a week with a ratio of 1:2 to 1:10 according to the following protocol. First, the cell layer was carefully rinsed with DPBS to remove remaining FCS which inhibits enzymatic detachment of the cells and dead cells. This was done by incubation with Trypsin/EDTA at 37 °C. After cells detached from the flask, the protease activity of trypsin was stopped by adding supplemented medium and cells were resuspended before splitting them according to their confluency. Fresh medium was added, and cells were returned to the incubator.

Table 13: Cells and corresponding medium.

Cells	**Medium**
Huh7	DMEM (+10% FCS, +1% Penicillin/Streptomycin)
HepG2	EMEM (+10% FCS, +1% Penicillin/Streptomycin)

Cells were used for approximately 35 passages before they were discarded since their genomic stability could not be guaranteed. The cells were continuously handled under sterile conditions to avoid contamination with bacteria, fungi or viruses.

3.2.1.1 Freezing cells

To freeze cells for storage, cells were treated with Trypsin/EDTA to detach them from the cell culture flask. After that, cells were centrifuged at 300 g at room temperature (RT). The sedimented cells were resuspended in FCS + 10% DMSO to preserve the cellular structure. Cells were stored at -80 °C in Mr. Frosty freezing containers and later transferred to storage boxes at -80 °C.

3.2.1.2 Thawing cells

To thaw cryoconserved cells, the cells were mixed with prewarmed medium (37 °C) and transferred stepwise into 10 ml of the cell culture medium. Cells were sedimented by centrifugation at 300 g for 5 min to remove the DMSO. The supernatant was discarded, and 10 ml fresh medium was added for resuspending the

cells. The suspension was directly transferred into a fresh T75-cell culture flask. On the following day, medium was exchanged, or cells were splitted if necessary.

3.2.1.3 Counting cells

Cells were counted with a *Neubauer* cell counting chamber. Briefly, 10 µl trypan blue dye were mixed with 10 µl cell suspension and transferred to the counting chamber. Since the dye can enter the cytoplasm of dead cells, these cells can be detected and were excluded from counting. Each big square of the counting chamber owns an area of 1 mm^2 with a depth of 0.1 mm which equals a volume of 0.1 mm^3 (0.001 µl). Cells within the four squares were counted and the average cell number per square was calculated. The cell number per ml was calculated according to Formula 1.

$$C = N \times 10^4 \times D$$

C = cells per ml

N = average cell number per square

10^4 = correction factor to calculate for 1 ml

D = dilution factor

Formula 1: Calculation of cell concentration.

After counting, cells were seeded into cell culture plates of different sizes depending on the experimental context.

3.2.2 Primary human hepatocytes (PHHs)

PHHs were kindly provided by PD Dr. Ruth Bröring, Department for Gastroenterology and Hepatology. Hepatocyte isolation, purification and seeding was performed according to Werner et al [220].

After seeding, PHHs were cultured in DMEM Ham's F12 medium supplemented with 1% Penicillin/Streptomycin in 6- or 12-well collagen-coated plates in an incubator with a humidified 5% CO_2 atmosphere at 37 °C over night. The next day, medium was exchanged, and experiments were performed as described for hepatocarcinoma cell lines (3.2.3 Cytokine treatment of hepatocarcinoma cell lines).

3.2.3 Cytokine treatment of hepatocarcinoma cell lines

To stimulate HepG2 and Huh7 cells with cytokines, cells were seeded into 6-well plates ($0.4x10^6$ cells/2ml) and incubated at 37 °C overnight. The next day, medium was exchanged prior to stimulation. The stimulation concentration varied, dependent on the experimental setup from 0.1 to 10 ng/ml for human interleukins and IFNγ and was 500 IU/ml for IFNα. After stimulation for various periods of time (from 15 min to 24 h 30 min), medium was aspirated, and the cells were rinsed once with ice cold DPBS which was aspirated again afterwards. Cells were lysed with 100 µl RIPA buffer /well supplemented with protease and phosphatase inhibitors to preserve the proteins of interest. With the help of a cell scraper, the cells were removed from the surface and collected in a 1.5 ml reaction tube. Finally, the cell lysates were centrifuged at 14,000 g for 10 min at 4 °C to remove the cellular debris and the supernatant containing the cellular proteins was collected in a new 1.5 ml reaction tube. The lysate was stored at -20 ° until further use.

3.2.4 Western Blot

Western blot analysis or immunoblot analysis is a method in molecular biology to separate and identify specific proteins in whole cell lysates. This is conducted by separating the proteins by size, then transfer to a carrier membrane and visualize the protein of interest using specific primary and secondary antibodies.

3.2.4.1 BCA Protein Assay

The Pierce BCA Protein Assay Kit was used for determination of protein concentrations in whole cell lysates that were obtained from HepG2 and Huh7 cells (see 3.2.3 Cytokine treatment of hepatocarcinoma cell lines). The assay was performed according to the manufacturer's instructions. Briefly, a colorimetric detection and quantification of the total protein level with reference to a BSA serial dilution was performed. The proteins in the measured samples reduce Cu^{2+} to Cu^{1+} in an alkaline medium which is in the end detected by adding bicinchoninic acid (BCA). Absorbance of the purple-coloured reaction increases nearly linearly with the protein concentration and was detected at 540 nm after 30 min incubation at 37 °C.

3.2.4.2 SDS-polyacrylamide-gel electrophoresis (SDS-PAGE) of proteins

SDS-PAGE was used to separate denatured proteins according to their molecular weights in an electronic field dependent on the amount of negatively charged SDS molecules bound to the length of the denatured proteins.

Prior to loading the polyacrylamide gels of 1.5 mm thickness the protein concentration of the samples was determined using a BCA protein assay (see 3.2.4 Western Blot

Western blot analysis or immunoblot analysis is a method in molecular biology to separate and identify specific proteins in whole cell lysates. This is conducted by separating the proteins by size, then transfer to a carrier membrane and visualize the protein of interest using specific primary and secondary antibodies.

3.2.4.1 BCA Protein Assay). 20 µg protein was mixed with 1 X Laemmli buffer (final concentration, f. c.) and denatured at 95 °C for 5 min. After cooling down, the samples were briefly centrifuged and loaded onto 10% acrylamide gels, prepared according to Table 14.

Table 14: Composition of resolving and stacking gels for SDS-PAGE. Quantities are stated in ml for one gel.

	Resolving gel, 10%	**Stacking gel**
Ultra Pure H_2O	4	3.4
Resolving gel buffer	2.6	-
Stacking gel buffer	-	1.4
50% Glycerol	0.2	-
10% SDS	0.1	0.1
Acrylamide	3.4	0.6
10% APS	0.04	0.04
TEMED	0.02	0.04

After polymerization, the gel was placed into the electrophoresis chamber, filled with 1 X TGS running buffer. Protein ladder as size control and the samples were loaded onto the gel and constant voltage was applied to run the gels (initially 80 V for 20 min followed by 150 V for approximately 1 h).

3.2.4.3 Immunoblotting

After electrophoretic separation of proteins, they were transferred onto a nitrocellulose membrane in a semi-dry transfer chamber. To this end, filter papers

and the nitrocellulose membrane were wetted with semi-dry transfer buffer (see Table 4: Buffers) and stacked in the transfer chamber together with the gel according to Figure 4.

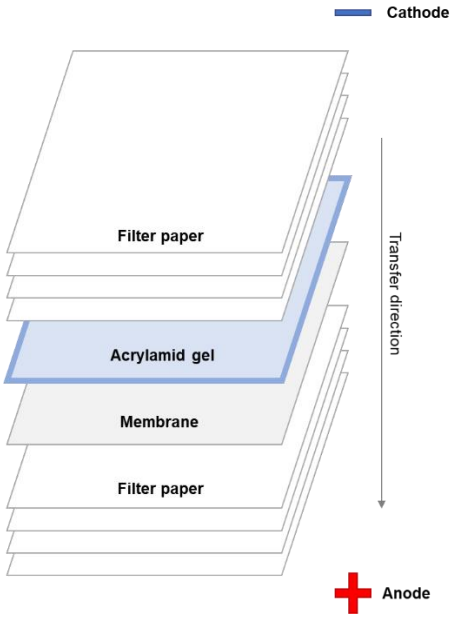

Figure 4: Schematic overview of the Immunoblot sandwich for semi-dry protein transfer.

The protein transfer was conducted at constant 0.6 A for 70 min. After transfer, membranes were blocked in 5% milk in TBS + 0.1% Tween-20 (TBS-T) for 60 min at RT. Primary antibodies to detect the protein of interest were diluted according to the data sheets 1:1000 or 1:5000 in 5% BSA in TBS-T and the membranes were incubated with the primary antibodies at 4 °C overnight. The next day, membranes were washed three times with TBS-T before incubation with the secondary antibody for 1 h at RT. The horseradish peroxidase (HRP)-conjugated secondary antibody was diluted 1:10,000. Protein bands were visualized using Immobilon® Forte Western HRP Substrate in an ECL Chemostar Imager (Intas).

3.2.5 RNA isolation from human cells

To isolate total RNA from cell culture cells or primary human hepatocytes (PHHs) the peqGOLD Total RNA Kit (VWR) was used which is a column-based method. RNA extraction was performed according to the manufacturer's instructions. Briefly, cells were lysed using RNA lysis buffer and transferred to a DNA Removing Column. After centrifugation and mixing the flow-through with 70% ethanol, the solution was loaded onto a PerfectBind RNA Column which binds the RNA from the sample to its matrix. After several washing steps and 5 min incubation of the column matrix in 50 µl

RNase-free water at RT, RNA was eluted via centrifugation. RNA concentration was measured at 260 nm using a N60 Nanophotometer (Implen).

3.2.5.1 Reverse transcription

Previously isolated RNA (see 3.2.5 RNA isolation from human cells) was transcribed into complementary DNA (cDNA) for later use in semiquantitative Real-Time PCR. To this end, the PrimeScript RT Reagent Kit was used and max. 500 ng of RNA template. The components were mixed for each sample as depicted in Table 15.

Table 15: Pipetting scheme for reverse transcription of an RNA template to cDNA using the PrimeScript RT Reagent Kit.

Vial	Reagent	Volume	Final concentration
V1	5x PrimeScript Buffer	2 µl	1 X
V2	PrimeScript RT Enzyme Mix	0.5 µl	
V3	Oligo dT Primer (50 µM)	0.5 µl	25 pmol
V4	Random hexamers	0.5 µl	50 pmol
	Template RNA	X µl (equal to max. 500 ng)	
V5	RNase-free water	Add up to 10 µl	

The prepared samples were briefly centrifuged to eliminate air bubbles and subsequently incubated in a SureCycler 8800 (Aligent) according to the program in Table 16.

Table 16: cDNA cycler protocol for reverse transcription.

Step	Temperature	Duration	Procedure
1	37 °C	15 min	Annealing + Elongation
2	85 °C	5 s	Denaturation of RNA and enzymes
3	4 °C	∞	Storage

After the reaction, samples were diluted with 90 µl Ultra-Pure water before being processed in the RT-PCR reaction.

3.2.5.2 SYBR® Green qRT-PCR

For semiquantitative analysis of previously transcribed cDNA (see 3.2.5.1 Reverse transcription), SYBR® Green PCR was applied which intercalates nonspecifically into

dsDNA and therefore allows measurement of the PCR product. The PCR mix was prepared according to Table 17. Primers were stored in working aliquots of 10 µM.

Table 17: Pipetting scheme for qRT-PCR.

Reagent	**Volume**
SYBR®Premix Ex Taq™ (Tli Rnase H Plus), ROX Plus	7.5 µl
Forward Primer	0.45 µl
Reverse Primer	0.45 µl
Ultra Pure water	5.6 µl
cDNA	1 µl

The reagents were mixed and briefly centrifuged to eliminate air bubbles and subsequently incubated in a CFX96 Teal TimeSystem Cycler (BioRad) according to the program in Table 18.

Table 18: Cycler program for semiquantitative real-time PCR.

Step		**Temperature**	**Duration**	**Procedure**
1		95 °C	10 min	Initial denaturation
2	40x	95 °C	20 s	Denaturation
3		Primer-dependent	30 s	Annealing
4		72 °C	1 min	Extension
5		72 °C	10 min	Final Extension

For annealing temperatures of the used primers see Table 10: Primer. The steps 2 to 4 were repeated for 40 cycles. GAPDH was used as a housekeeping gene control which is equally expressed in every sample. Gene expression was calculated and based on Threshold Cycle (ct-) value of the respective target gene. Analysis was performed using Bio-Rad CFX Manager software (BioRad). The subsequent calculation was used to determine the $2^{-\Delta\Delta ct}$ value with $\Delta ct = ct_{(gene\ of\ interest)} - ct_{(housekeeper)}$ and $\Delta\Delta ct = \Delta ct_{stimulated)} - \Delta ct_{(untreated)}$.

3.2.6 Colorimetric WST-1 cellular viability assay

With help of the WST assay, cell proliferation and viability were quantified. In the colorimetric assay the tetrazolium salts of the WST-1 reagent are cleaved to formazan by cellular enzymes. An increased cell number leads to augmented enzyme activity and therefore an increased amount of formazan dye quantifiable by

absorbance measurement at 440 nm. The amount of formazan dye correlates to the number of metabolically active cells.

To perform the assay, Huh7 and HepG2 cells were harvested by trypsinization and resuspended in DMEM (Huh7) or EMEM (HepG2) supplemented with 10% FCS and 1% Penicillin/Streptomycin. The cells were subsequently plated at a density of $1x10^4$ cells per well into a 96-well plate and incubated overnight at 37 °C and 5% CO_2. The next day, medium was exchanged to fresh medium with 10% FCS and cells were stimulated with recombinant cytokines (IL-22, IL-6, IFNα, IFNγ) at a concentration of 5 ng/ml (final concentration) or 500 IU/ml for IFNα. Each cell line was incubated for 6 h and 12 h, respectively. PBS + 0.1% BSA was added in the control group. 10 µl/well Cell Proliferation Reagent WST-1 was added according to the manufacturer's instructions 2 h prior to the end of stimulation. The plates were shaken for 1 min on an orbital shaker. Absorbance measurement of the samples against a background control was performed with a microplate reader (FluoStar Omega, BMG) at a wavelength of 440 nm. The reference wavelength was at 650 nm.

3.2.7 Isolation of human peripheral blood mononuclear cells (PBMCs) from blood samples

Primary immune cells were isolated from blood samples obtained from patients or healthy donors by Ficoll gradient centrifugation. Samples were centrifuged at 3000 g for 15 min at 4 °C. The remaining blood without the excess plasma was transferred carefully in a 15 ml tube containing 5 ml Ficoll solution to create two layers. After centrifugation at 500 g for 15 min without break, the PBMCs were separated from the remaining blood cells according to Figure 5. The interphase containing the PBMCs was transferred into a new 50 ml tube and filled up with DPBS, followed by centrifugation at 300 g for 10 min. This washing step was repeated after discarding the supernatant. In case of remaining erythrocytes in the cell pellet, 2 ml ACK lysis buffer was added and incubated for 2 min in between the washing steps. PBMCs were frozen in 1 ml freezing medium (FCS + 10% DMSO).
The cells were stored at -80 °C until further use.

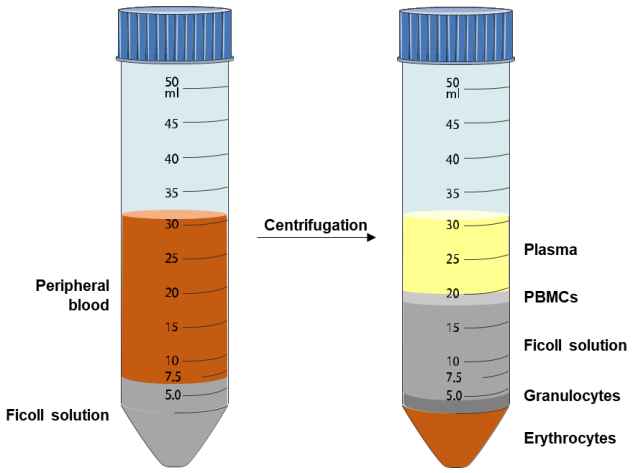

Figure 5: Schematic depiction of density gradient centrifugation.
Upon centrifugation the different layers become separated. PBMCs can be removed and used for further experiments.

3.2.7.1 Stimulation of PBMCs

Previously isolated PBMCs that were stored at -80 °C were thawed and resuspended in 4 °C RPMI medium supplemented with 10% FCS and 1% P/S. Cells were centrifuged at 500 g for 5 min at 4 °C. The supernatant was discarded to resuspend the PBMCs in 1 ml RPMI medium. Cells were counted and were seeded in a 24-well plate. About 50,000 cells were frozen separately in RNA lysis buffer for RNA isolation. The seeded cells were stimulated with 50 ng/ml IL-6 or IFNγ or a combination dependent on the experimental setup. The incubation time varied from 30 min up to 3 h and 30 min.

3.2.7.2 Staining for flow cytometric analysis

Stimulated PBMCs from patients and healthy donors were harvested by resuspending them and collected in a 1.5 ml reaction tube. All following steps were performed on ice. The cells were centrifuged at 500 g for 5 min at 4 °C, the supernatant was discarded, cells were taken up in 100 µl staining buffer and transferred into a 96-well plate. After another centrifugation step, cells were resuspended in 50 µl staining buffer supplemented with human Fc-block solution (1:25) to block the Fc-receptors on the cell's surfaces for 10 min. The antibodies from "Prä Fix/Perm staining Mix" (see Table 19) were mixed in 50 µl Brilliant Stain Buffer per well and added to the cells for 20 min on ice in the dark. Afterwards, the cells were washed with 200 µl staining buffer at 500 g for 5 min at 4 °C. The supernatant was aspirated, and cells were fixed with 200 µl/well PFA-containing Fixation Buffer in

the dark at RT for 20 min. Cells were centrifuged again at 500 g for 5 min at 4 °C and washed with staining buffer as described above. After discarding the supernatant, cells were permeabilized with 100% ice cold methanol on ice for 10 min. Again, cells were washed with staining buffer and prepared for staining with “Post Fix/Perm staining Mix 1” (see Table 19; 100 µl Brilliant Staining Buffer per well) for 60 min at RT in the dark. Thereafter, cells were sedimented and washed before they were stained with “Post Fix/Perm staining Mix 2” (see Table 19; 100 µl Brilliant Staining Buffer per well) for 20 min on ice in the dark. A final washing step was performed before cells were resuspended in 200 µl staining buffer for fluorescence measurement at flow cytometer CytoflexS (Beckman Coulter). For data analysis FlowJo Software was used.

Table 19: Pipetting scheme for multicolour flow cytometric staining of PBMCs.

Antibody mix	**Target**	**Fluorochrome**	**Clone**	**Cat. #**	**Manufacturer**	**Amount in 100 µl**
Prä Fix/Perm staining Mix	CD3	Alexa700	UCHT1	300424	BioLegend	2 µl
	CD4	BV605	OKT4	317438	BioLegend	1 µl
	CD8	APF/Fire 750	RPA-T8	301066	BioLegend	0.5 µl
	gp130	BV650	AM64	564154	BD Biosciences	5 µl
	Zombie Aqua	BV510		77143	BioLegend	0.1 µl
Post Fix/Perm staining Mix 1	pStat3	FITC	4/P-STAT3	557814	BD Biosciences	20 µl
	Stat3	PE	M59-50	560391	BD Biosciences	20 µl
Post Fix/Perm staining Mix 2	CD14	PerCP-Cy5.5	HCD14	325622	BioLegend	2 µl
	CD45RA	PE-Dazzle594	HI100	304146	BioLegend	0.5 µl
	IL-6Rα (CD126)	PE-Cy7	UV4	352810	BioLegend	5 µl

Immune cell populations were gated and analysed as displayed in Figure 6.

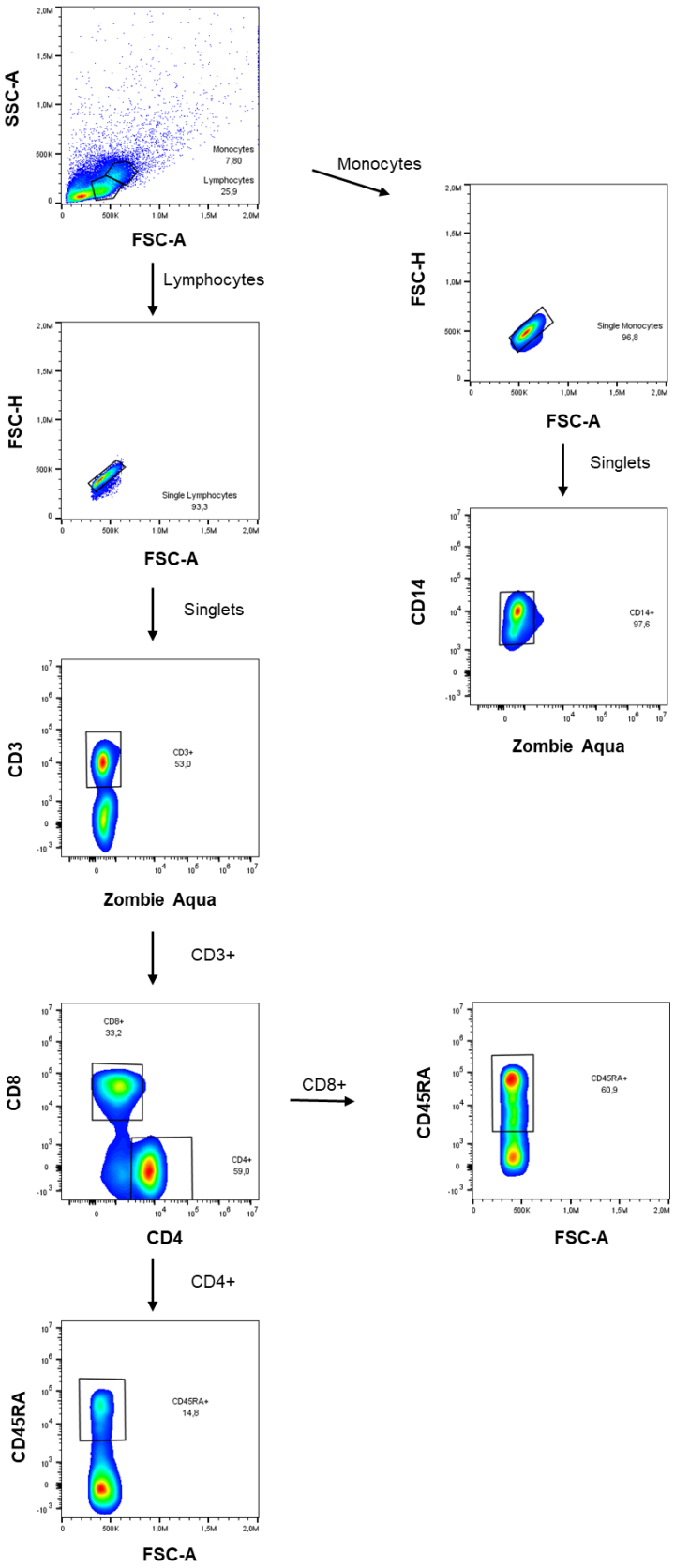

Figure 6: Gating strategy for multicolour flow cytometry.
Firstly, the lymphocyte and monocyte populations were separated. This was followed by singlet gating in each cellular subset. Living cells were determined by live-dead staining Zombie Aqua. Zombie Aqua vs. CD14 reveals the living monocyte subset while Zombie Aqua vs CD3 in the lymphocyte subset separated the T cells. These were further divided into $CD8^+CD45RA^+$ and $CD4^+CD45RA^+$ T cells.

The final cell populations were investigated regarding their levels of CD126 and CD130 as well as their content of phosphorylated and total Stat1 and Stat3.

3.2.8 Patients

Between November 2018 and October 2021, patients diagnosed with compensated liver cirrhosis (Child-Pugh A), decompensated liver cirrhosis (Child-Pugh B and C) or acute-on-chronic liver failure were included in our cohort study. The state of liver disease was assigned to the patients referring to the criteria of the EASL-CLIF consortium [144]. Patients suffering from hepatocellular carcinoma (HCC) beyond MILAN criteria were excluded from the study as well as pregnant or breast-feeding patients and patients infected with the human immunodeficiency virus (HIV). Patients that donated blood for this study signed the written consent of the study which was performed in cooperation with the Westdeutsche Biobank at the University Hospital Essen, Germany. Human biological samples and related data were provided by the Westdeutsche Biobank Essen (WBE, University Hospital Essen, University of Duisburg-Essen, Germany; approval WBE-071).

3.2.9 Statistics

Statistical analysis and graph creation were performed with the software GraphPad Prism (Version 8, GraphPad Software, San Diego, Ca, USA). Tests for significance were performed dependent on whether the data was distributed normally (One- or two-way ANOVA) or not (Kruskal-Wallis-test). *P* values <0.05 were considered as statistically significant with * = <0.05, **= <0.01, *** = <0.001. Group differences were assessed using X^2-contingency test

4 Results

4.1 The influence of various cytokines on hepatocarcinoma cell lines and primary human hepatocytes (PHHs)

Initially, the influence of various cytokines on hepatocarcinoma cell lines and primary human hepatocytes (PHHs) was investigated. Cytokines which were described as influential in the context of LC and ACLF were considered, namely IL-6, IL-10, IL-13, IL-26 and G-CSF [65, 133, 189, 191]. It was known from previous works in our group that for instance IL-22 can be used for *in vitro* assays at a concentration of 5 ng/ml to effectively induce Jak-Stat-signalling pathway activation in the hepatocarcinoma cell lines HepG2 and Huh7 [185]. Furthermore, IFNα and IFNγ were used in our working group at concentrations of 500 IU/ml and 5 ng/ml, respectively [173, 175]. To figure out an appropriate working concentration for IL-6 and other mentioned cytokines such as G-CSF, IL-13 or IL-10 for our *in vitro* assays, several time and concentration kinetic experiments were performed with HepG2 and Huh7 cells which are two frequently used hepatocarcinoma cell lines in liver related research. Additionally, PHHs were also included and treated with IL-6, IL-13 and G-CSF. The used cytokines are described to function via the Jak-Stat signalling pathway as described for IL-6 in chapter 1.1.1.1.2 Interleukin 6, so pathway activation was controlled by detection of phosphorylated Stat molecules via immunoblot analysis. Control samples received treatment with PBS supplemented with 0.1% BSA as this was the condition in which the cytokines were all stored and diluted.

4.1.1 Time kinetic experiments with various cytokines

In Western blot experiments both cell lines show a strong Stat1 and Stat3 phosphorylation within the initial 60 min after IL-6 stimulation with 10 ng/ml (Figure 7). For further stimulation experiments the 30 min time point was chosen to show successful pathway activation by Stat1 and Stat3 phosphorylation. This is consistent with previous findings of our group regarding IL-22 [185].

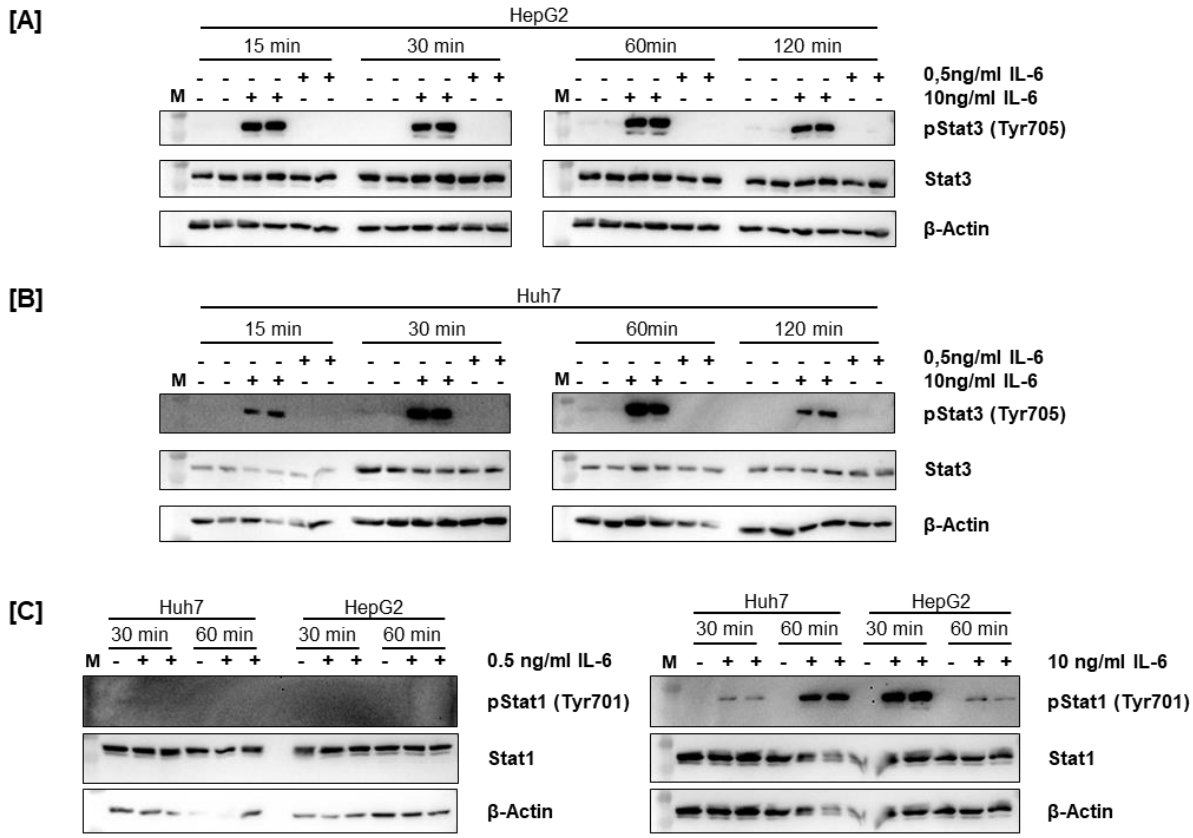

Figure 7: Stat phosphorylation after IL-6 stimulation in HepG2 and Huh7 cells.
HepG2 cells [A], [C] and Huh7 cells [B], [C] were stimulated with IL-6 at a dose of 0.5 ng/ml and 10 ng/ml for the indicated time points. Phosphorylation of Stat1 at Tyr701 and of Stat3 at Tyr705 was assessed via Immunoblotting with β-Actin as reference. One experiment is shown as demonstration. M = Marker lane.

Analogous to the described time kinetic experiments with IL-6, other cytokines, namely IL-26, IL-10, IL-13 and G-CSF were tested regarding Stat phosphorylation induction (Figure 8). Based on this selection only IL-13 and G-CSF showed satisfactory Stat3 phosphorylation in HepG2 cells (Figure 8 [E], [F]). In line with the findings for IL-6, the strongest phosphorylation was detected after 30 to 60 min of stimulation.

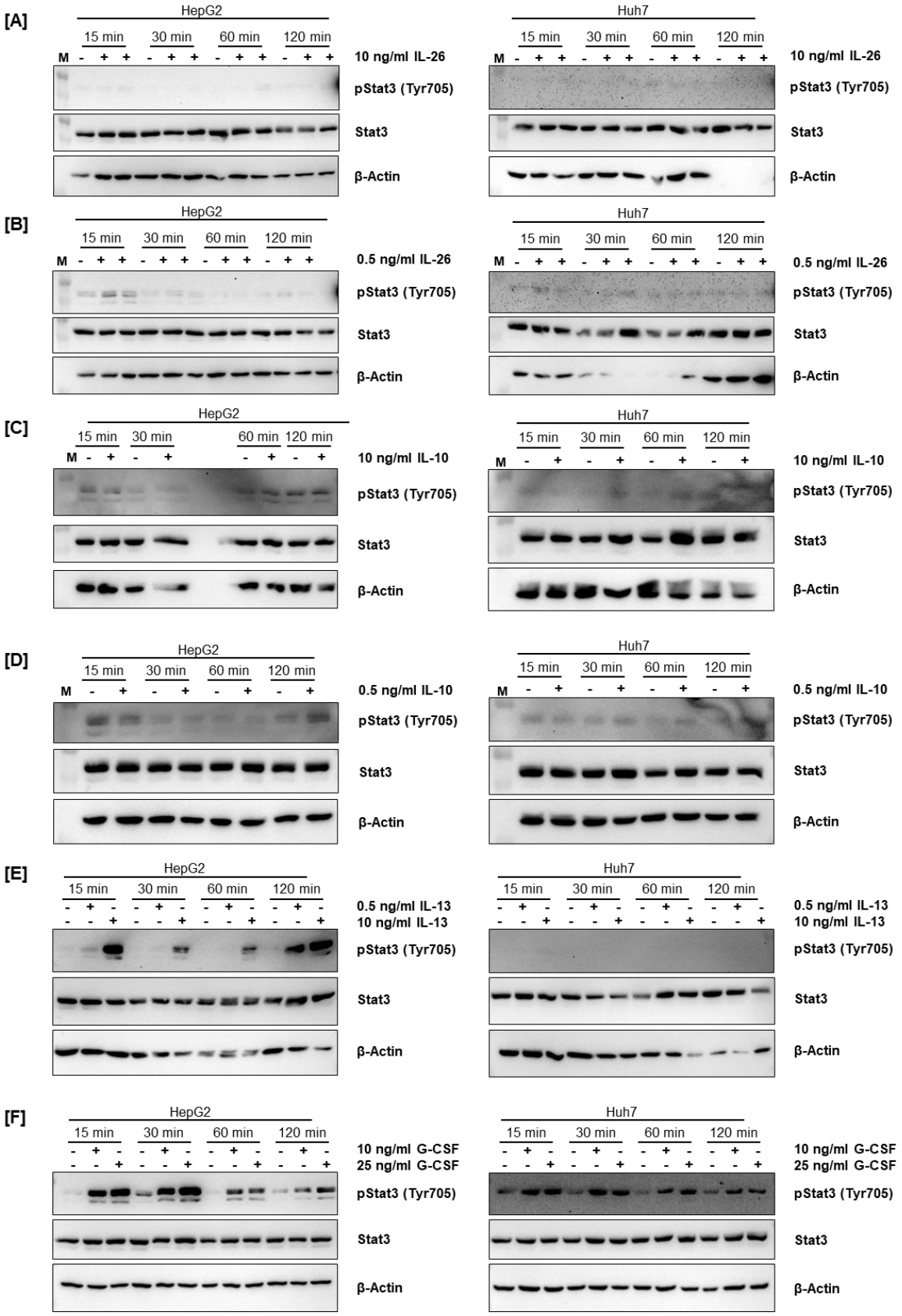

Figure 8: Stat phosphorylation in HepG2 and Huh7 cells after stimulation with various cytokines.
HepG2 cells [A-E, left panel] and Huh7 cells [A-E, right panel] were stimulated with IL-26 [A], [B], IL-10 [C], [D], IL-13 [E] and G-CSF [F] at a dose of 0.5 ng/ml,10 ng/ml or 25 ng/ml, respectively, for the indicated time points. Phosphorylation of Stat3 at Tyr705 was assessed via Immunoblotting with β-Actin as reference. One experiment is shown as demonstration. M = Marker lane.

Stat phosphorylation was additionally inducible in primary human hepatocytes that were kindly provided by PD Dr. Ruth Bröring. PHHs were cultured in DMEM Ham's F12 without supplemented FCS as this reduced the background phosphorylation of Stats. Figure 9 [A-C] shows the results for PHHs stimulated with IL-6, IL-13 and G-CSF, respectively. Comparable to the cell line experiments Stat phosphorylation was strongest within the initial 30 min after stimulation and declines afterwards.

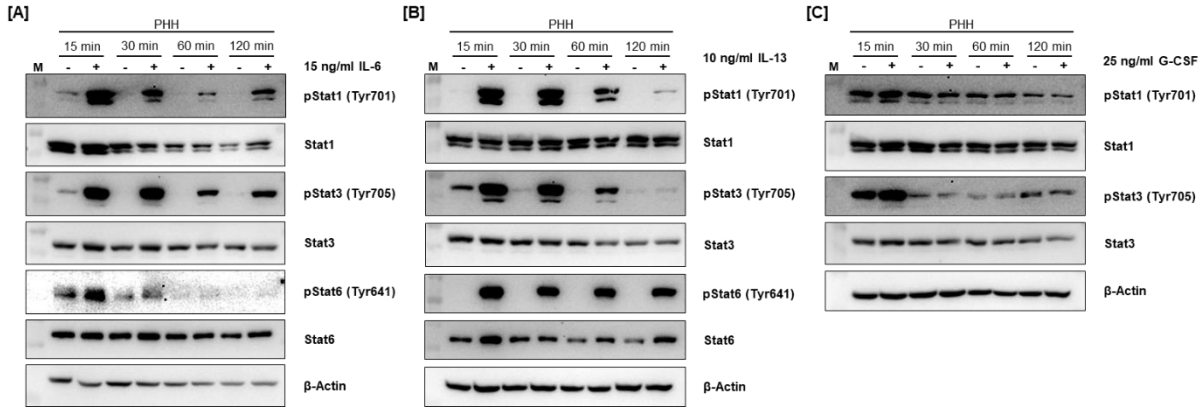

Figure 9: Stat phosphorylation in PHHs.
PHHs [A-C] were stimulated with IL-6 [A], IL-13 [B] and G-CSF [C] at a dose of 15 ng/ml, 10 ng/ml and 25 ng/ml, respectively, for the indicated time periods. Phosphorylation of Stat1 at Tyr701, Stat3 at Tyr705 and Stat6 at Tyr641 was assessed via Immunoblotting with β-Actin as reference. One experiment is shown as demonstration. M = Marker lane.

To sum up, IL-6, IL-13 and G-CSF induce a rapid Stat phosphorylation peak in hepatocarcinoma cell lines and PHHs which declines afterwards.

4.1.2 Concentration kinetic experiments with various cytokines

The next step was to evaluate the ideal cytokine concentration for the future stimulation experiments. Therefore, HepG2 and Huh7 cell were stimulated with various amounts of IL-6, IL-26, IL-10, IL-13 and G-CSF for 15 min and Western blot analysis was performed to control the Stat phosphorylation levels. The results are shown in Figure 10. Throughout the different stimulations, a concentration between 1 ng/ml and 10 ng/ml was found to be necessary to induce a solid phosphorylation signal. For the next experiments, 5 and 10 ng/ml were taken as fix concentrations for the respective cytokines.

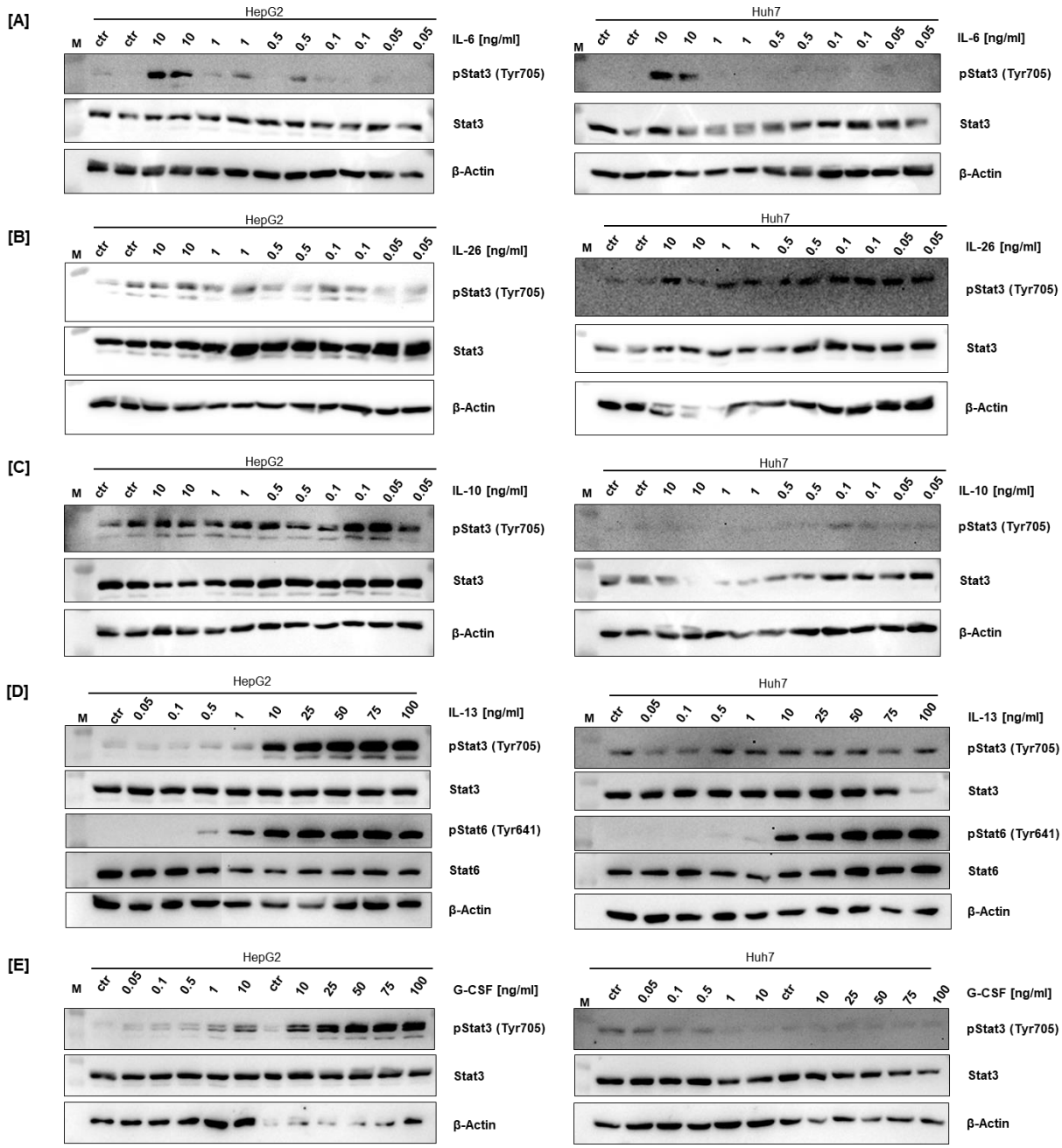

Figure 10: Phosphorylation of Stats alters dependent on cytokine concentration.
HepG2 cells [A-E, left panel] and Huh7 cells [A-E, right panel] were stimulated with IL-6 [A], IL-26 [B], IL-10 [C], IL-13 [D] and G-CSF [E] with a dose range from 0.05 ng/ml to 10 or 100 ng/ml, respectively, for 15 min. Phosphorylation of Stat3 at Tyr705 was assessed via Immunoblotting with β-Actin as reference. One experiment is shown as demonstration. M = Marker lane.

After the time and concentration kinetic experiments, IL-6, IL-22, IL-13 and G-CSF were considered as candidates for further investigations as IL-10 and IL-26 did not induce a solid Stat phosphorylation that could be shown in the used cell lines.

4.2 Cytokine combinations synergistically enhance Stat phosphorylation in hepatocarcinoma cell lines and PHHs

In the next experimental approaches, we aimed to assess whether the selected cytokines influence each other in terms of signalling pathway activation. Therefore, several single cytokine doses and combinations were applied in the defined concentrations to HepG2 and Huh7 cells simultaneously or one after another. IL-22 was one of the cytokines in each treatment pair due to its previously described important role in LC and ACLF [185, 186]. After 30 min total stimulation time the phosphorylation of Stat molecules was investigated by Western Blot analysis and quantified relative to the corresponding β-Actin signal from the Western Blots using the software ImageJ. The results are depicted in the Figure 11, Figure 12, Figure 13 and Figure 14. In the following, especially the single stimulation conditions (lane 2) and 3)) and the condition where both cytokines were applied for 30 min simultaneously (lane 6)) are compared.

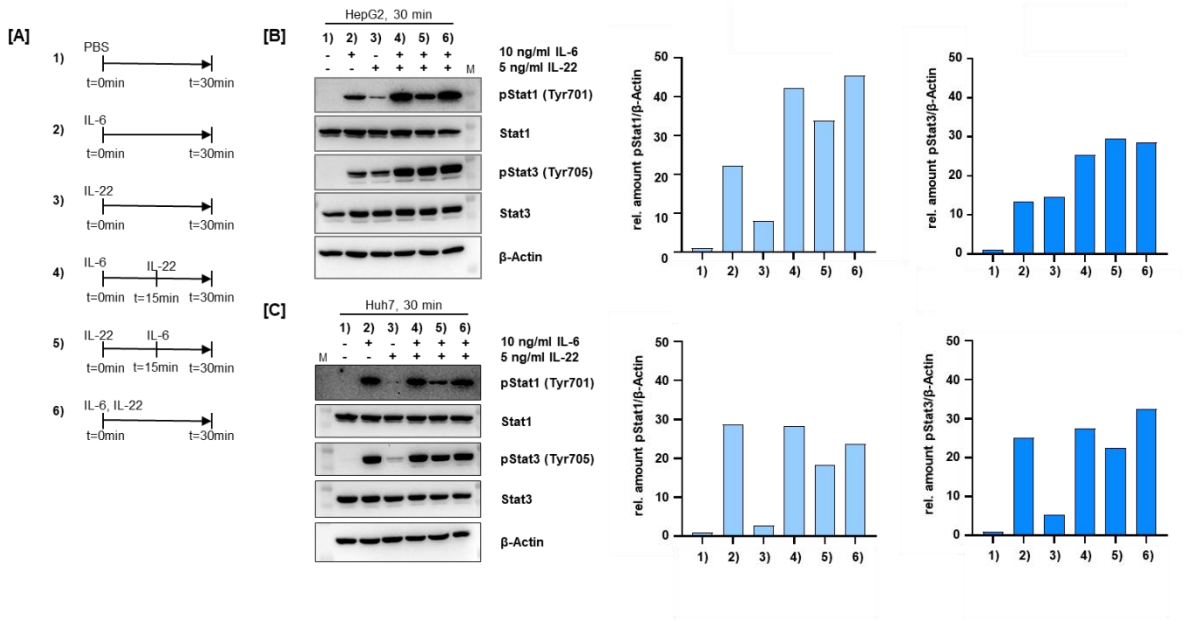

Figure 11: IL-6 and IL-22 synergistically enhance short-term Stat phosphorylation in hepatocarcinoma cell lines.
HepG2 cells [B] and Huh7 cells [C] were stimulated with 10 ng/ml IL-6 and/or 5 ng/ml IL-22 as indicated in [A] and the relative amount of phosphorylated Stat1 and Stat3 was quantified relative to the corresponding β-Actin band. Phosphorylation of Stat1 at Tyr701 and of Stat3 at Tyr705 was assessed via Immunoblotting with β-Actin as reference. One experiment is shown as demonstration. M = Marker lane.

The combined stimulation with IL-6 and IL-22 (Figure 11) shows that single cytokine treatments with both cytokines lead to successful phosphorylation of Stat1 and Stat3. The detailed stimulation scheme is depicted in Figure 11 [A]. It becomes especially

visible in HepG2 cells (Figure 11 [B]) that a combination of both cytokines resulted in increased phosphorylation levels of Stat1 and Stat3 suggesting a synergistic mode of action.

This effect could also be observed regarding the IL-13 and IL-22 combination as shown in Figure 12. Here, the pStat1 level in HepG2 cells was considerably enhanced when both cytokines were combined in the treatment. Stat6 is not a shared signalling molecule of both cytokines so we expected no effect upon the combined treatment.

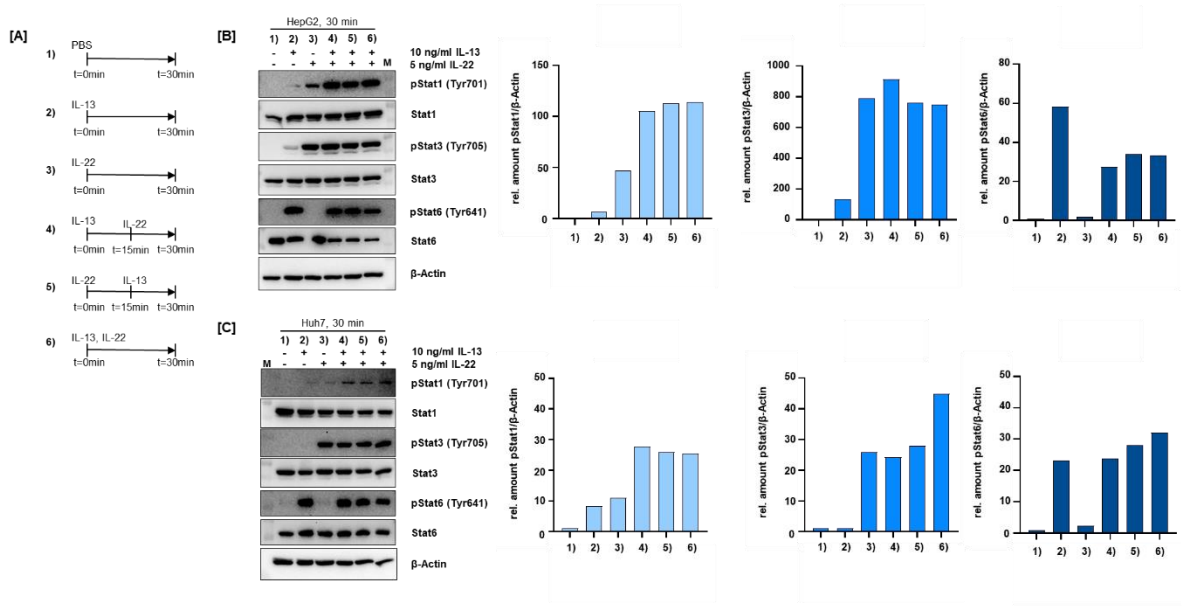

Figure 12: IL-13 and IL-22 combination influences short-term STAT phosphorylation in hepatocarcinoma cell lines.
HepG2 cells [B] and Huh7 cells [C] were stimulated with 10 ng/ml IL-13 and/or 5 ng/ml IL-22 as indicated in [A] and the relative amount of phosphorylated Stat1, Stat3 and Stat6 was quantified relative to the corresponding β-Actin band. Phosphorylation of Stat1 at Tyr701 and of Stat3 at Tyr705 was assessed via Immunoblotting with β-Actin as reference. One experiment is shown as demonstration. M = Marker lane.

Regarding the combination of IFNα and IL-22, the pStat1 level of single and combined stimulation need to be compared as Stat1 is the shared signalling molecule of both cytokines (Figure 13). Phosphorylation was stronger induced in HepG2 cells compared to Huh7 cells but nevertheless both cytokines combined lead to an increased phosphorylation of Stat1 which suggests stronger pathway activation.

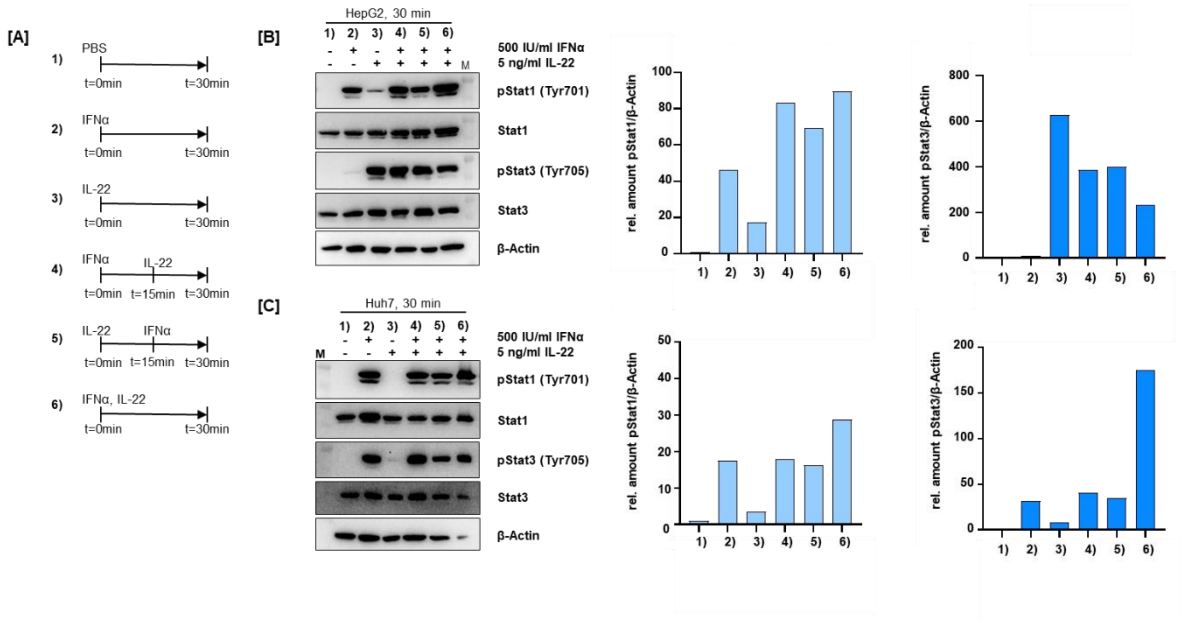

Figure 13: IFNα and IL-22 influence short-term STAT phosphorylation in hepatocarcinoma cell lines.
HepG2 cells [B] and Huh7 cells [C] were stimulated with 500 IU/ml IFNα and/or 5 ng/ml IL-22 as indicated in [A] and the relative amount of phosphorylated Stat1 and Stat3 was quantified relative to the corresponding β-Actin band. Phosphorylation of Stat1 at Tyr701 and of Stat3 at Tyr705 was assessed via Immunoblotting with β-Actin as reference. One experiment is shown as demonstration. M = Marker lane.

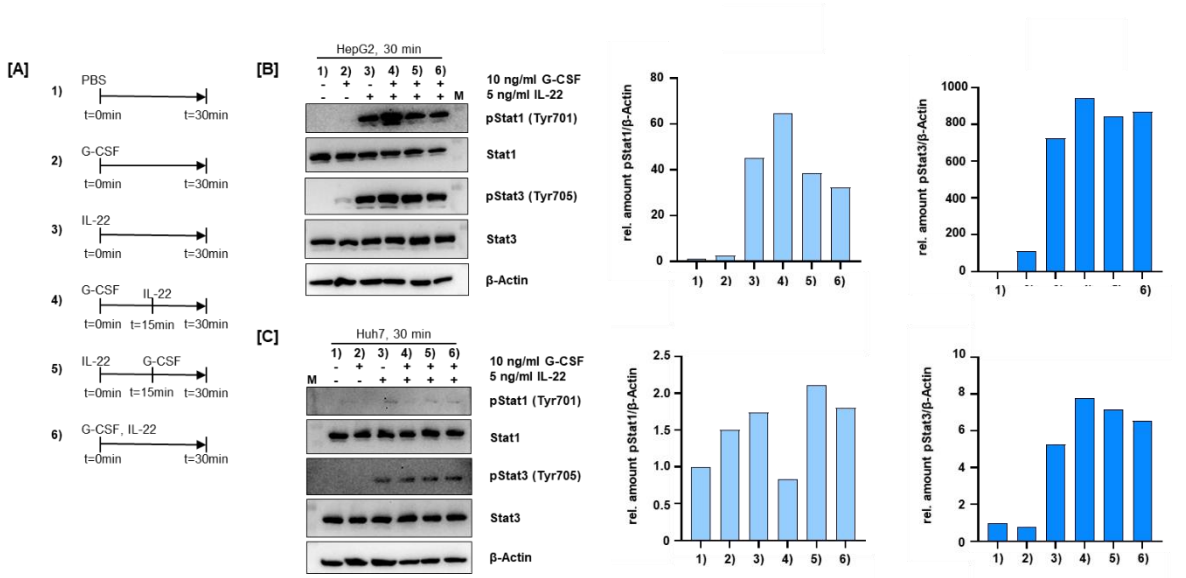

Figure 14: G-CSF and IL-22 influence short-term STAT phosphorylation in hepatocarcinoma cell lines.
HepG2 cells [B] and Huh7 cells [C] were stimulated with 10 ng/ml G-CSF and/or 5 ng/ml IL-22 as indicated in [A] and the relative amount of phosphorylated Stat1 and Stat3 was quantified relative to the corresponding β-Actin band. Phosphorylation of Stat1 at Tyr701 and of Stat3 at Tyr705 was assessed via Immunoblotting with β-Actin as reference. One experiment is shown as demonstration. M = Marker lane.

Figure 14 shows the treatment of HepG2 and Huh7 cells with G-CSF and IL-22. In this treatment combination no clear synergistic effect was detected. The Stat phosphorylation levels resulting from single or combined cytokine treatment did not differ much. Therefore, this combination was no longer considered.

Overall, the combinatory treatment worked best in HepG2 cells and the combinations of IL-6 with IL-22 showed the most promising effect together. This combination was selected for further investigations as both cytokines seem to influence each other in a synergistic way when both are present. Hence, the experimental setup using IL-6 and IL-22 was repeated in a setting that included extended stimulation times up to 45 min to see whether the effect of both cytokines alters. In addition, the stimulation concentration of IL-6 was adjusted to 5 ng/ml deviating from the previous experiments (Figure 11). Analogous to the previous figures, Figure 15 [A] shows the detailed stimulation scheme for the experiment to outline when single cytokine doses or a combination was applied to the cells. Figure 15 [B] and [C] show the Western blots and quantification for HepG2 and Huh7 cells, respectively. Lane 3) to 8) display a total stimulation time of 30 min while samples blotted in lane 9) to 14) were stimulated for 45 min.

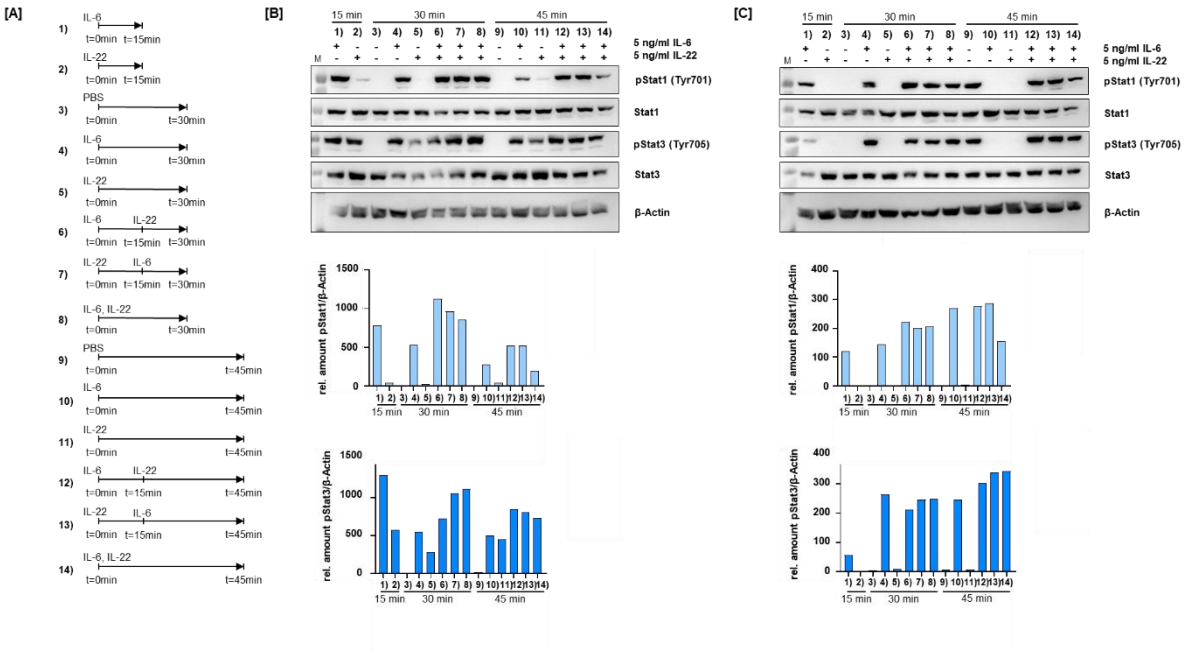

Figure 15: IL-6 and IL-22 synergistically enhance short-term STAT phosphorylation with a maximum after 30 min.
HepG2 cells [B] and Huh7 cells [C] were stimulated with 5 ng/ml IL-6 and/or 5 ng/ml IL-22 as indicated in [A] and the relative amount of phosphorylated Stat1 and Stat3 was quantified relative to the corresponding β-Actin band. Phosphorylation of Stat1 at Tyr701 and of Stat3 at Tyr705 was assessed via Immunoblotting with β-Actin as reference. One out of three independent experiments is shown as demonstration. M = Marker lane.

Figure 15 shows that the synergistic effect of both cytokines in terms of Stat1 and Stat3 phosphorylation peaks after a total stimulation time of 30 min. The results are comparable to the previously presented and confirm the synergistic effect of both cytokines concerning enhanced Stat phosphorylation. This further confirms the results from the time and concentration kinetic experiments as after 45 min the Stat1 and Stat3 phosphorylation signal is barely detectable compared to earlier time points (see chapter 4.1 The influence of various cytokines on hepatocarcinoma cell lines and primary human hepatocytes (PHHs)).

Additional to cells line experiments, the combined treatment with IL-6 and IL-22 was also performed with PHHs (Figure 16). Here, the effect of both cytokines applied simultaneously compared to single cytokine stimulations is even clearer visible than in HepG2 cells. After each period of 15 min, 30 min or 45 min total stimulation time, the combinatory treatment with both cytokines leads to a stronger Stat1 and Stat3 phosphorylation.

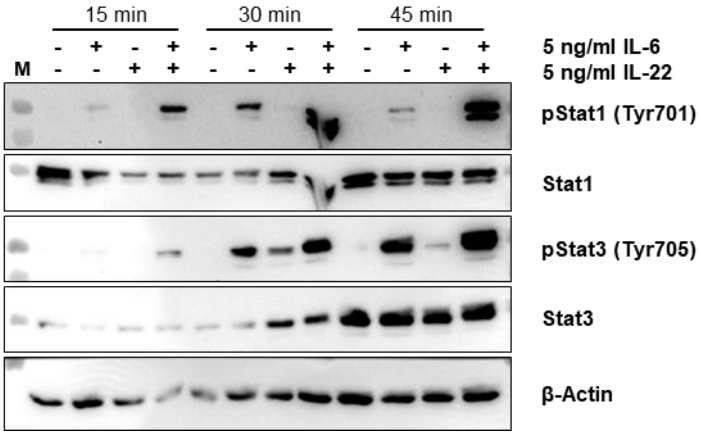

Figure 16: IL-6 and IL-22 synergistically enhance short-term Stat phosphorylation in PHHs.
PHHs were stimulated with 5 ng/ml IL-6 and/or 5 ng/ml IL-22 as indicated. Phosphorylation of Stat1 at Tyr701 and of Stat3 at Tyr705 was assessed via Immunoblotting with β-Actin as reference. One experiment is shown as demonstration. M = Marker lane.

Overall, the depicted results show that cytokines using the same signalling pathway often influence each other's signalling. Particularly, the combination of IL-6 and IL-22 synergistically enhances short-term phosphorylation of Stat1 and Stat3.

4.3 IL-6 and IL-22 combined treatment enhances anti-microbial activity

As a next step, we aimed to investigate whether the enhanced Stat phosphorylation due to combined cytokine treatment has an influence on downstream target genes of

the respective cytokines. Therefore, HepG2, Huh7 cells and PHHs were stimulated with different single cytokine doses and their combinations as depicted in the following chapters. Stimulation was performed for 6 or 12 h in the cell line while for PHHs the 24 h time point was added. After stimulation, the cells were lysed and RNA was isolated as described previously (3.2.5 RNA isolation from human cells) to perform SYBR® Green qPCR with GAPDH as the housekeeping gene (see 3.2.5.1 Reverse transcription and 3.2.5.2 SYBR® Green qRT-PCR). We assessed the fold change (f. c.) in target gene expression relative to an unstimulated control sample.

The evaluated genes are either described target genes of IL-6, IL-22 or both. Accordingly, cells were stimulated with the combination of IL-6 with IL-22, IL-6 or IL-22 with IFNα and IL-6 or IL-22 with IFNγ.

Bcl-2 is an antiapoptotic protein induced by IL-6 among other cytokines via Stat3 as its transcriptional activator. It is described to have a variety of functions for instance to support cell survival and protection from autophagy [3, 160].

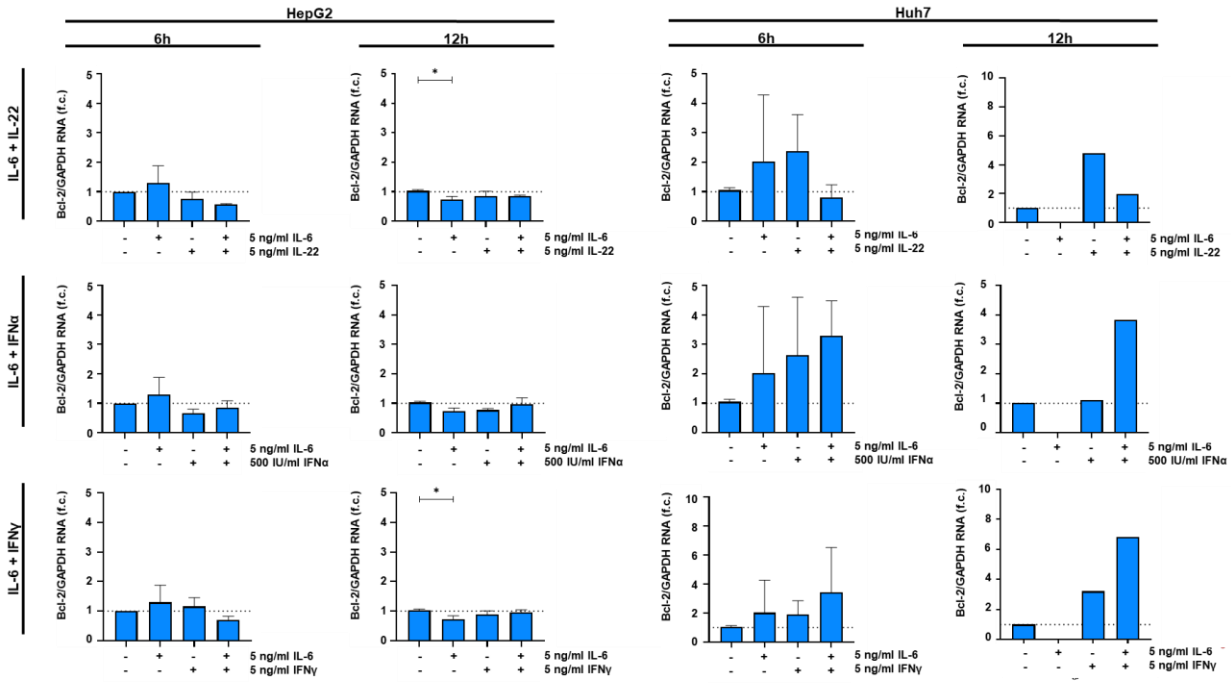

Figure 17: Quantification of mRNA levels of Bcl-2.
HepG2 cells (left side) and Huh7 cells (right side) were treated with 5 ng/ml of IL-6, IL-22 or a combination for 6 h or 12 h, respectively. The cells were treated with 5 ng/ml IL-6, 5 ng/ml IL-22, 500 IU/ml IFNα, 5 ng/ml IFNγ or a combination as indicated in the different rows. Total RNA was extracted and the changes in induction of Bcl-2 was assessed by SYBR Green qPCR with GAPDH as the housekeeping gene. Mean and standard deviation (SD) of three independent experiments are shown. Statistical significance was tested using One-way ANOVA or Kruskal-Wallis test. * = <0.05, **= <0.01, *** = <0.001 dependent on data distribution.

Bcl-2 RNA was barely shown to be induced by IL-6, IL-22, IFNα, IFNγ or a combination in the described settings as displayed in Figure 17. Furthermore, in many cases the RNA amount detected during PCR was at the detection limit.

IRF1 as the next investigated gene is known to be induced by IL-6 and IFNγ mainly via Stat1. As a tumour suppressor and a transcriptional regulator, it contributes to the processes of inhibiting tumour cell growth and support immune responses towards bacterial or viral infections. Furthermore, it influences cell proliferation and apoptosis [104, 150, 196]. The results are depicted in Figure 18.

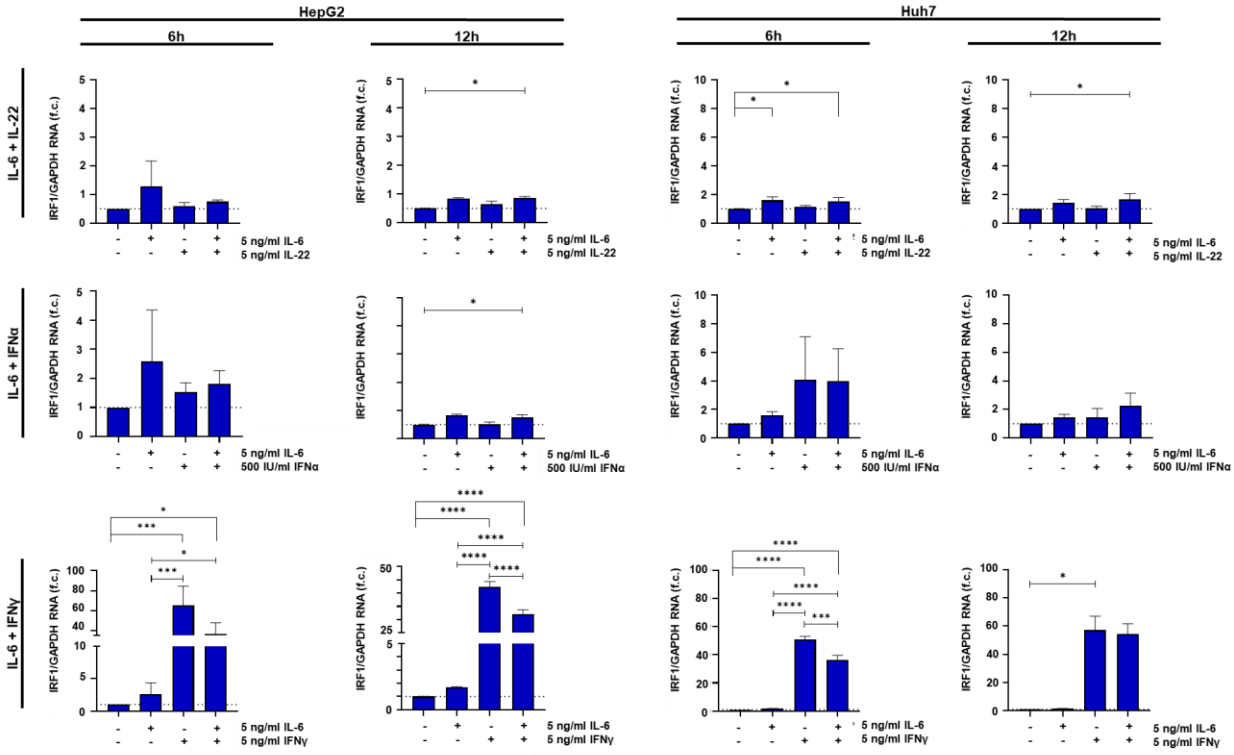

Figure 18: Quantification of mRNA levels of IRF1.
HepG2 cells (left side) and Huh7 cells (right side) were treated with 5 ng/ml of IL-6, IL-22 or a combination for 6 h or 12 h, respectively. The cells were treated with 5 ng/ml IL-6, 5 ng/ml IL-22, 500 IU/ml IFNα, 5 ng/ml IFNγ or a combination as indicated in the different rows. Total RNA was extracted and the changes in induction of IRF1 were assessed by SYBR Green qPCR with GAPDH as the housekeeping gene. Mean and standard deviation (SD) of three independent experiments are shown. Statistical significance was tested using One-way ANOVA or Kruskal-Wallis test. * = <0.05, **= <0.01, *** = <0.001 dependent on data distribution.

The single or combinatory treatment with IL-6, IL-22 or IFNα did induce few IRF1 RNA but there were no significant differences between single and combinatory stimulation conditions. However, while IL-6 showed only little IRF1 induction, IFNγ strongly induced this protein's RNA. The combination of both cytokines led to RNA induction that was significantly higher than the single IL-6 stimulation but also significantly lower than the single IFNγ treatment. Thus, these data suggest IL-6 is

weakening the effect of IFNγ in HepG2 cells after 12 h and in Huh7 cells earlier after 6 h of stimulation.

A comparable result can be found regarding TIMP-1 RNA induction upon IL-6 and IFNγ stimulation. TIMP-1 belongs to a protein family of inhibitors of matrix metalloproteinases (MMPs) which are involved in ECM degradation [16]. Additionally, it is described to be a biomarker in liver fibrosis patients [122, 138]. According to the results in Figure 19, stimulation of Huh7 cells with the different cytokines did not induce TIMP-1 RNA. However, in HepG2 cells treatment with IL-6 resulted in TIMP-1 induction. In the case of IL-6 and IFNγ co-stimulation the amount of induced TIMP-1 RNA was still induced compared to the untreated control but significantly reduced compared to the IL-6 single stimulation after 12 h.

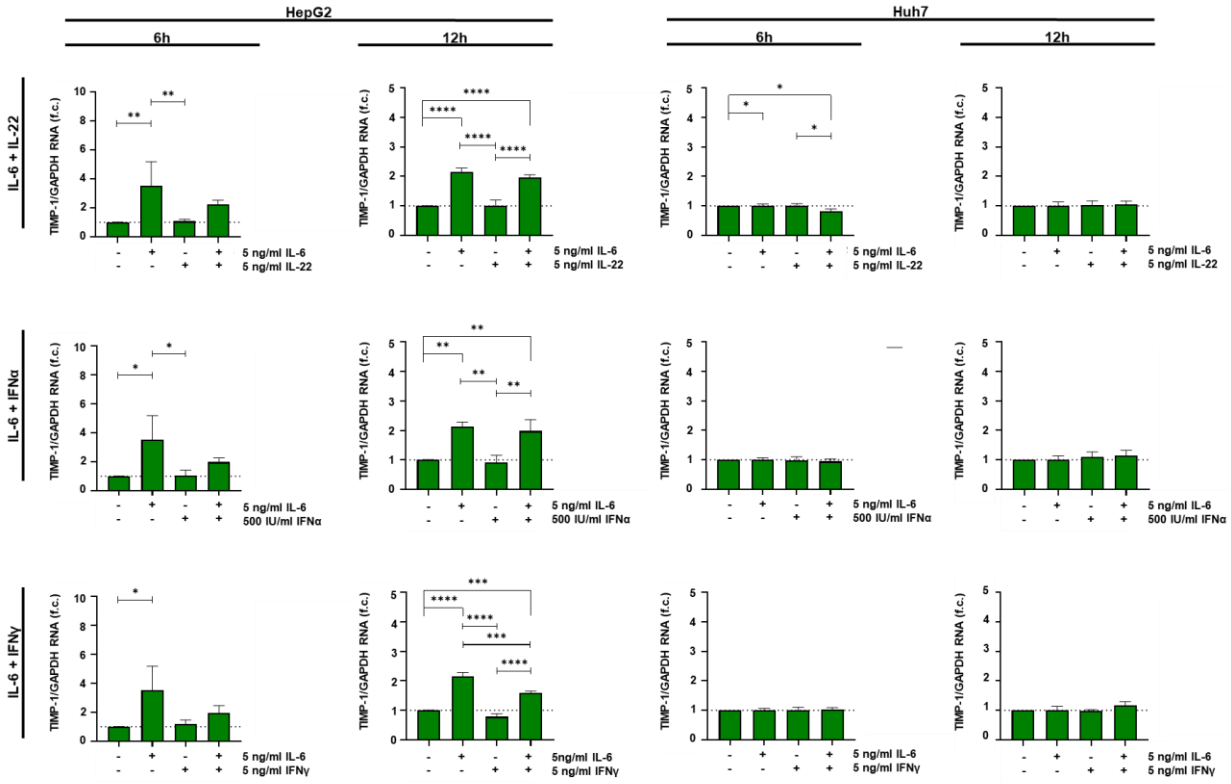

Figure 19: Quantification of mRNA levels of TIMP-1.
HepG2 cells (left side) and Huh7 cells (right side) were treated with 5 ng/ml of IL-6, IL-22 or a combination for 6 h or 12 h, respectively. The cells were treated with 5 ng/ml IL-6, 5 ng/ml IL-22, 500 IU/ml IFNα, 5 ng/ml IFNγ or a combination as indicated in the different rows. Total RNA was extracted and the changes in induction of TIMP-1 were assessed by SYBR Green qPCR with GAPDH as the housekeeping gene. Mean and standard deviation (SD) of three independent experiments are shown. Statistical significance was tested using One-way ANOVA or Kruskal-Wallis test. * = <0.05, **= <0.01, *** = <0.001 dependent on data distribution.

The proteinase inhibitor α1-antichymotrypsin is an acute phase protein induced in the liver upon IL-6 and IL-22 stimulation as part of an acute phase response towards infections [89, 123, 195, 203, 224]. We observed RNA induction upon IL-6 stimulation

in our two investigated cell lines (Figure 20). IL-22 stimulation and stimulation with IFNα, IFNγ or a combination among each other does not lead to a stronger induction of α1-antichymotrypsin RNA compared to the single cytokine treatment.

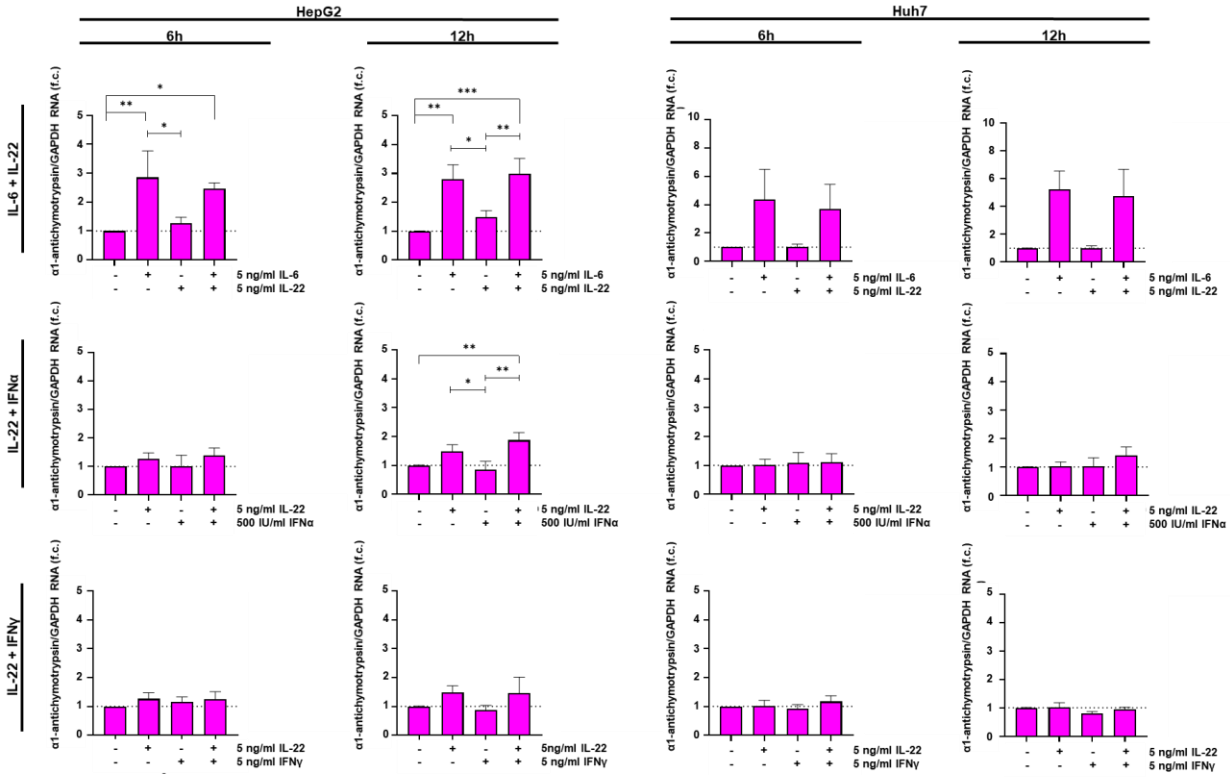

Figure 20: Quantification of mRNA levels of α1-antichymotrypsin.
HepG2 cells (left side) and Huh7 cells (right side) were treated with 5 ng/ml of IL-6, IL-22 or a combination for 6 h or 12 h, respectively. The cells were treated with 5 ng/ml IL-6, 5 ng/ml IL-22, 500 IU/ml IFNα, 5 ng/ml IFNγ or a combination as indicated in the different rows. Total RNA was extracted and the changes in induction of α1-antichymotrypsin were assessed by SYBR Green qPCR with GAPDH as the housekeeping gene. Mean and standard deviation (SD) of three independent experiments are shown. Statistical significance was tested using One-way ANOVA or Kruskal-Wallis test. * = <0.05, **= <0.01, *** = <0.001 dependent on data distribution.

The last investigated target gene of IL-6 and IL-22 induced in hepatocytes is the lipopolysaccharide-binding protein (LBP) [57, 185, 207, 226]. It is an acute phase protein and a suggested marker of infection. LBP binds to lipopolysaccharide (LPS) originating from gram-negative bacteria where it is a glycolipid in the outer membrane. Upon binding, LBP facilitates binding to CD14 receptors on monocyte- and macrophage-like cells which in turn initiates cytokine production [76]. The results from the various single or combinatory cytokine stimulations are shown in Figure 21. In general, Huh7 cells were less responsive to IL-6 or any other cytokine stimulation compared to HepG2 cells. In HepG2 cells especially after 12 h of cytokine stimulation, we observed an increase in LBP RNA when cells were stimulated with

IL-6 and IL-22 simultaneously compared to the single cytokine stimulations. This is also true for the IL-6 and IFNα combination.

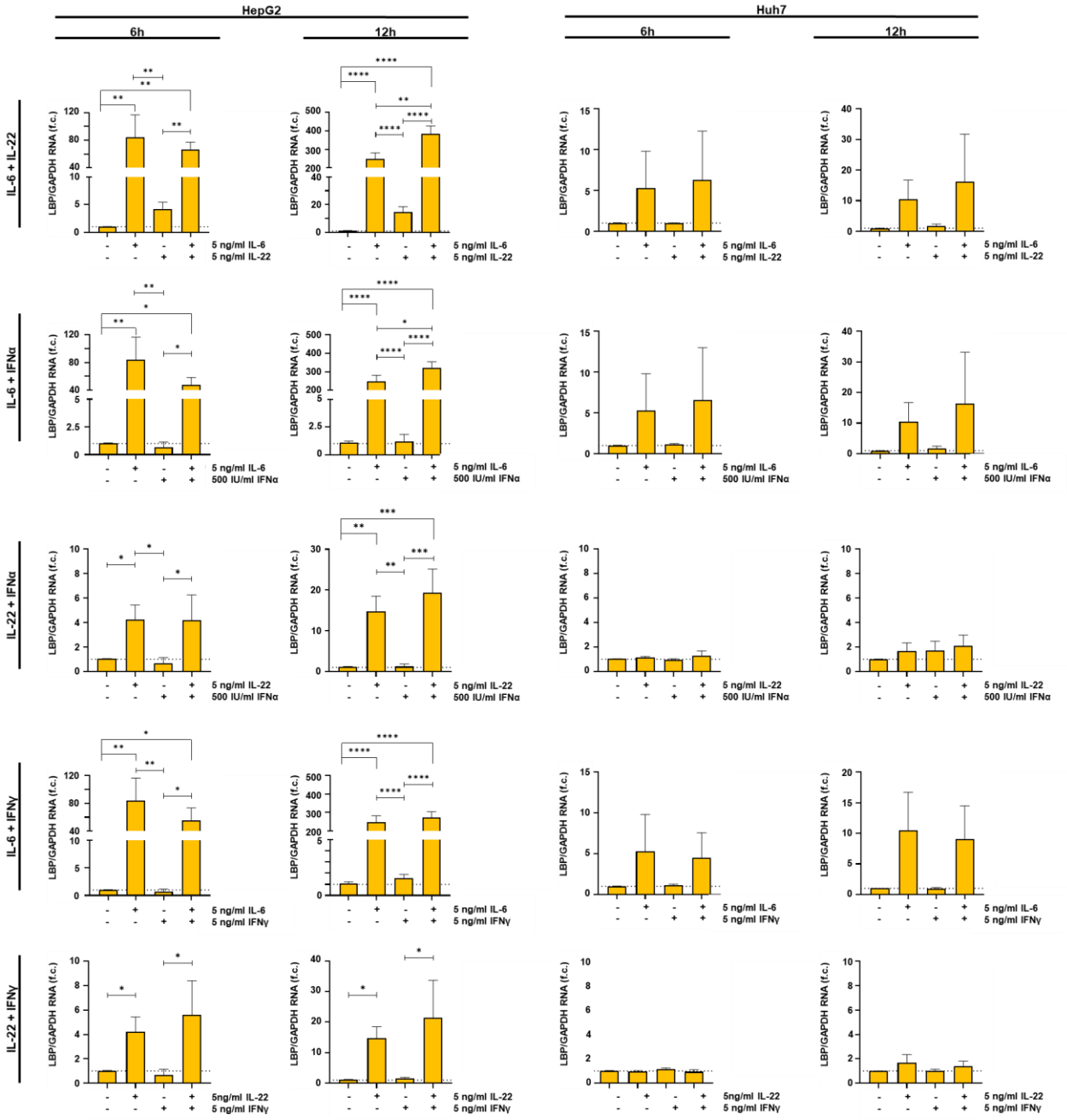

Figure 21: Quantification of mRNA levels of LBP.
HepG2 cells (left side) and Huh7 cells (right side) were treated with 5 ng/ml of IL-6, IL-22 or a combination for 6 h or 12 h, respectively. The cells were treated with 5 ng/ml IL-6, 5 ng/ml IL-22, 500 IU/ml IFNα, 5 ng/ml IFNγ or a combination as indicated in the different rows. Total RNA was extracted and the changes in induction of LBP were assessed by SYBR Green qPCR with GAPDH as the housekeeping gene. Mean and standard deviation (SD) of three independent experiments are shown. Statistical significance was tested using One-way ANOVA or Kruskal-Wallis test. * = <0.05, **= <0.01, *** = <0.001 dependent on data distribution.

Overall, IL-6 and IFNγ might use the same signalling pathway but our data suggest that both do not have synergistic effects on TIMP-1 and IRF1 as a combined treatment led to a decreased RNA induction compared with the single IFNγ

stimulation. However, IL-6 combined with IL-22 or IFNα show mutual enhancement of LBP RNA expression in HepG2 cells after 12 h of stimulation.

These data suggest that the combination of IL-6 and IL-22 supports anti-microbial activity.

4.3.1 Target gene expression upon combined cytokine stimulation in PHHs

Based on the results with the HepG2 cell line described earlier in this chapter, where an enhanced LBP RNA induction was observed due to a combined cytokine treatment with IL-6 and IL-22, primary human hepatocytes were used to verify these findings. PHHs were stimulated with IL-6, IL-22 or a combination for 6 h, 12 h and 24 h. After stimulation, the cells were lysed and RNA was isolated as described previously (3.2.5 RNA isolation from human cells) to perform quantitative real time PCR (see 3.2.5.1 Reverse transcription and 3.2.5.2 SYBR® Green qRT-PCR). We assessed the fold change (f. c.) in target gene expression relative to an untreated control sample. The results are shown in Figure 22.

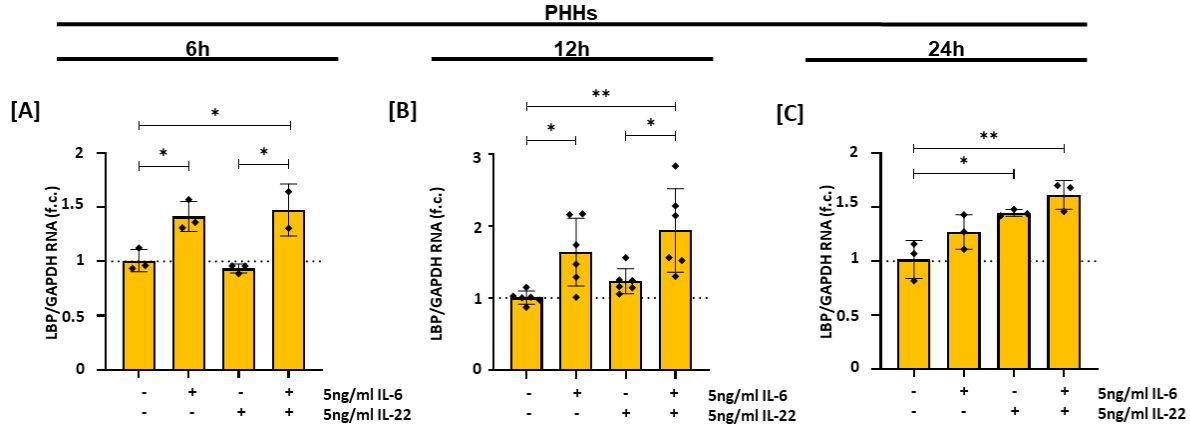

Figure 22: Quantification of mRNA levels of LBP in PHHs.
PHHs were treated with 5 ng/ml of IL-6, IL-22 or a combination for 6 h [A] or 12 h [B] or 24 h [C]. Total RNA was extracted and the changes in induction of several target genes were assessed by SYBR Green qPCR with GAPDH as the housekeeping gene. Mean and standard deviation (SD) of one to two independent experiments are shown. Statistical significance was tested using One-way ANOVA or Kruskal-Wallis test. p-values * = <0.05, **= <0.01, *** = <0.001 dependent on data distribution.

In contrast to the results in HepG2 cells, no significant differences between a single IL-6 stimulation and combinatory stimulation with IL-22 could be detected. However, there is the tendency after 6 h and 12 h that a cytokine combination led to an enhanced LBP RNA induction.

4.4 Influence of repeated cytokine treatment of hepatocytes

Based on the results that a cytokine combination can enhance the phosphorylation signal it raised the question whether a repeated treatment with the same cytokine could also have this effect. Therefore, IL-6 and IL-22 were selected for the next experiments. Huh7 cells, HepG2 cells and PHHs were treated repeatedly with IL-6 or IL-22 for up to 24 h. The cytokines were applied in the beginning and then again after 3 h, 6 h, 12 h and 24 h. 30 min after the last application at every time point, cells were lysed, and the phosphorylated proteins were detected using immunoblot analysis. The results are shown in Figure 23. At the single time points of cell lysis, the treated samples were always compared to an untreated sample from the same time point.

Figure 23 shows clearly that neither in HepG2 cells [A] nor in Huh7 cells [B] a repeated cytokine treatment with 5 ng/ml IL-6 or IL-22 led to an increase in the amount of phosphorylated Stat1 or Stat3. Rather, regarding pStat1 levels, there is an initial Stat1 phosphorylation that cannot be maintained over time or reinduced by an iterated application of the cytokine. The treated cells remained unresponsive to the stimulus. This is already the case after 3 h and 30 min of stimulation time. For Stat3, a certain level of phosphorylation can be maintained throughout repeated treatments over 24 hours, but the signal was strongly reduced and could not return to the initial levels after 30 min of stimulation. The phenomenon of signalling becoming refractory in cells within hours after stimulation was described elsewhere for IFNα signalling in the context of HBV and HCV immune therapy and termed refractoriness [70, 176].

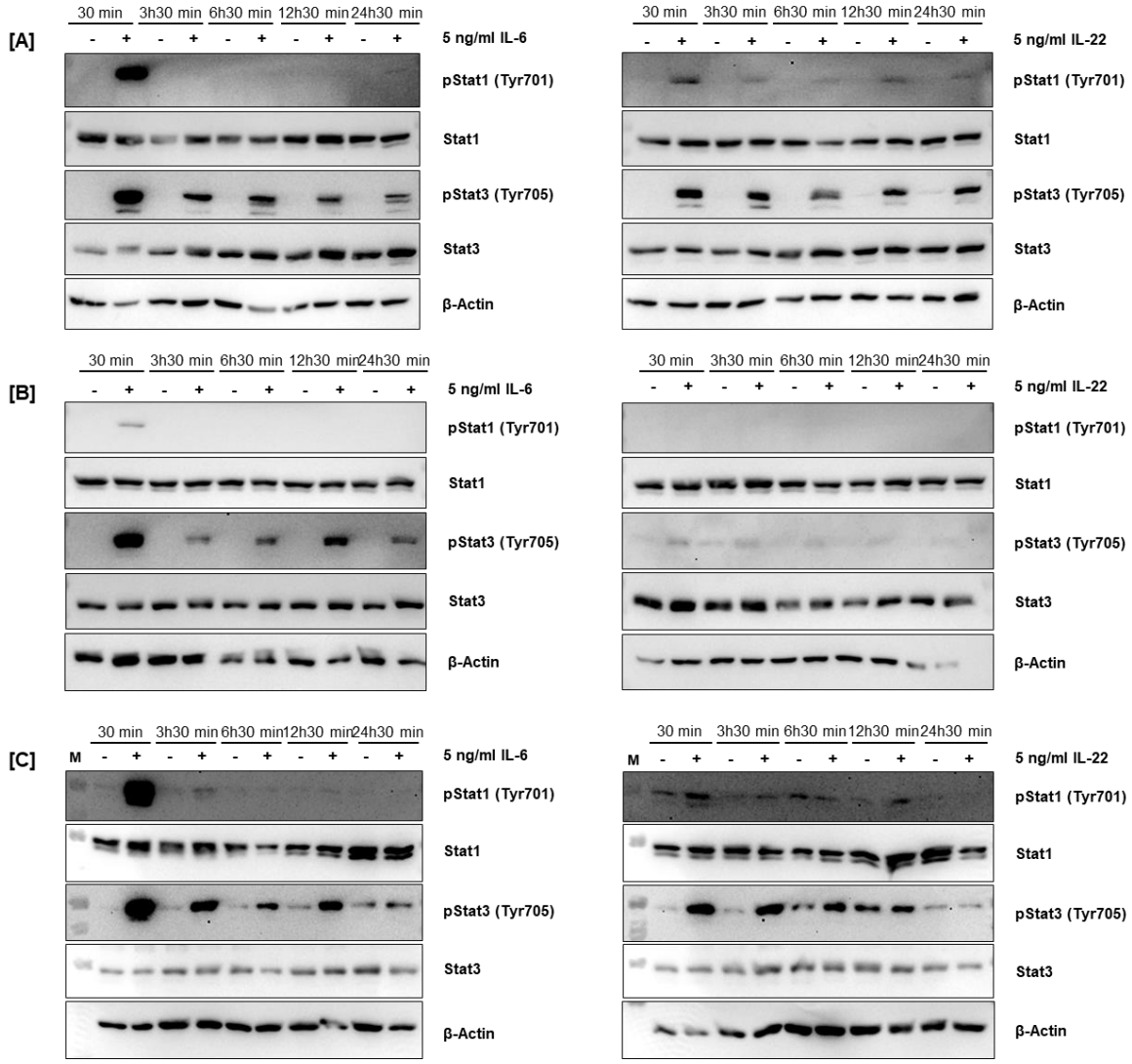

Figure 23: Cellular response to repeated cytokine treatment with IL-6 and IL-22.
HepG2 cells [A] and Huh7 cells [B] were treated with 5 ng/ml IL-6 (left panel) or IL-22 (right panel) for the indicated total durations (cytokines were provided a t=0 h, t=3 h, t=6 h, t=12 h and t=24 h). One out of three independent experiments is shown as demonstration. [C] PHHs were treated with several doses of 5 ng/ml IL-6 (left panel) or IL-22 (right panel) for the displayed total durations (Cytokines were provided a t=0 h, t=3 h, t=6 h, t=12 h and t=24 h), n=3. Phosphorylation of Stat1 at Tyr701 was assessed via Immunoblotting with β-Actin as reference. One experiment is shown as demonstration.

The phenomenon of refractoriness observed in the cell lines was mirrored in the primary hepatocytes Figure 23 [C]. Stat1 and Stat3 phosphorylation could not be reinduced within 24 hours compared to the initial level after 30 min.

4.4.1 The cellular response to repeated doses of stimulation is cytokine specific

Besides IL-6 and IL-22, IFNγ did also show an influence on cellular gene expression when used in combination with IL-6. Therefore, it was investigated how IFNγ influences Stat phosphorylation when it is repeatedly applied to hepatocarcinoma cell

lines (Figure 24). Once again, we could observe decreased Stat1 phosphorylation over time and after repeated cytokine treatment but in contrast to IL-6 and IL-22, this could only be detected in HepG2 cells (Figure 24 [A]) and to a smaller extend in Huh7 cells (Figure 24 [B]). Further, the unresponsiveness of the cells to the cytokine treatment seems to recover after 6 h compared to IL-6 and IL-22 treatment where the unresponsiveness was persistent throughout the experiment (Figure 23). This findings for type II interferons are in contrast with earlier published results for type I and type III interferons which showed refractory signalling upon repeated stimulation [70].

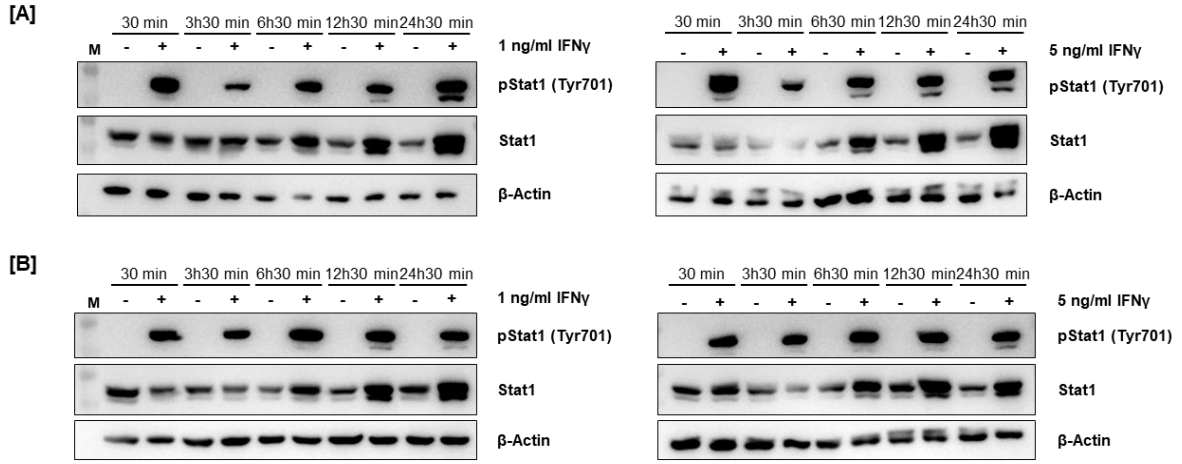

Figure 24: Cellular response to repeated cytokine treatment with IFNγ.
HepG2 cells [A] and Huh7 cells [B] were treated with 1 ng/ml of IFNγ (left panel) or 5 ng/ml of IFNγ (right panel) for the indicated total durations (cytokines were provided a t=0 h, t=3 h, t=6h, t=12 h and t=24 h). Phosphorylation of Stat1 at Tyr701 was assessed via Immunoblotting with β-Actin as reference. One experiment is shown as demonstration.

This suggests that unresponsiveness of cells concerning Stat phosphorylation due to repeated cytokine administration is dependent on the respective cytokine.

4.4.2 Refractoriness of cell lines to repeated cytokine administration on a functional level

The next step was to investigate whether the unresponsiveness of HepG2 cells to repeated IL-6 and IL-22 administration can also be determined on a functional level. Therefore, HepG2 cells were treated with the IL-6 or IL-22 at the time points 0 h, 3 h, 6 h and 12 h followed by a final 12 h incubation time which resulted in total stimulation times from 12 h to 24 h. Afterwards, the cells were lysed and the amount of LBP RNA was quantified using SYBR® Green qPCR with GAPDH as the housekeeping gene (see 3.2.5.1 Reverse transcription and 3.2.5.2 SYBR® Green

qRT-PCR). We assessed the fold change (f. c.) in LBP RNA expression relative to an unstimulated control sample.

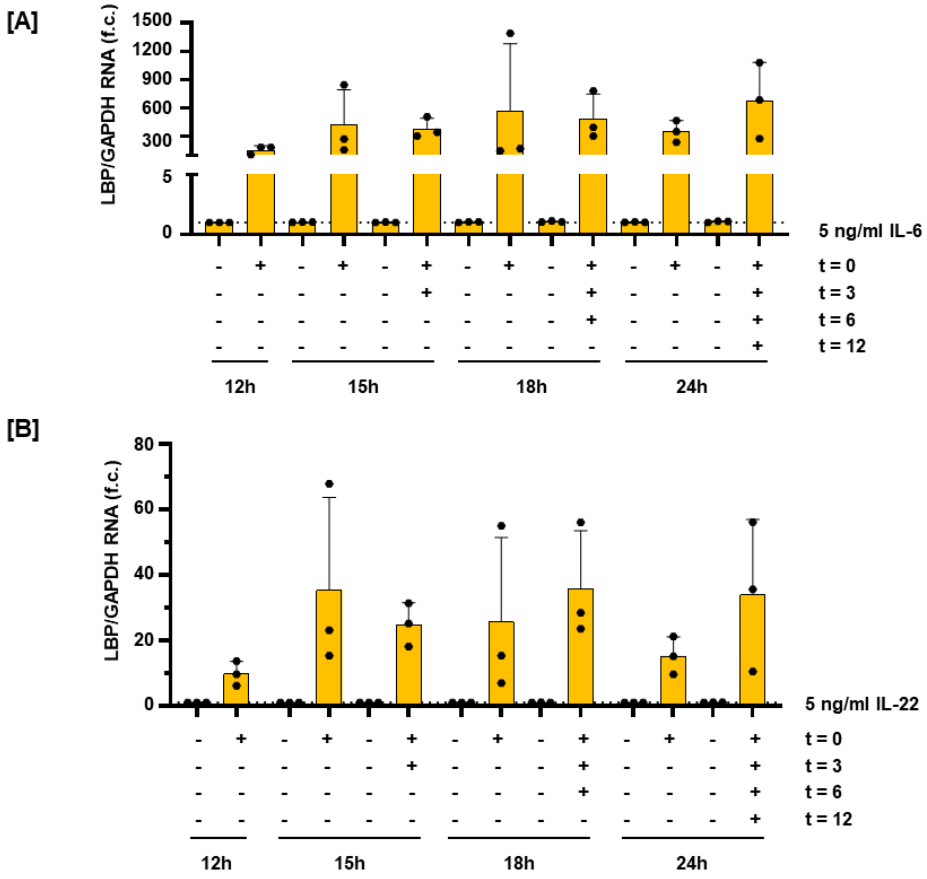

Figure 25: Repeated cytokine treatment does not enhance LBP-RNA levels compared to single cytokine stimulations within 24 h.
HepG2 cells were treated with 5 ng/ml of IL-6 [A] or IL-22 [B]. Cytokines were provided a t=0 h, t=3 h, t=6 h and t=12 h. 12 h after the last cytokine administration cells were lysed. Total RNA was extracted and the changes in induction of LBP was assessed by SYBR Green qPCR with GAPDH as the housekeeping gene. Mean and standard deviation (SD) of three independent experiments are shown. Statistical significance was tested using One-way ANOVA or Kruskal-Wallis test. p-values * = <0.05, **= <0.01, *** = <0.001.

According to the results depicted in Figure 25, there are no significant differences between a single cytokine stimulation for 12 h and single or repeated cytokine administrations for longer time periods up to 24 h of total stimulation time. This finding is the same for IL-6 (Figure 25 [A]) and IL-22 (Figure 25 [B]) treatment. Additionally, a direct comparison between a single cytokine stimulation and a repeated cytokine stimulation for the same total stimulation time did not lead to significantly increased LBP RNA levels. Thus, a repeated cytokine treatment did not enhance LBP RNA levels compared to single cytokine stimulations within 24 h. However, LBP RNA are maintained over 24 h even after a single cytokine stimulation

although the amount of phosphorylated Stat molecules which work as transcriptional activators decrease over time as seen in Figure 23.

4.5 Mechanistic approach to examine cellular refractoriness to cytokine stimulation

The previous chapters showed that a repeated cytokine administration of the same cytokine was not able to enhance the Stat phosphorylation. The question arose whether another cytokine which induces the same Stat phosphorylation is able to do so and therefore circumvent the unresponsiveness of the treated liver cells.

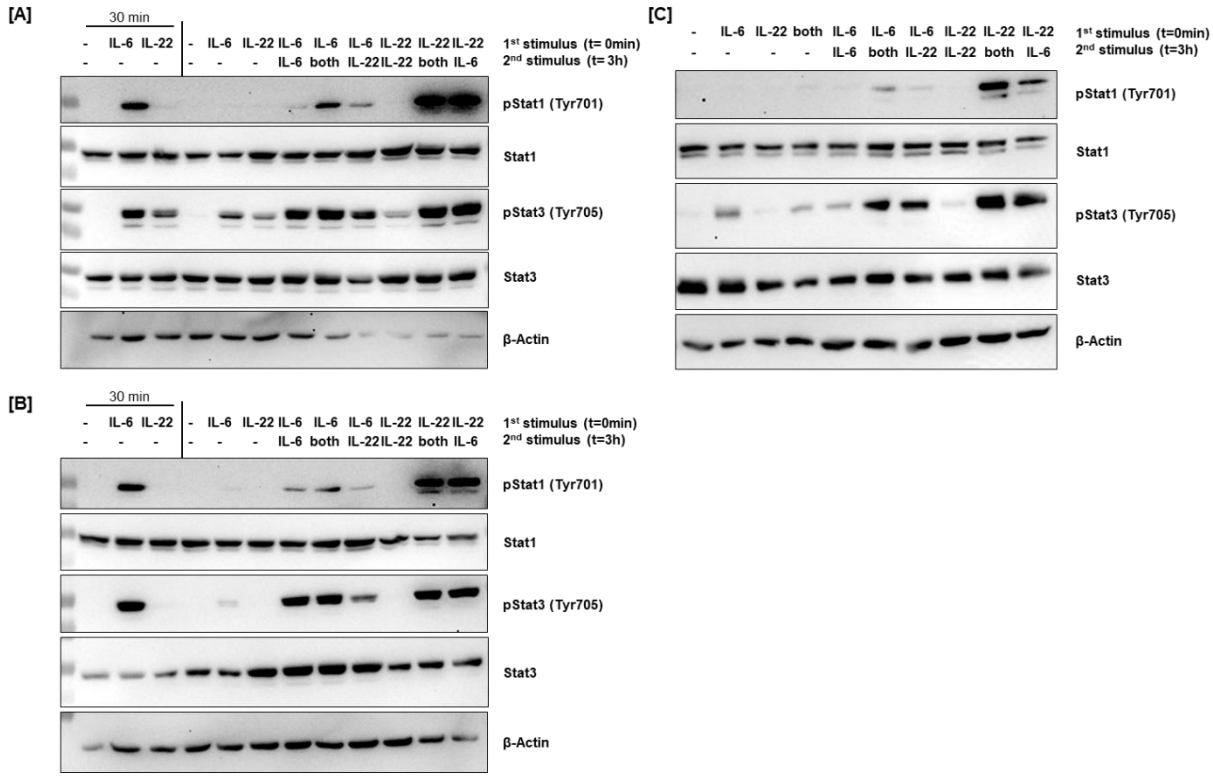

Figure 26: Alternate stimulation with IL-6 and IL-22 circumvents unresponsiveness to repeated single cytokine administration.
HepG2 cells [A] and Huh7 cells [B] were stimulated with 5 ng/ml IL-6 and/or 5 ng/ml IL-22 as indicated at t=0 h and t=3 h for the displayed total duration of 3 h 30 min, One out of three experiments is shown as demonstration. PHHs [C] were treated with several doses of 5 ng/ml IL-6 and/or IL-22 at t=0 h and t=3 h for the displayed total duration of 3 h 30 min. One experiment is shown as demonstration. Phosphorylation of Stat1 at Tyr701 and of Stat3 at Tyr705 was assessed via Immunoblotting with β-Actin as reference. One experiment is shown as demonstration. M = Marker lane.

Consequently, as shown in Figure 26, we stimulated HepG2 cells (Figure 26 [A]), Huh7 cells (Figure 26 [B]) and PHHs (Figure 26 [C]) with IL-6 and IL-22 for 30 min or 3 h and 30 min. It can be seen for both cell lines that after 30 min of stimulation, IL-6 and IL-22 induce phosphorylation of Stat1 and Stat3. A single cytokine stimulation for 3 h and 30 min led to a weaker signal that was in part barely detectable by

immunoblot analysis which is in line with the previous results. A second stimulation at the 3 h timepoint with the same cytokine that was used initially showed a slightly stronger phosphorylation. But when stimulated the other cytokine that was not used initially the Stat phosphorylation was even stronger, especially visible for pStat1. These findings were also figured out in primary human hepatocytes (Figure 26 [C]).

The same experimental setup was also performed using IL-6 and IFNγ as a pair for hepatocarcinoma cell line stimulation (Figure 27). Both cytokines induce Stat1 phosphorylation. Here again, especially regarding HepG2 cells (Figure 27 [A]), when two different cytokines are used for treatment over 3 h and 30 min the phosphorylation signal is stronger compared to stimulations where the same cytokine is used at both stimulation time points.

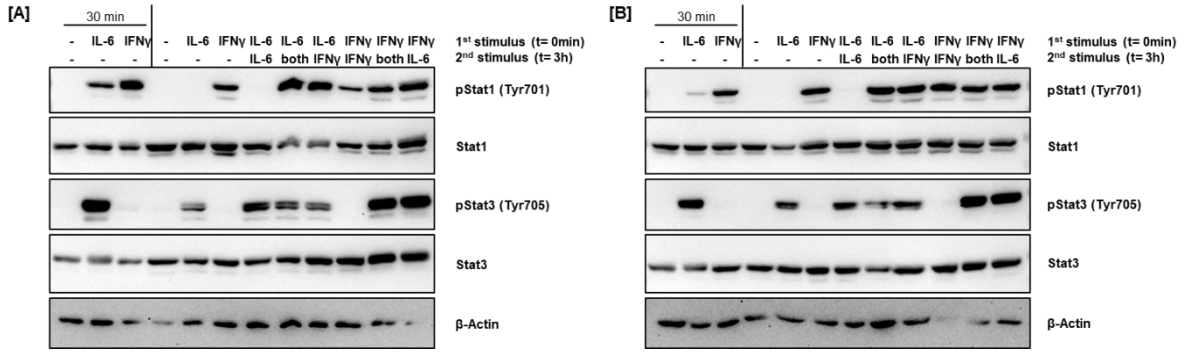

Figure 27: Alternate stimulation with IL-6 and IFNγ circumvents unresponsiveness to repeated single cytokine administration.
HepG2 cells [A] and Huh7 cells [B] were stimulated with 5 ng/ml IL-6 and/or 5 ng/ml IFNγ as indicated at t=0 h and t=3 h for the displayed total duration of 3 h 30 min. Phosphorylation of Stat1 at Tyr701 and of Stat3 at Tyr705 was assessed via Immunoblotting with β-Actin as reference. One out of three experiments is shown as demonstration.

So overall it can be stated that cytokine refractoriness is not based on a general unresponsiveness of Stat phosphorylation itself as it is still inducible by stimulation with another cytokine that used the same Stat signalling molecules.

4.6 Cytokines influence on cell viability

As for instance IL-6 and IL-22 are linked to cellular regeneration and proliferation, we performed a WST-1 viability staining. Therefore, and as the cytokines were used in previous experiments for stimulation, HepG2 and Huh7 cells were stimulated with IL-6, IL-22 and IFNγ either with single doses or in combinations as indicated in Figure 28 for 6 h and 24 h, respectively. WST-1 reagent was added 2 h prior to the end of

stimulation and viability according to the absorbance at 440 nm was studied as shown in Figure 28. Stimulated cells were compared to untreated control cells.

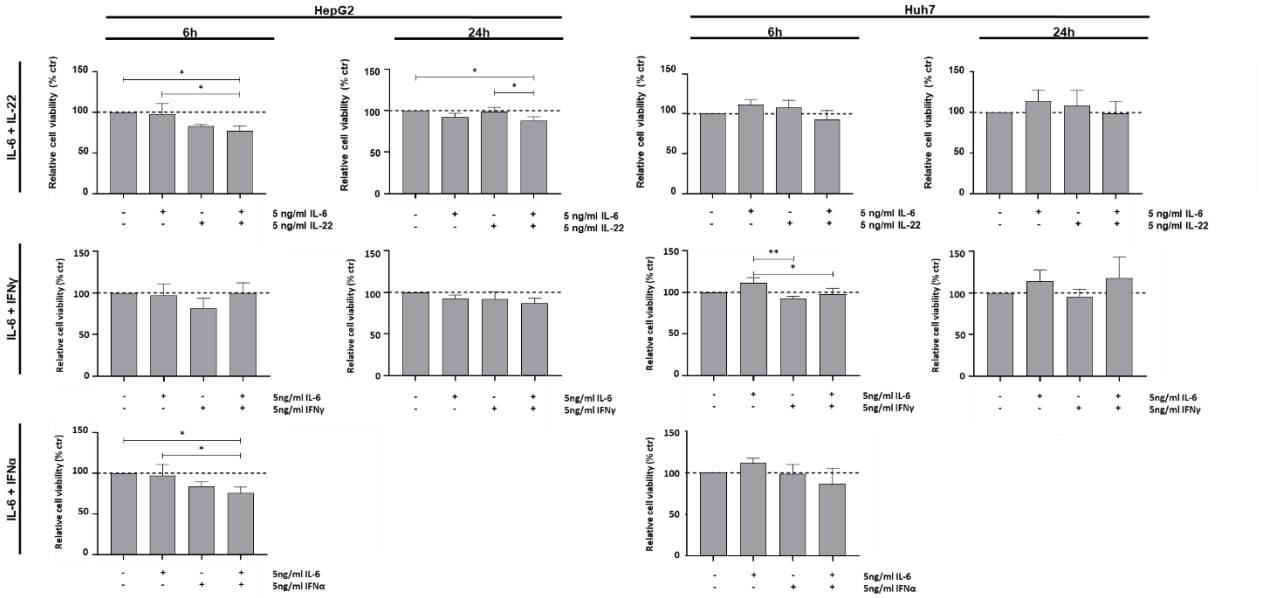

Figure 28 Hepatocarcinoma cell viability after treatment with IL-6, IL-22, IFNα, IFNγ or a combination. HepG2 cells (left panel) and Huh7 cells (right panel) were treated with 5 ng/ml IL-6, IL-22, IFNα, IFNγ or a combination for 6 h or 24 h, as indicated. 2 directly after stimulation. Mean and standard deviation (SD) of three independent experiments are shown. Statistical significance was tested using One-way ANOVA or Kruskal-Wallis test. p-values * = <0.05, **= <0.01, *** = <0.001.

The absorbance was slightly decreased in the 6 h HepG2 cells treated with IL-6 and IL-22 or IL-6 and IFNα. This influence seems to recover regarding the 24 h timepoint. Other treatments did not influence cellular viability in our experiments in a significant way.

4.7 HepG2 cells responsiveness to cytokine stimulation after cytokine withdrawal

So far, in all experiments that described unresponsiveness of cells to cytokine stimulation with IL-6 and IL-22, the cytokines were not removed but still present when further doses were added. Next, we wanted to assess whether Stat phosphorylation can be reinduced faster in HepG2 cells when the initial cytokine dose is removed for a certain time prior to the next stimulation. To this end, HepG2 cells were stimulated with IL-6 (Figure 29 [A]) or IL-22 (Figure 29 [B]) for initial 30 min. Hereafter, the medium containing the cytokine was removed and new medium was added to the cells for further incubation between 1 h and 6 h. This was followed by a second 30 min stimulation with the same cytokine as used initially. By the end of stimulation,

cells were lysed and phosphorylation of Stat1 and Stat3 was investigated using Western blot analysis.

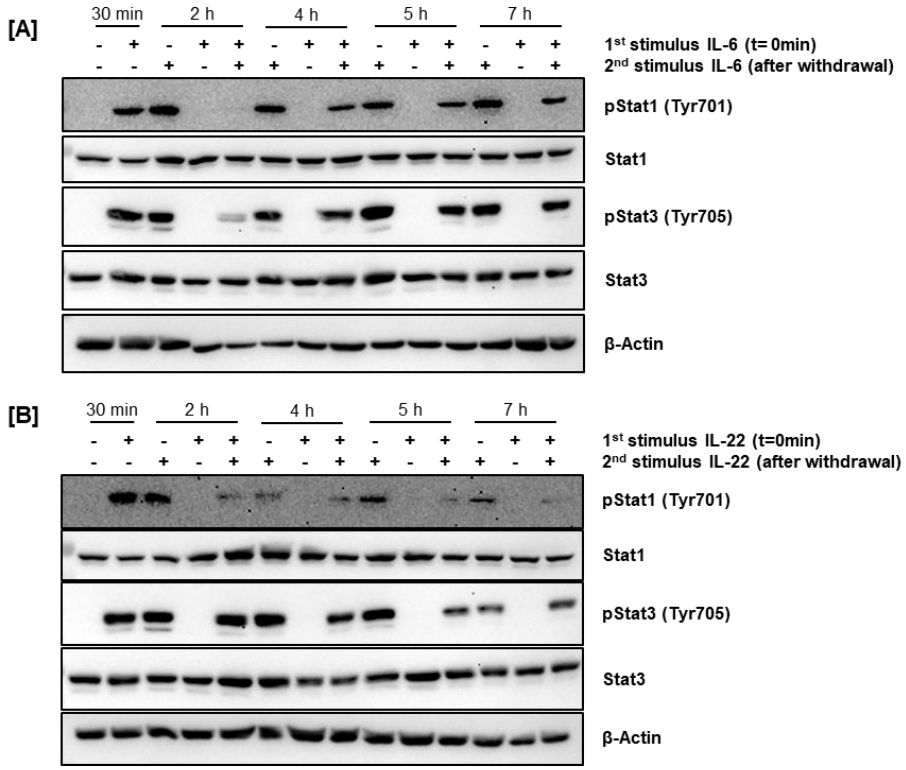

Figure 29: The influence of cytokine stimulation after withdrawal on HepG2 cells.
HepG2 cells were stimulated with 5 ng/ml IL-6 [A] and/or 5 ng/ml IL-22 [B] for the initial and last 30 min of the displayed total duration of 30 min/2 h/4 h/5 h and 7 h. Phosphorylation of Stat1 at Tyr701 and of Stat3 at Tyr705 was assessed via Immunoblotting with β-Actin as reference. One experiment is shown as demonstration.

Both cell lines show Stat phosphorylation after 30 min but not after 2 h or longer single cytokine stimulation which is in line with the results presented earlier in this project. It is noteworthy that after a cytokine withdrawal for one hour the Stat1 phosphorylation for both cytokine treatments was either absent or weak compared to the 30 min signal. The pStat3 signal of the double stimulated samples at this time point was barely detectable after IL-6 stimulation cells but strong after IL-22 stimulation. After a cytokine withdrawal of 3 h, pStat1 was reinducable by IL-6 stimulation which could not be observed earlier when the second cytokine dose was added without previous medium exchange (see 4.4 Influence of repeated cytokine treatment of hepatocytes) or with a cytokine withdrawal of 1 h. Additionally, the pStat3 signal after a 3 h cytokine withdrawal was comparable to the initial signal after 30 min. Regarding treatment with IL-22, a 3 h removal of the initial cytokine dose was sufficient to induce a Stat1 and Stat3 phosphorylation that is comparable to the

30 min time point. These results suggest that the absence of the respective cytokine might reduce cellular refractory behaviour.

4.8 The influence of IL-6 and IFNγ on peripheral blood mononuclear cells

After intensive studying on the influence of cytokines on hepatocarcinoma cell lines and primary human hepatocytes, we asked the question whether also other cells are affected by the cytokines' influence such as blood immune cells; they might also be directly affected by elevated cytokine levels in LC and ACLF patients. Furthermore, future immune therapeutic approaches will have influence on them so studying their behaviour towards single and repeated cytokine stimulation will give valuable insights. To this end, PBMCs from healthy donors and patients with compensated LC, AD and ACLF were collected as described in chapter 3.2.7 Isolation of human peripheral blood mononuclear cells (PBMCs) from blood samples to investigate their immune biology. Isolated PBMCs were stored at -80 °C and thawed for this experiment. After seeding, the PBMCs were directly stimulated with either IL-6 or IFNγ for 30 min. In a parallel setting, PBMCs were stimulated with IL-6 or IFNγ for 3 h and directly afterwards again for additional 30 min with either the same cytokine that was initially used or the other. This approach is comparable to the one in chapter 4.5 Mechanistic approach to examine cellular refractoriness to cytokine stimulation to evaluate the PBMC's potential to be restimulated. After stimulation, PBMCs were harvested and stained for multicolour (phospho-) flowcytometric analysis as described in the method section 3.2.7.2 Staining for flow cytometric analysis. In the end, $CD14^+$ monocytes and lymphocyte populations, namely $CD3^+CD4^+$, $CD3^+CD4^+CD45RA^+$, $CD3^+CD8^+$ and $CD3^+CD8^+CD45RA^+$ T cells, were investigated further. The $CD45RA^+$ populations comprise naïve and effector T cells and provide further inside into the entire $CD3^+CD4^+$ or $CD3^+CD8^+$ population [129]. Stained target structures besides the surface markers were the two IL-6 receptor chains, namely CD126 (IL-6Rα) and CD130 (gp130) as well as intracellular located unphosphorylated and phosphorylated Stat3 proteins, the latter indicating a successful signalling response to the cytokine stimulation. In addition, differences between healthy donor PBMCs and patient PBMCs were assessed. IL-22 could not be used in this experimental setup as immune cells do usually not express the IL-22R1 receptor subunit [149, 223].

4.8.1 Patient characteristics

A total of 45 patients were included in the present analyses. Sample collection and exclusion criteria are summarized in the method section (3.2.8 Patients). The selection criteria were previously defined referring to the criteria of the EASL-CLIF consortium [144]. Of the selected patients, 15 each had compensated LC, acute decompensation or ACLF. While compensated patients differed in their etiology of liver disease, acute decompensated patients and ACLF patients tend to share alcoholic etiology with 40% and 73%, respectively. As expected, patients with AD and ACLF differ from compensated patients as they have significantly higher serum levels of CRP, IL-6 and bilirubin and lower levels of albumin. Characteristics of all included patients are displayed in Table 20.

Table 20: Characteristics and laboratory results of included patients.

				p-value		
	Compensated (n=15)	**Acute decompensated (n=15)**	**ACLF (n=15)**	**Compensated vs AD**	**Compensated vs ACLF**	**AD vs ACLF**
Age (years), mean (SD)	49.87 (16.16)	54.20 (10.70)	53.47 (14.89)	n.s.	n.s.	n.s.
Gender male/female, n (%)	6/9 (40/60)	11/4 (73.3/26.7)	8/7 (53.3/46.7)	n.s.	n.s.	n.s.
Etiology of liver disease, n						
viral	0	2	1	n.s.	n.s.	n.s.
NASH	2	2	1	n.s.	n.s.	n.s.
alcoholic	2	6	11	n.s.	0.0009	n.s.
cholestatic	3	2	1	n.s.	n.s.	n.s.
other	5	3	1	n.s.	n.s.	n.s.
Leucocytes (/nl), mean (SD)	5.9 (1.7)	5.9 (2.9)	7.2 (3.5)	n.s.	n.s.	n.s.
Hemoglobin (g/dl), mean (SD)	12.1 (2.3)	10.1 (2.4)	8.0 (1.2)	n.s.	<0.0001	n.s.
Thrombocytes (/nl), mean (SD)	140.8 (77.8)	109.3 (64.5)	88.9 (55.2)	n.s.	n.s.	n.s.
CRP (mg/dl), mean (SD)	0.8 (1.0)	2.5 (2.4)	3.8 (2.7)	n.s.	0.0004	n.s.
Bilirubin (mg/dl), mean (SD)	1.0 (0.4)	3.5 (2.1)	11.1 (10.6)	0.0037	<0.0001	n.s.
Albumin (g/dl), mean (SD)	4.3 (0.3)	3.1 (0.6)	3.3 (0.9)	<0.0001	0.004	n.s.
IL-6 (pg/ml), mean (SD)	1.0 (3.8)	37.9 (57.2)	72.3 (52.9)	0.0065	<0.0001	n.s.
CLIF OF Score, mean (SD)	7.1 (1.8)	6.9 (1.2)	9.7 (1.5)	n.s.	0.0004	0.0007
CLIF C AD /ACLF Score, mean (SD)	32.8 (8.3)	35.5 (7.1)	46.8 (10.4)	n.s.	0.0003	0.0035
MELD, mean (SD)	7.9 (2.0)	16.8 (4.3)	26.6 (9.8)	0.0005	<0.0001	n.s.
Child Pugh, mean (SD)	5.2 (0.4)	8.7 (1.3)	10.4 (1.3)	0.0004	<0.0001	n.s.

4.8.2 Basal expression level of pStat3, Stat3, CD126 and CD130 in PBMCs

First, the basal expression levels of phosphorylated and unphosphorylated Stat3, CD126 and CD130 were investigated in unstimulated $CD3^+CD4^+$, $CD3^+CD4^+CD45RA^+$, $CD3^+CD8^+$ and $CD3^+CD8^+CD45RA^+$ T cells and $CD14^+$ monocytes (Figure 30, Figure 31, Figure 32).

We found similar levels of basal total Stat3, phosphorylated Stat3, CD126 and CD130 in all investigated cell types with only little exceptions.

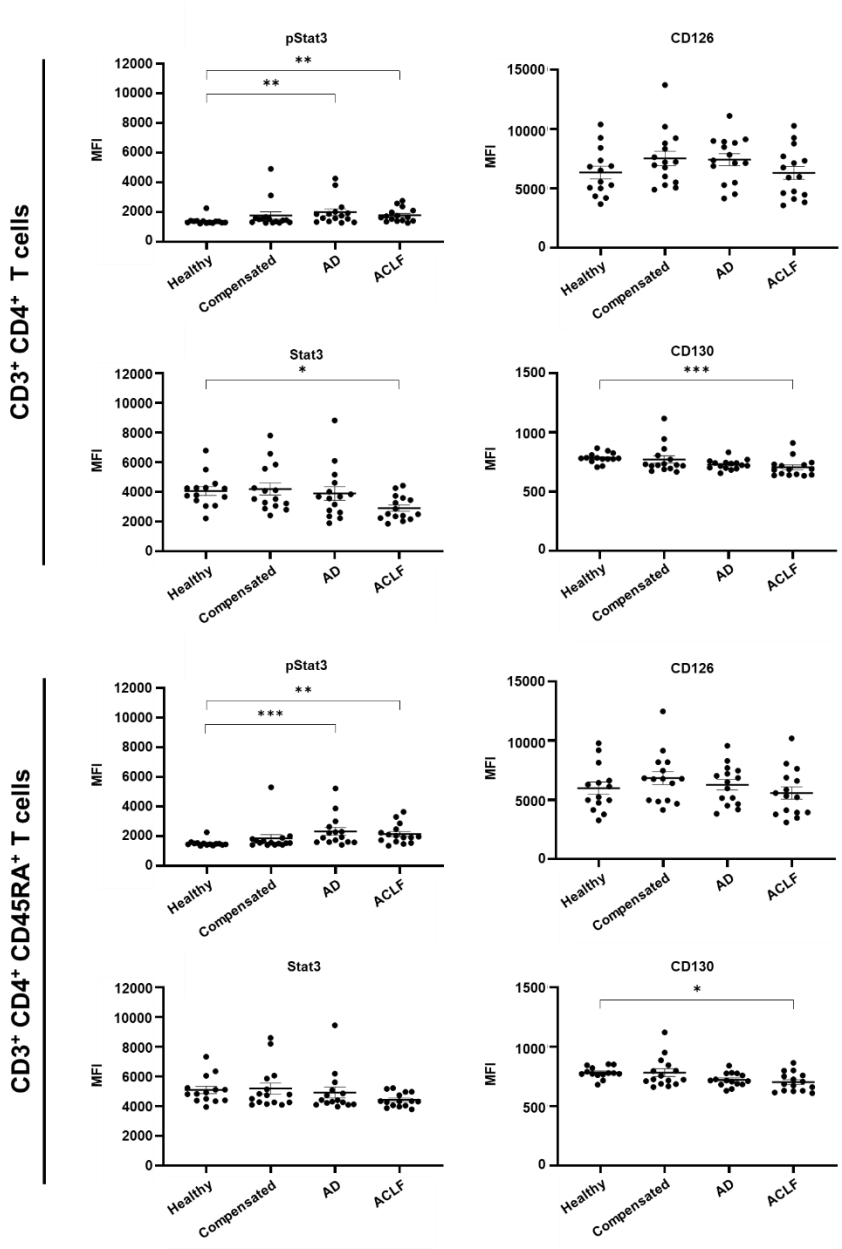

Figure 30: Basal expression levels of (p)Stat3, CD126, CD130 in unstimulated $CD3^+CD4^+$ and $CD3^+CD4^+CD45RA^+$ T cells.
The expression levels of intracellular Stat3, phosphorylated Stat3 and surface CD126 and CD130 in unstimulated $CD3^+CD4^+$ (upper panel) and $CD3^+CD4^+CD45RA^+$ (lower panel) T cells from healthy donors and patients with different stages of liver disease (n=15 in each group) were determined by flow cytometry. Anti-pStat3(pY705) antibody was used to determine phosphorylation. Mean and standard error of the mean (SEM) are shown. Statistical significance was tested using One-way ANOVA or Kruskal-Wallis test. p-values * = <0.05, **= <0.01, *** = <0.001 dependent on data distribution. MFI = median fluorescence intensity.

For instance, we observed slightly changed Stat3, pStat3, and CD130 levels in patient samples compared to the healthy controls. Usually, the changes were found in AD and ACLF patients and predominantly in $CD3^+CD4^+(CD45RA^+)$ cell populations (Figure 30).

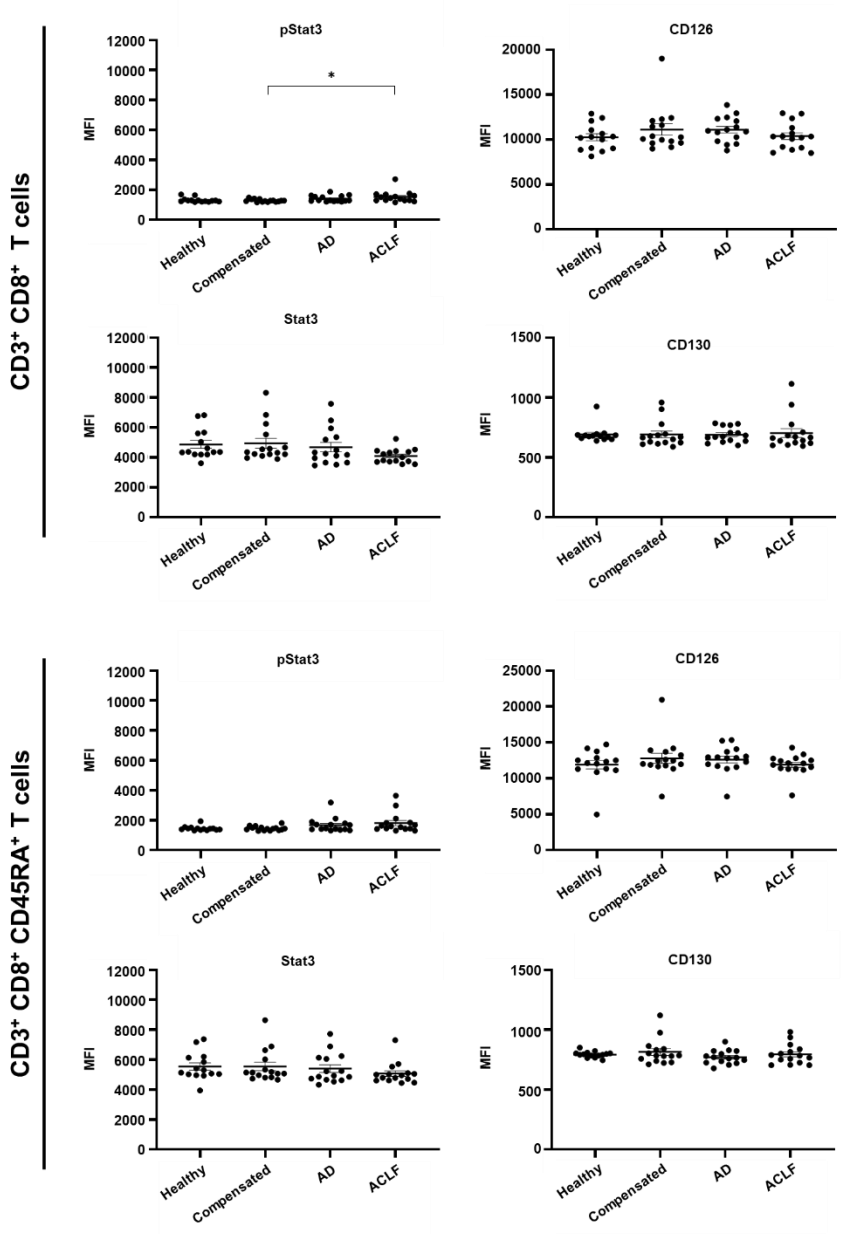

Figure 31: Basal expression levels of (p)Stat3, CD126, CD130 in unstimulated $CD3^+CD8^+$ and $CD3^+CD8^+CD45RA^+$ T cells.
The expression levels of intracellular Stat3, phosphorylated Stat3 and surface CD126 and CD130 in unstimulated $CD3^+CD8^+$ (upper panel) and $CD3^+CD8^+CD45RA^+$ (lower panel) T cells from healthy donors and patients with different stages of liver disease (n=15 in each group) were determined by flow cytometry. Anti-pStat3(pY705) antibody was used to determine phosphorylation. Mean and standard error of the mean (SEM) are shown. Statistical significance was tested using One-way ANOVA or Kruskal-Wallis test. p-values * = <0.05, **= <0.01, *** = <0.001 dependent on data distribution. MFI = median fluorescence intensity.

The $CD3^+CD8^+$ T cell populations showed a slightly reduced overall expression level of pStat3 towards ACLF patients compared with healthy controls (Figure 31). On the other hand, the $CD45RA^+$ subpopulation did not display different basal expression levels of the investigated target proteins.

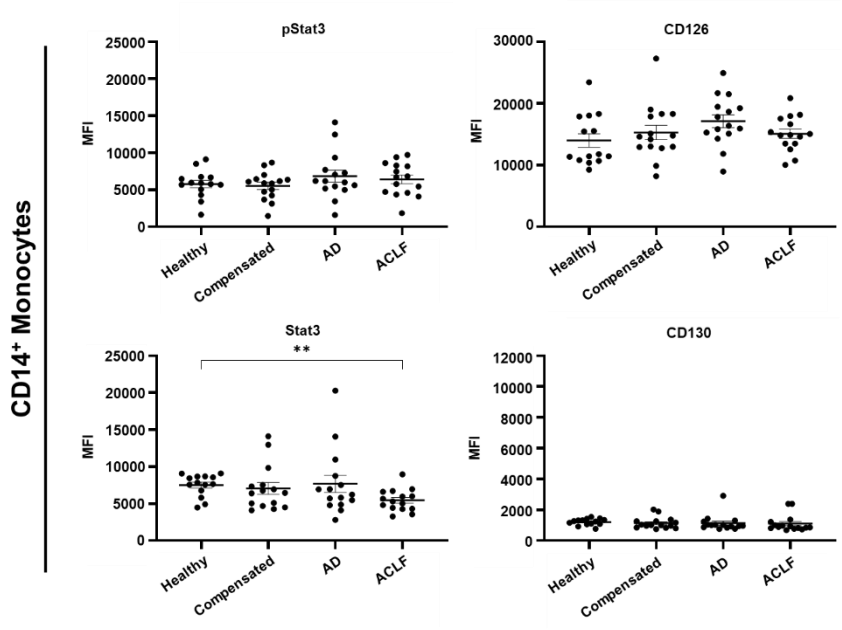

Figure 32: Basal expression levels of (p)Stat3, CD126, CD130 in unstimulated CD14⁺ monocytes.
The expression levels of intracellular Stat3, phosphorylated Stat3 and surface CD126 and CD130 in unstimulated CD14⁺ monocytes from healthy donors and patients with different stages of liver disease (n=15 in each group) were determined by flow cytometry. Anti-pStat3(pY705) antibody was used to determine phosphorylation. Mean and standard error of the mean (SEM) are shown. Statistical significance was tested using One-way ANOVA or Kruskal-Wallis test. p-values * = <0.05, **= <0.01, *** = <0.001 dependent on data distribution. MFI = median fluorescence intensity.

CD14⁺ monocytes showed equal basal level of all investigated proteins in all investigated groups except for Stat3. Here, we see a decrease in ACLF patients compared to healthy donor monocytes. In general, for this cell type higher MFI values were detected compared to the T cell populations.

4.8.3 Impaired IL-6 signalling response in liver cirrhosis patients

Next, PBMCs stimulated with IL-6 for 30 min were investigated for their signalling response by analysing Stat3 phosphorylation. The signalling response (ΔMFI) was calculated by subtracting unstimulated Stats median fluorescence intensity (MFI) from IL-6 stimulated MFI. We examined $CD3^+CD4^+$, $CD3^+CD4^+CD45RA^+$, $CD3^+CD8^+$ and $CD3^+CD8^+CD45RA^+$ T cells and $CD14^+$ monocytes. The results are shown in Figure 33.

We observed that IL-6 induced phosphorylation of Stat3 in liver disease patients was lower than that in healthy donors. This was significant for nearly all stages of liver disease and in all investigated cell types. More specifically, the most significant differences compared to healthy donors were found in $CD8^+$ T cells from acute

decompensated patients. Furthermore, in this exact cell types the signalling response to IL-6 seems to improve during later stages of liver disease when AD patients are compared to ACLF patients, but the levels of healthy donors can not be reached. These results suggest a dysfunctional IL-6-Stat3 pathway in liver cirrhosis patients that aggravates during the course of disease.

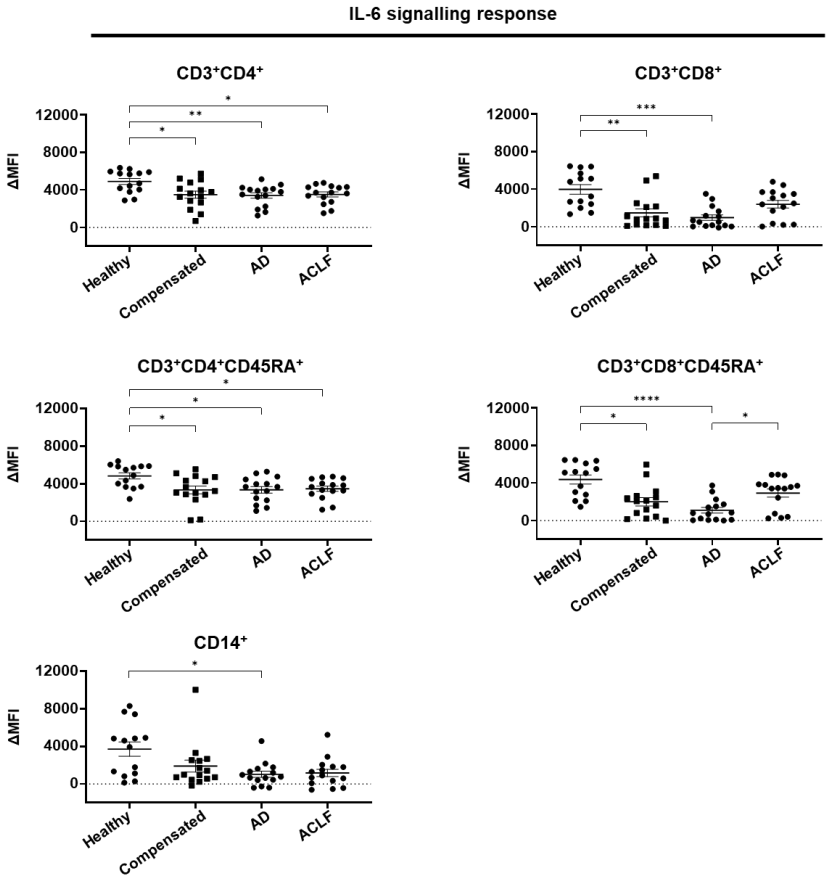

Figure 33: IL-6 signalling response in PBMC subpopulations from healthy donors and liver disease patients.
IL-6 (50 ng/ml) induced phosphorylation of Stat3 after 30 min total stimulation time was determined by flow cytometry in PBMC subsets, namely $CD3^+CD4^+$, $CD3^+CD4^+CD45RA^+$, $CD3^+CD8^+$ $CD3^+CD8^+CD45RA^+$ T cells and $CD14^+$ monocytes. Anti-pStat3(pY705) antibody was used to determine phosphorylation. Mean and standard error of the mean (SEM) are shown. Statistical significance was tested using One-way ANOVA or Kruskal-Wallis test. p-values * = <0.05, **= <0.01, *** = <0.001 dependent on data distribution. ΔMFI = delta median fluorescence intensity.

4.8.4 Repeated cytokine stimulation in PBMCs of healthy donors and liver cirrhosis patients

To investigate whether PBMCs also show an unresponsive behaviour to repeated cytokine stimulation and whether PBMCs from patients in different stages of liver cirrhosis react differently, PBMCs were seeded and stimulated as described before. Additional to the 30 min stimulation samples, further samples were stimulated with a

second cytokine dose 3 h after the initial stimulation for again 30 min. The results for the repeated IL-6 stimulation are presented in chapter 4.9.4.1 IL-6 stimulated PBMCs while the results from the repeated IFNγ stimulation are presented in chapter 4.9.4.2 IFNγ stimulated PBMCs.

4.9.4.1 IL-6 stimulated PBMCs

Previous experiments from our working group (unpublished data) have already shown that PBMCs from healthy donors have a comparable fast phosphorylation kinetic as Stat1 and Stat3 phosphorylation upon IL-6 stimulation was strongly induced after 30 min but was strongly reduced again after 1 h. After 3 h of IL-6 stimulation, the initial Stat3 phosphorylation was not detectable anymore by Western blot experiments. Therefore, any phosphorylation present in the following results that occurs after 3 h and 30 min was considered to be induced by the second stimulation dose after 3 h.

The results for the $CD3^+CD4^+$ and $CD3^+CD4^+CD45RA^+$ T helper cells are depicted in Figure 34. We could observe that the total Stat3 levels were not significantly different in the samples that were stimulated in this experiment. pStat3 was strongly induced within 30 min of stimulation with IL-6 in $CD3^+CD4^+$ T cells (Figure 34, left panel) in healthy donors and every investigated stage of liver cirrhosis. The second IL-6 stimulation dose resulted in a slight induction of Stat3 phosphorylation which was significantly lower compared to the 30 min signal. pStat3 phosphorylation after the second stimulation in cells from healthy donors were still significantly higher compared to unstimulated control samples. This changed when healthy donors are compared with compensated, acute decompensated and ACLF patients. Notably, there are no significant differences between unstimulated samples and samples that were stimulated twice. The difference in Stat3 phosphorylation between a single and a second IL-6 dose becomes larger towards AD and ACLF patients. Additionally, in healthy donors there is still a difference in Stat3 phosphorylation wen the second cytokine dose is IFNγ compared to unstimulated $CD3^+CD4^+$ T cells but with disease progression this contrast vanishes.

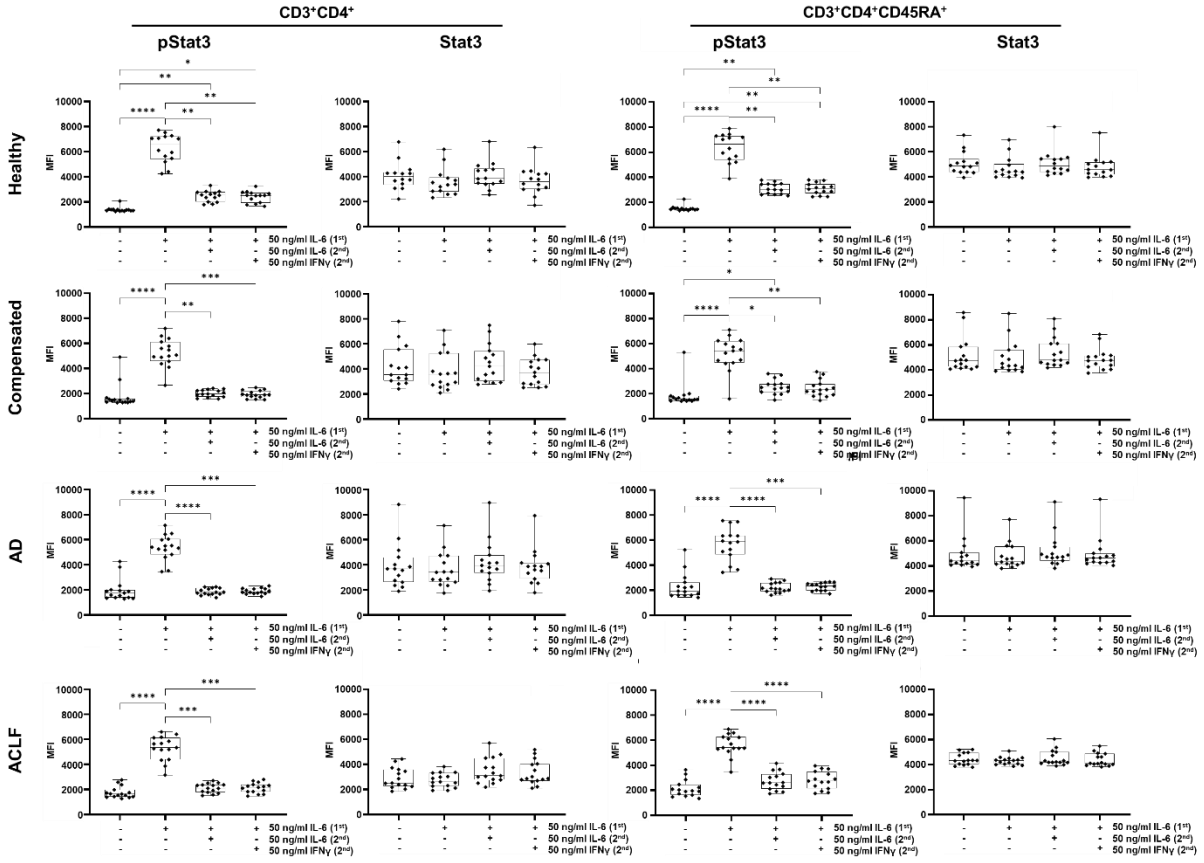

Figure 34: Repeated IL-6 stimulation of CD3$^+$CD4$^+$ and CD3$^+$CD4$^+$CD45RA$^+$ T cells.
Induction of IL-6 signalling response after repeated cytokine application was determined after one stimulus IL-6 (50 ng/ml, 1st) for 30 min and 30 min after a second stimulus with either IL-6 or IFNγ (50 ng/ml, 2nd) at the time point 3 h after the first stimulation. CD3$^+$CD4$^+$ T cells (left panel) and CD3$^+$CD4$^+$CD45RA$^+$ T cells are shown. Phosphorylation of Stat3 (anti-pStat3(pY705) antibody) was determined. Data is shown as boxplots with whiskers (min to max). Statistical significance was tested using One-way ANOVA or Kruskal-Wallis test. p-values * = <0.05, **= <0.01, *** = <0.001 dependent on data distribution. MFI = median fluorescence intensity.

The results described for CD3$^+$CD4$^+$ T cells also apply for the CD3$^+$CD4$^+$CD45RA$^+$ T cell subpopulation (Figure 34, right panel). Here, the difference between single and second dose IL-6 in healthy donors and compensated patients compared to AD and ACLF patients is even stronger. However, the data suggest that the general ability to phosphorylate Stat3 in all four patient groups remains highly significant and does not change during course of disease.

The results for the CD3$^+$CD8$^+$ and CD3$^+$CD8$^+$CD45RA$^+$ cytotoxic T cells are depicted in Figure 35. Again, the total Stat3 levels are equal in the different samples so changes in the phosphorylation levels do not origin from thereof. Cells from healthy donors are effectively stimulatable with IL-6 which induces Stat3 phosphorylation. Repeated stimulation with IL-6 or IFNγ still showed elevated pStat3 levels compared to the unstimulated control but significantly lower than after a single IL-6 stimulation. Unlike the CD4$^+$ T cell populations described above, the differences between healthy

donor cells and patient cells become more definite. In $CD3^+CD8^+$ cytotoxic T cells from compensated patients pStat3 is still inducible but to a much lower extend than in healthy donors. Also, the differences to the samples that received a second cytokine stimulation with IL-6 or IFNγ disappear. This effect is even more prominent in AD patients where there is barely any Stat3 phosphorylation after a single 30 min treatment. In this stadium of liver disease there is no difference in Stat3 phosphorylation when unstimulated cells are compared to two times stimulated cells.

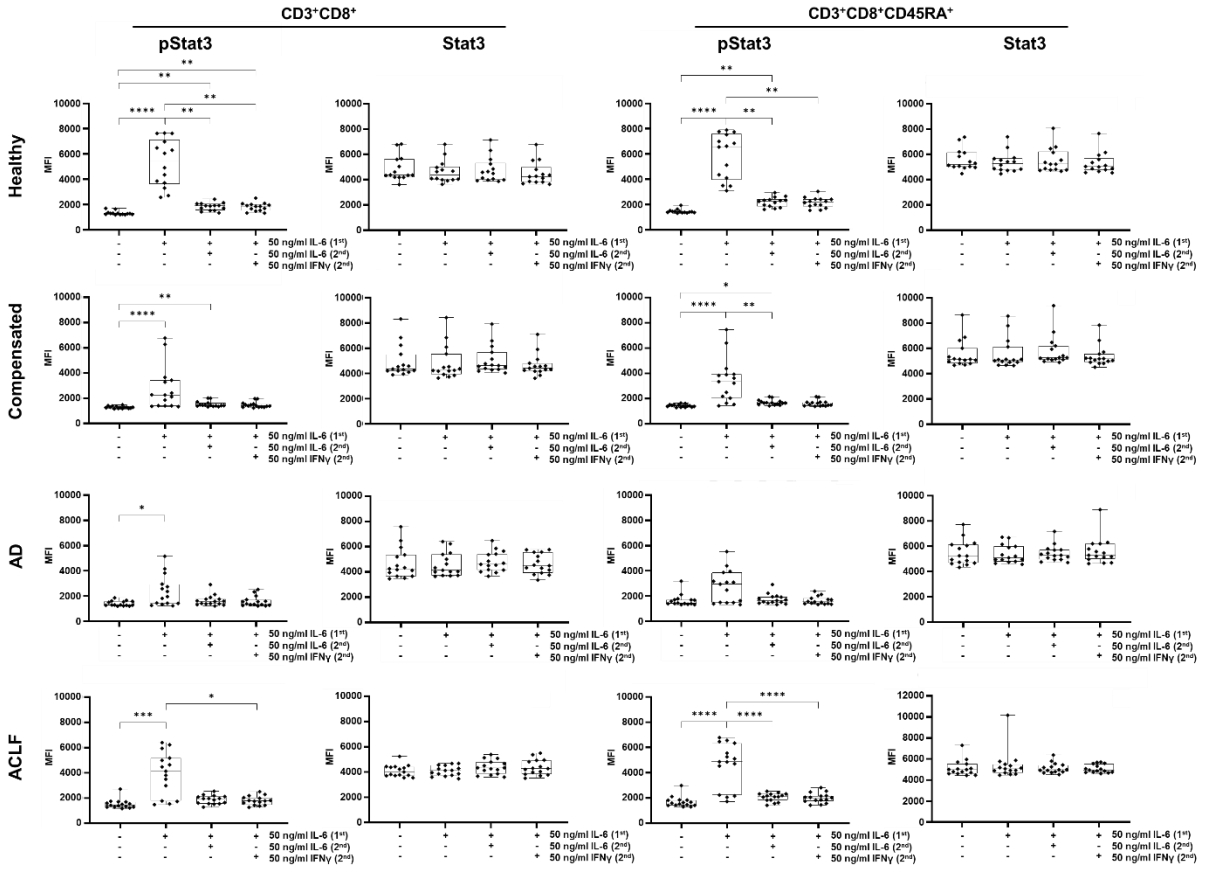

Figure 35: Repeated IL-6 stimulation of $CD3^+CD8^+$ and $CD3^+CD8^+CD45RA^+$ T cells.
Induction of IL-6 signalling response after repeated cytokine application was determined after one stimulus IL-6 (50 ng/ml, 1st) for 30 min and 30 min after a second stimulus with either IL-6 or IFNγ (50 ng/ml, 2nd) at the time point 3 h after the first stimulation. $CD3^+CD8^+$ T cells (left panel) and $CD3^+CD8^+CD45RA^+$ T cells are shown. Phosphorylation of Stat3 (anti-pStat3(pY705) antibody) was determined. Data is shown as boxplots with whiskers (min to max). Statistical significance was tested using One-way ANOVA or Kruskal-Wallis test. p-values * = <0.05, **= <0.01, *** = <0.001 dependent on data distribution. MFI = median fluorescence intensity.

Regarding cells from ACLF patients, the single IL-6 stimulation is more effective concerning the 30 min single stimulation, but the cells are still not responsive to a second cytokine dose. In $CD3^+CD8^+CD45RA^+$ T cells (Figure 35, right panel) the reaction to IL-6 stimulations is again comparable to their parent population of $CD3^+CD8^+$ T cells. As described above, cells from AD patients can barely be

stimulated with IL-6 to induce a Stat3 phosphorylation response. This seems to recover in ACLF patients where Stat3 phosphorylation can be induced again but a second cytokine stimulation does not show a difference compared to unstimulated control samples.

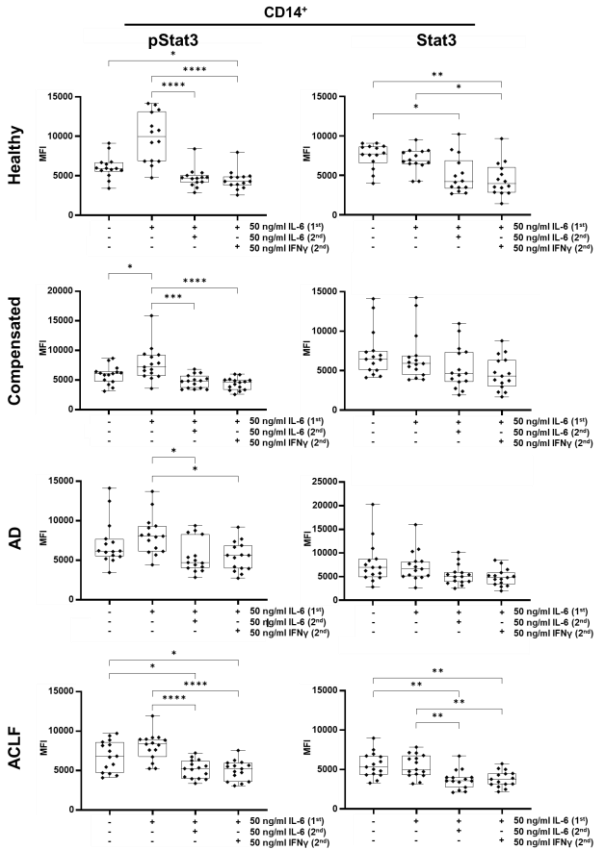

Figure 36: Repeated IL-6 stimulation of CD14⁺ monocytes.
Induction of IL-6 signalling response after repeated cytokine application was determined after one stimulus IL-6 (50 ng/ml, 1st) for 30 min and 30 min after a second stimulus with either IL-6 or IFNγ (50 ng/ml, 2nd) at the time point 3 h after the first stimulation. Phosphorylation of Stat3 (anti-pStat3(pY705) antibody) was determined. Data is shown as boxplots with whiskers (min to max). Statistical significance was tested using One-way ANOVA or Kruskal-Wallis test. p-values * = <0.05, **= <0.01, *** = <0.001 dependent on data distribution. MFI = median fluorescence intensity.

In CD14⁺ monocytes (Figure 36) there is only a weak increase of pStat3 levels upon a single IL-6 stimulation which is only significant in compensated patients. After 3h and 30 min stimulation time for those samples that received a second cytokine dose the pStat3 levels are significantly lower compared to unstimulated control cells and especially to the cells that received a single IL-6 stimulation. Furthermore, the total Stat3 levels tend to decrease in the samples that incubated longer during the stimulation. This trend is significant in healthy donors and ACLF patients. These data suggest a strong pre-activation of the Stat3 pathway in monocytes in our experimental setting. The pre-activation seems to be reduced when the cells

incubate for over 3 h during stimulation time. Within this time, instead of inducing a Stat3 signalling response, the pre-activation is reduced which can be seen in the depicted data in the decrease of pStat3 and Stat3 levels over time. Moreover, Stat3 seems to be degraded in the monocytes over time.

4.9.4.2 IFNγ stimulated PBMCs

The data presented in this section resulted from PBMC stimulation experiments that were performed as described for the previous chapter (4.8.4 Repeated cytokine stimulation in PBMCs of healthy donors and liver cirrhosis patients). For these results, PBMCs were seeded and stimulated with IFNγ instead of IL-6. The treatment was either a single cytokine application for 30 min or a repeated cytokine application where the second dose was given after 3 h for additional 30 min. The second dose was either IFNγ or IL-6 as indicated in the following figures.

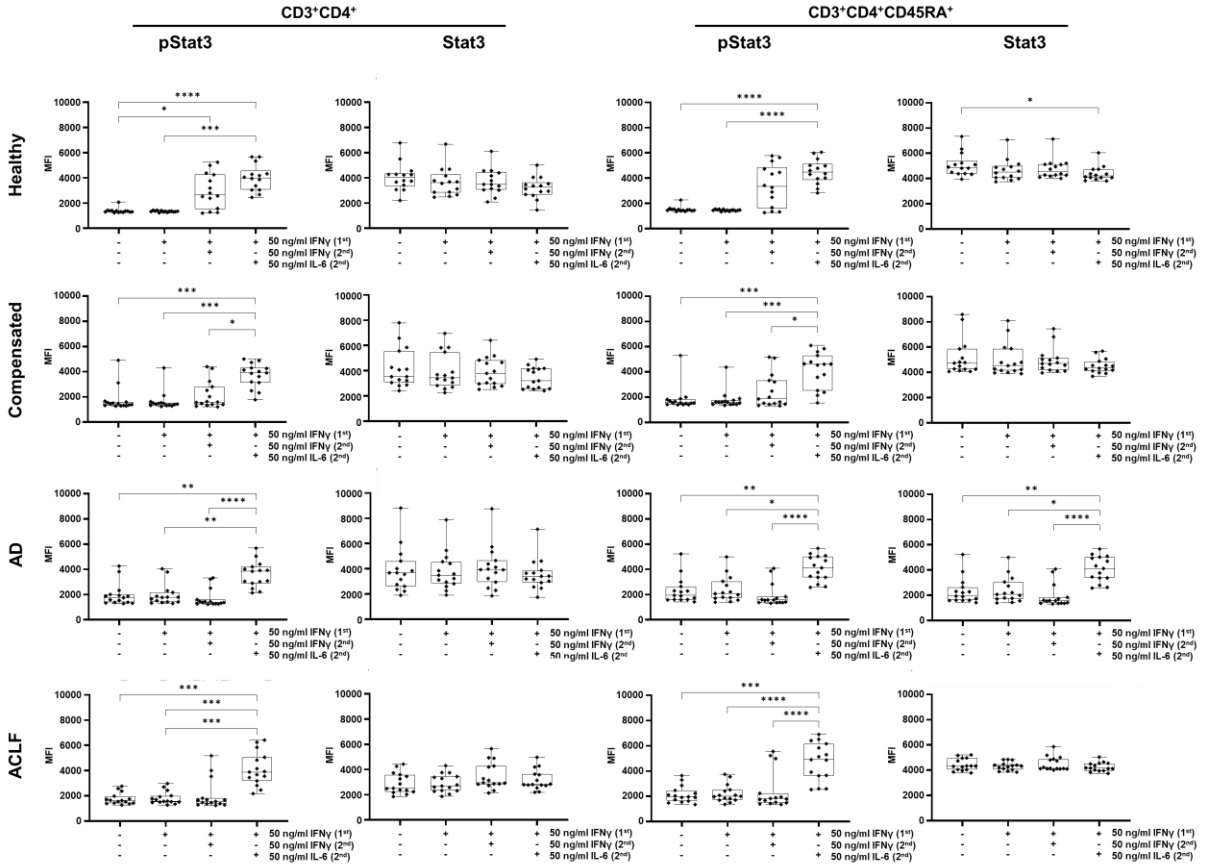

Figure 37: Repeated IFNγ stimulation of CD3⁺CD4⁺ and CD3⁺CD4⁺CD45RA⁺ T cells.
Induction of IFNγ signalling response after repeated cytokine application was determined after one stimulus IL-6 (50 ng/ml, 1st) for 30 min and 30 min after a second stimulus with either IFNγ or IL-6 (50 ng/ml, 2nd) at the time point 3 h after the first stimulation. $CD3^+CD4^+$ T cells (left panel) and $CD3^+CD4^+CD45RA^+$ T cells are shown. Phosphorylation of Stat3 (anti-pStat3(pY705) antibody) was determined. Data is shown as boxplots with whiskers (min to max). Statistical significance was tested using One-way ANOVA or Kruskal-Wallis test. p-values * = <0.05, **= <0.01, *** = <0.001 dependent on data distribution. MFI = median fluorescence intensity.

The results for the $CD3^+CD4^+$ and $CD3^+CD4^+CD45RA^+$ T helper cells are shown in Figure 37 (left and right panel, respectively). We observed equally distributed total Stat3 levels. They were not significantly different in the samples that were stimulated throughout the experiment. As expected, pStat3 was not strongly induced upon a single IFNγ treatment but when IL-6 was given as second cytokine dose. Interestingly, when IFNγ was given as the second cytokine dose, healthy donor $CD3^+CD4^+$ and $CD3^+CD4^+CD45RA^+$ T cells displayed Stat3 phosphorylation that was significantly different to unstimulated control cells. This effect was no longer present in patients with compensated LC, AD or ACLF.

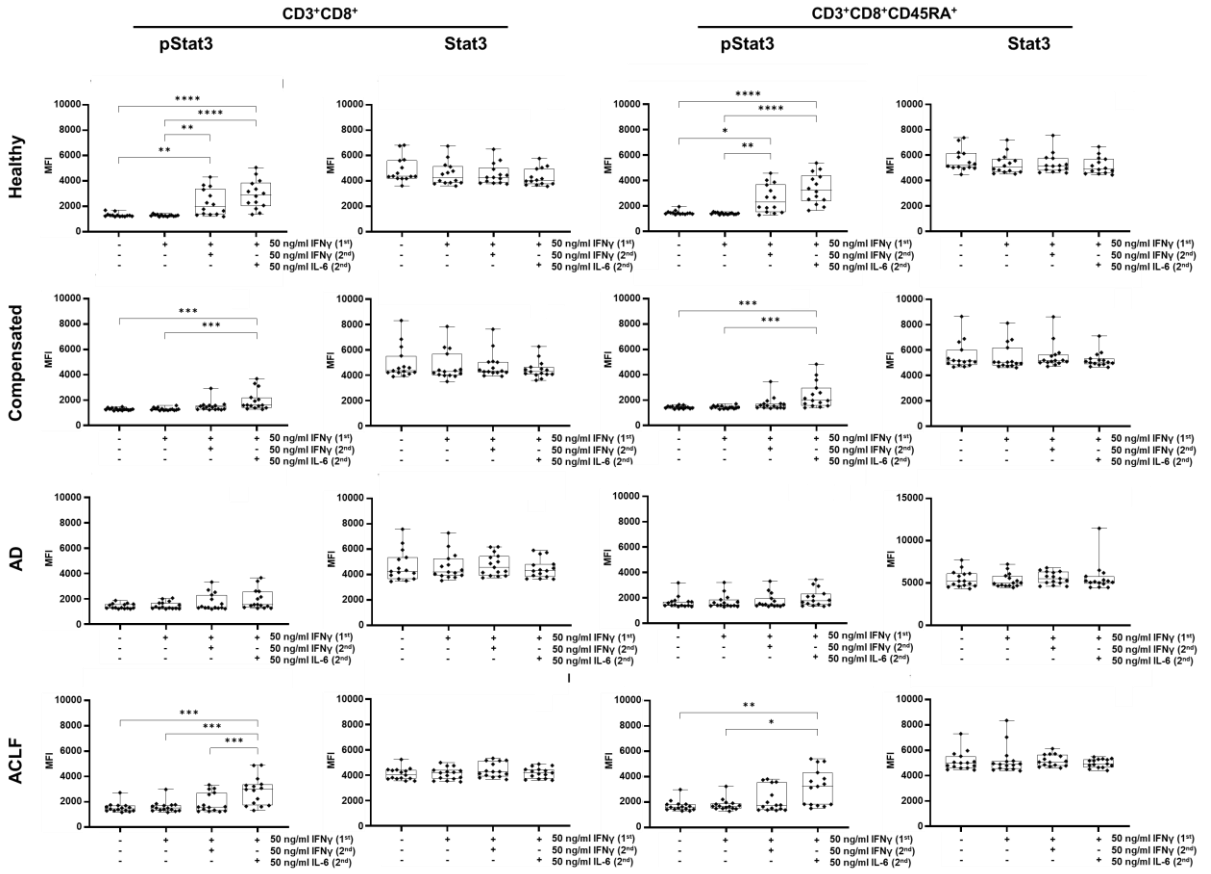

Figure 38: Repeated IFNγ stimulation of $CD3^+CD8^+$ and $CD3^+CD8^+CD45RA^+$ T cells.
Induction of IFNγ signalling response after repeated cytokine application was determined after one stimulus IL-6 (50 ng/ml, 1st) for 30 min and 30 min after a second stimulus with either IFNγ or IL-6 (50 ng/ml, 2nd) at the time point 3 h after the first stimulation. $CD3^+CD8^+$ T cells (left panel) and $CD3^+CD8^+CD45RA^+$ T cells are shown. Phosphorylation of Stat3 (anti-pStat3(pY705) antibody) was determined. Data is shown as boxplots with whiskers (min to max). Statistical significance was tested using One-way ANOVA or Kruskal-Wallis test. p-values * = <0.05, **= <0.01, *** = <0.001 dependent on data distribution. MFI = median fluorescence intensity.

The results for the $CD3^+CD8^+$ and $CD3^+CD8^+CD45RA^+$ cytotoxic T cells are depicted in Figure 38 (left and right panel, respectively). Stat3 levels are equal in the different samples. Cells from healthy donors stimulated with IFNγ again showed induction of

Stat3 phosphorylation and therefore pathway activation compare to unstimulated or single stimulated cells. The differences in the healthy $CD8^+$ cells are more significant as in the $CD4^+$ cell populations. When it comes to patient samples, this pStat3 induction cannot be observed.

In the case that the second cytokine dose was IL-6, Stat3 becomes phosphorylated in healthy donors. With further disease progression, the capacity to react to IL-6 decreases and reaches its minimum in AD patients in both $CD3^+CD8^+$ and $CD3^+CD8^+CD45RA^+$ T cells. This mirrors the results from the previous chapter when even a single stimulation dose of IL-6 was barely or not able to induce Stat3 phosphorylation successfully (Figure 35) in AD patients.

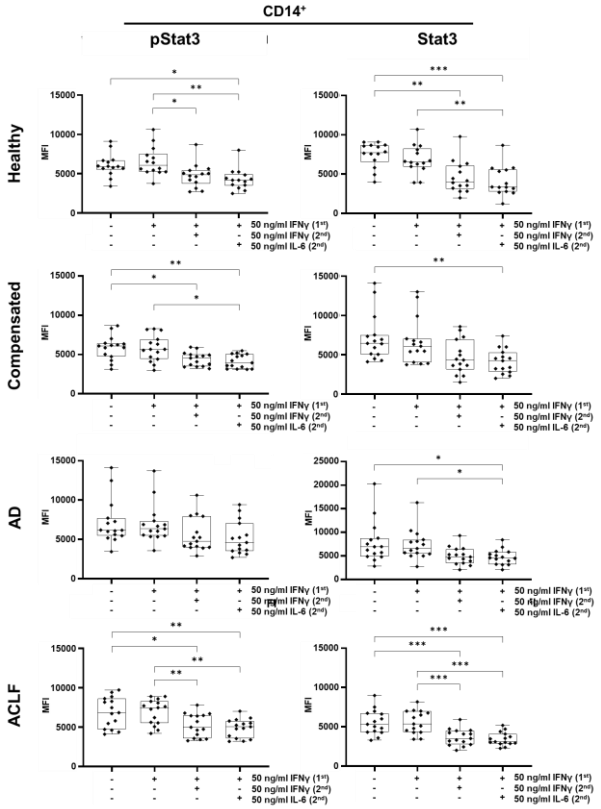

Figure 39: Repeated IFNγ stimulation of $CD14^+$ monocytes.
Induction of IFNγ signalling response after repeated cytokine application was determined after one stimulus IL-6 (50 ng/ml, 1st) for 30 min and 30 min after a second stimulus with either IFNγ or IL-6 (50 ng/ml, 2nd) at the time point 3 h after the first stimulation. Phosphorylation of Stat3 (anti-pStat3(pY705) antibody) was determined. Data is shown as boxplots with whiskers (min to max). Statistical significance was tested using One-way ANOVA or Kruskal-Wallis test. p-values * = <0.05, **= <0.01, *** = <0.001 dependent on data distribution. MFI = median fluorescence intensity.

As expected, there is no increase of Stat3 phosphorylation upon a single IFNγ stimulation in $CD14^+$ monocytes (Figure 39). After 3h and 30 min stimulation, for those samples that received a second cytokine dose the pStat3 levels decrease

significantly compared to unstimulated control cells or show the trend to decrease over the time of the experiment. Furthermore, the total Stat3 levels also tend to decrease in the samples that incubated longer during the stimulation. This trend is significant in all investigated groups. These results underline the suggested pre-activation of the Stat3 pathway in monocytes in our experimental setting. The pre-activation might be reduced when the cells incubate for over 3 h during stimulation time. Within this time, instead of inducing a Stat3 signalling response, the pre-activation is reduced which can be seen in the depicted data in the decrease of pStat3 and Stat3 levels over time. It was expected that upon a second stimulation with IL-6, Stat3 phosphorylation would have been induced which was not the case as the detected pStat3 level of this condition is lower than the pStat3 level of unstimulated cells in all investigated patient groups and healthy donors.

5 Discussion

Liver cirrhosis is the leading cause for liver-related deaths [43]. Progressing liver cirrhosis might lead to development of acute-on-chronic liver failure (ACLF), a defined syndrome characterized by acute decompensation, organ failure and a high short-term mortality up to 76% in 28 days [144]. Both, liver cirrhosis and ACLF are associated with immune dysregulation and systemic inflammation along with elevated levels of pro- and anti-inflammatory cytokines in the patients [5, 42, 205]. These factors are thought to contribute to organ failure in liver cirrhosis patients and worse outcome. Current immunotherapeutic options to treat patients is to counteract the symptoms and etiological factors among others [87]. Besides that, different cytokines are already considered for immunotherapeutic approaches such as IL-22 as treatment of alcoholic hepatitis [8, 180, 229] or G-CSF to improve the survival rate of ACLF patients [56, 65, 79]. However, little is known about the interplay between the different upregulated cytokines. A deeper understanding is necessary to evaluate and improve immunotherapies.

5.1 Combined cytokine treatments reveal synergistic and antagonistic effects on signalling and RNA level

This thesis takes a closer look at the interplay between various cytokines that were described in the context of liver cirrhosis, ACLF and liver injury with emphasis on IL-6, IL-22 and lFNγ. It aims to improve the understanding of the interdependence of the different cytokines on hepatocytes as in these states of disease they are exposed to a whole network of cytokines. It was shown that cytokine combinations such as IL-6, IL-13, IL-22 and G-CSF influence each other's signalling response in hepatocarcinoma cell lines (Figure 11 to Figure 15). The combination of IL-6 and IL-22 also elevated phosphorylated Stat1 and Stat3 protein levels in primary human hepatocytes (Figure 16). Pursuing this effect to the induction of target genes, we found that LBP RNA amounts were elevated in hepatocytes that were stimulated with both, IL-6 and IL-22, simultaneously (Figure 21). IL-6 and IL-22 are especially described to be elevated in the serum of LC and ACLF patients and associated with worse outcome although they are attributed with positive properties such as involvement in liver regeneration, hepatoprotection and cell proliferation [42, 57, 77, 162, 185]. In our experiments, co-stimulation of both cytokines resulted in enhanced

LBP RNA levels suggesting an enhanced antimicrobial response by hepatocytes. It has been described recently, that IL-22 has an enhancing effect on IL-1β and TNFα stimulated CXCL8 secretion. CXCL8 mRNA expression was also significantly increased indicating the enhancing effect of IL-22 on the intracellular signalling level [236]. The authors described the p38 MAPK signalling pathway being involved in the enhancing effect of IL-22 on TNF-α-stimulated CXCL8 secretion. Our data might suggest an enhancing effect of IL-22 on IL-6 stimulated LBP RNA expression in hepatocytes. It is of further interest for future experiments how cytokine combinations affect other cells or tissues such as the gastrointestinal barrier function that is described to influenced and preserved by IL-22 [11, 109, 124, 217]. Measurement of transepithelial electric resistance (TEER) of cytokine stimulated cells might provide further insight into the influence of high levels of different cytokines on the intestinal integrity as it can be found in our patients.

Upon the presented cytokine combinatory treatments IL-6 and IFNγ led to altered RNA expression of TIMP-1 and IRF1. In this case, a combination did not lead to an enhanced but diminished RNA expression of the mentioned target genes (Figure 18, Figure 19) despite synergism in Stat phosphorylation. TIMP-1 RNA expression was upregulated by IL-6 treatment and cytokine combination with IFNγ led to a decrease while IRF1 RNA was upregulated by IFNγ and diminished by addition of IL-6. As IRF1 is a mediator of IFNγ for cell cycle arrest and apoptosis in hepatocytes, it is thinkable that IL-6-mediated regenerative and hepatoprotective properties counteract IFNγ treatment [107]. IL-6-mediated TIMP-1 RNA induction might serve tissue remodelling to support the process of liver regeneration that might be opposed by IFNγ. Other studies revealed that IL-6 induced TIMP-1 plays major role in chemotherapy resistance in cancer which supports its pro-survival properties [230].

5.2 IL-6 and IL-22 induce refractoriness in hepatocytes

Next, experiments were performed to determine whether a repeated cytokine stimulation would lead to a comparable effect of enhanced Stat phosphorylation and target gene expression regarding IL-6 and IL-22. Our *in vitro* studies revealed refractoriness of the Stat-pathway after repetitive cytokine stimulation for Stat1 and Stat3 (Figure 23) whereby Stat1 refractoriness was stronger and long-lasting compared to Stat3. Such refractoriness had been described earlier for IFNα stimulated murine hepatocytes depending on upregulation of USP18/UBP43, a

negative regulator of the IFN signalling [163, 176]. Silencing of USP18 led to enhanced ability of IFNα to inhibit HCV-RNA replication [163]. Furthermore, Read et. al. suggest PPARα agonists to increase sensitivity to IFN treatment in HCV infections [164].

Experiments to further determine the mechanism behind showed that cytokine refractoriness due to IL-6 or IL-22 stimulation is not based on a general unresponsiveness of Stat phosphorylation itself as it is still inducible by stimulation with another cytokine that used the same Stat signalling molecules (Figure 26). IL-6 and IL-22 both use the same proteins of the Jak protein family, namely Jak1 and Tyk2, to transduce the signal and phosphorylate Stat molecules although Tyk2 is not necessarily essential for successful IL-6 signalling in mice and human [121, 159, 181, 190]. This suggests that an inhibition of the Jak protein family seems not to be likely for cytokine refractoriness but needs to be further investigated to exclude this option. The data suggest that refractoriness' origin needs to be on an upstream levels where both pathways use different signalling molecules for instance on the receptor level. IL-6 uses the IL-6Rα and gp130 as receptors to initiate signalling while IL-22 uses a receptor dimer composed of IL-22R1 and IL-10R2 [22, 55]. Therefore, receptor internalization or inhibition in their signal transmission but also individual signalling pathway inhibitors like the SOCS protein family might play a role in cellular refractoriness and need to be further investigated. Of note, refractoriness is independent of the investigated cell types but dependent on the respective cytokine. We could show IL-6 refractoriness in hepatocarcinaoma cell lines, PHHs, $CD4^+$/$CD8^+$ T cell subpopulations (Figure 34, Figure 35) and monocytes (Figure 36). On the other hand, HepG2 and Huh7 cells did only show a mild unresponsiveness towards repetitive IFNγ stimulation (Figure 24) but Stat1 phosphorylation could be reinduced when cells initially stimulated with IL-6 were treated with IFNγ as second stimulus (Figure 27). Additionally, upon a cytokine withdrawal between the repeated cytokine stimulations with IL-6 or IL-22, refractoriness could be reduced and Stat phosphorylation was induced ealier (Figure 29). This provides a valuble insight into IL-6 and IL-22 signalling dynamics and can be used for future immunotherapeutic approaches. For example, it is conceivable to use a pathway antagonist or blocking antibody to inhibit the cytokine signalling with the purpose to then give a cytokine boost that might enhance its desired effects. This would interfere with the continuous cytokine exposure and reinduce sensitivity of the treated cells.

However, cytokine refractoriness might follow different rules regarding target gene expression of the respective cytokine. Our data show that in HepG2 cells LBP RNA expression was not enhanced after repetitive stimulation with IL-6 and IL-22 (Figure 25). A direct comparison between a single cytokine stimulation and a repeated cytokine stimulation for the same total stimulation time did not lead to significantly increased RNA levels over at least 24 hours. We conclude that at least for LBP it does not matter whether HepG2 cells are repeatedly stimulated or not to induce gene transcription. It is of further interest to identify more genes whose expression is influenced by the simultaneous presence of for instance IL-6 and IL-22 and whether those genes show divergent regulation.

Further investigations in this context are needed as the amount and time point of cytokine treatment seem to play a crucial role in immune therapy. Recently, it was shown that the order of administration of cytokines in combination therapies (IL-2 and IFNα) can decouple toxicity from efficacy in syngeneic mouse tumour models [172]. Protein engineering of IL-22 resulted in a high affinity variant of IL-22 that primarily induces Stat3 phosphorylation and therefore promotes regeneration and epithelial protection while negative effects mediated via Stat1 were reduced [180]. Given our measurements regarding the fast peaking answer to cytokine stimulation, a treatment with cytokines modified for high-affinity rather than long-lasting stability might be a valuable approach for future cytokine therapies.

In this context, it raises the question how IL-6-trans signalling is implicated as this was not especially addressed this project. IL-6 trans-signalling is thought to mediate primarily pro-inflammatory effects and contributes to cancer development [94, 210, 228] but it also is described to play an essential role in liver regeneration after partial hepatectomy in mice [55, 67]. Further insight is needed whether IL-6 classic and trans signalling respond differently to repetitive cytokine stimulation.

The data from our patient cohort revealed that the basic levels of the surface receptor CD126 (IL-6Rα) remained the same throughout the different stages of liver disease while gp130 was diminished in patients suffering from ACLF. It would be interesting to further evaluate the soluble gp130 levels in the patients and whether they differ from healthy controls to draw conclusions about altered involvement of IL-6 trans signalling and its contribution to the patient’s stage of disease.

5.3 T cells from liver cirrhosis patients show a dysfunctional IL-6-Stat3 pathway after IL-6 stimulation

Taking a closer look at our investigated patient cohort it was observed that changes in Stat3 phosphorylation due to IL-6 cytokine treatment (Figure 33) were not related to changes in the total amounts of Stat3 in the patients as it was not significantly elevated throughout the different stages of liver cirrhosis and ACLF (Figure 30, Figure 31, Figure 32).

The overall results from the single and repeated cytokine stimulations of the patient's PBMCs suggest a dysfunctional IL-6-Stat3 pathway in liver cirrhosis patients that aggravates during the course of disease (Figure 34, Figure 35). Especially in $CD3^+CD8^+$ cells and their $CD45RA^+$ subpopulation which comprises effector and naïve T cells, even a single IL-6 stimulation dose not induce a Stat3 phosphorylation that is significantly different from unstimulated cells in acute decompensated patients. IL-6 is a pleiotropic cytokine as described before and has profound effect on T cells as hepatocytes and leukocytes are the cell types mostly expressing IL-6Rα [181]. As reviewed by Dienz et. al. [54] IL-6 enhances T cell proliferation and downregulates FasL which prevents apoptosis. Furthermore, increased migration and plays a role in supporting the effector and memory T cell populations. IL-6 is an important modulator of $CD4^+$ T cell effector functions. Additionally, IL-6 promotes T helper cell differentiation towards Th2 and Th17 subsets by inhibiting Th1 polarization [53]. Th17 cells are involved in the defence mechanisms against pathogens at mucosal tissues for instance by maintaining barrier functions [86]. Overall, IL-6 strongly contributes to effector functions of $CD4^+$ T cell subsets. IL-6 has regulatory functions regarding $CD8^+$ T cells. Among others, IL-6 supports differentiation of naïve $CD8^+$ T cells into IL-21 producing effector T cells which support B cells' isotype switching that in turn contributes to production of virus-protective IgG antibodies [234]. Together with other cytokines such as IL-7 or IL-15, IL-6 stimulates $CD8^+$ T cell proliferation [75]. $CD4^+$ and $CD8^+$ T cell from liver cirrhosis and ACLF patients showed inappropriate functions after stimulation with PMA/ionomycin which resulted in diminished IFNγ and TNFα production compared to healthy controls [174]. From our results, we can conclude that $CD4^+$ and $CD8^+$ T cells from patients with liver cirrhosis and ACLF have an impaired IL-6-Stat3-signalling which might result from systemically elevated IL-6 levels in the patients. We could see a preactivation of Stat3 with disease

aggravation (Figure 30), especially in $CD4^+$ T cells which can contribute to the observed impaired response to IL-6. This might contribute to the described impaired functions of these cell populations in the patients, particularly as protein degradation might already have started to terminate the signal. While preactivation was stronger in $CD4^+$ T cells, the unresponsiveness to IL-6 was more pronounced in $CD8^+$ T cells (Figure 35). As refractoriness upon IL-6 stimulation was also observed in the T cell subsets and to a greater extend in AD and ACLF patients, this might be another hint that indicates inappropriate T cell function. One can speculate whether the isolation procedure of the PBMCs was long enough to make cells again sensitive towards IL-6 stimulation in the first stimulation attempt. However, as a repeated stimulation only led to a strongly diminished Stat3 phosphorylation this could mirror the reaction in the patients that display high IL-6 serum levels. The resulting implications for T-cell functions in the context of liver cirrhosis and ACLF need to be further investigated. For future experiments, one should focus on distinction of the T cell population. In this project, the overall populations of $CD4^+$ and $CD8^+$ T cells and the $CD45RA^+$ subset was evaluated. As $CD45RA^+$ T cells comprise naïve and effector T cells it would be interesting whether these cells react differently to cytokine stimulation or whether they are affected both. This can be achieved using one additional surface marker, namely CCR7. This marker would further facilitate the differentiation between naïve, central memory, effector and effector memory T cell [129]. As described before, repetitive cytokine stimulation led to diminished Stat3 phosphorylation in the T cells of patients compared to healthy donor T cells (Figure 34, Figure 35). The extent of the refractoriness increased with disease progression which might be associated with the increasing IL-6 levels that are constantly observed in liver cirrhosis and ACLF patients. Increasing unresponsiveness to IL-6 stimulation during disease progression was not based on receptor internalization as seen in Figure 30 for $CD4^+$ T cells, in Figure 31 for $CD8^+$ T cells and Figure 32 for $CD14^+$ monocytes. Again, it would be interesting to further investigate the role of IL-6-trans-signalling in the investigated patients. Using an ELISA assay, one could examine the levels of sIL-6R. Differences might in the receptor amount might help to gain further insight into the signalling mechanism during liver disease.

IFNγ usually has a broad spectrum of effects on T cells such as Th1/Th2 differentiation and direct suppressive and proapoptotic properties while indirect effects are associated with enhanced $CD8^+$ T cell activity [221]. IFNγ signalling

mainly uses Stat1 but also Stat3 is described to be part of the signalling as it forms heterodimers with Stat1 [95, 161]. This explains the enhanced Stat3 phosphorylation that was observed in repetitively IFNγ-stimulated T cells (Figure 37, Figure 38). Unfortunately, Stat1 phosphorylation could not be investigated due to problems with the multicolour flow cytometry staining of pStat1. This limits the data interpretation.

We further investigated the impact of IL-6 and IFNγ stimulation on healthy and patient's $CD14^+$ monocyte population. Monocytes are precursor cells that have the potential to differentiate into macrophages or dendritic cells which is stimulated by the cytokines M-CSF or GM-CSF and IL-4, respectively [38]. IL-6 and IFNγ both support the differentiation step towards the macrophage phenotype [38, 51]. In our experiments, we observed the trend of IL-6 to induce Stat3 phosphorylation while these changes were not significant. What was more striking is that pStat3 level decreased in both stimulation settings (Figure 36, Figure 39) after more than 30 min stimulation time. The same was observed for the total Stat3 amounts in these cells. This might indicate a pre-activation of the monocytes during the experimental procedure so that after 30 min there was no discrimination between IL-6 induced pStat3 and pStat3 due to pre-activation. Over time, both pStat3 and Stat3 might be degraded. Nevertheless, we could observe a slight activation of Stat3 upon IL-6 single stimulations that was reduced in patients suffering from (decompensated) liver cirrhosis. So, also the monocytes seem to have an impaired IL-6-Stat3 signalling axis. The preactivation supports the observation that monocytes could not be stimulated effectively by IL-6 and the refractoriness theory. Consequently, a therapeutic treatment with IL-6 will have only little influence. As the Stat3 activation seems to be affected in monocytes it would be of further interest whether this also affects the differentiation into macrophages and furthermore the polarization into M1 and M2 macrophages. Mauer et. al. [134] described the role of IL-6 signalling in murine macrophages and found IL-6 to be central for promoting M2 polarization and limiting LPS-induced endotoxemia. Dysfunctional response to IL-6 stimulation in our experiments might contribute to the fact that patients with late stage liver disease and ACLF incline to suffer from infections [69].

Collectively, this thesis could show new facets of the interdependence of different cytokines in hepatocytes and in the context of liver cirrhosis and ACLF. Cytokine combinations such as IL-6 and IL-22 increased the anti-microbial activity of hepatocytes without major negative influence on cell viability. Additionally,

hepatocytes showed refractoriness after repetitive cytokine stimulation for IL-6 and IL-22 which was also shown to occur in immune cells of liver disease patients. Furthermore, with disease aggravation, T cell subpopulations were less sensitive to IL-6 stimulation in general which need to be considered for future immune therapies. Considering cellular refractoriness for different cytokines might shape future application patterns. A deeper understanding of the whole cytokine network and the interplays between the different components is crucial to develop new therapeutic strategies. Moreover, new methods like machine learning approaches predict and facilitate identification of new combinatorial functions and synergistic or antagonistic mechanisms might be considered to expand the current knowledge [31]. Mouse models that mimic chronic liver disease might help to further elucidate the influence of combined cytokines *in vivo*. An example is the mouse model of the National Institute on Alcohol Abuse and Alcoholism (NIAAA) model from Bertola et. al [20]. It is a chronic-plus-binge alcohol feeding model that mimics the drinking pattern of patients with alcoholic liver disease. This the main experiment only lasts for eleven days plus 5 days for acclimatisation to tube feeding which is a huge advantage to other long-time chronic ethanol feeding models. Therapeutic cytokine doses can be administered easily during this time to evaluate the therapeutic potential of cytokine combinations.

6 Summaries

6.1 Summary and Outlook

Liver cirrhosis is the leading cause for liver-related deaths and may progress to development of ACLF. Cirrhosis-related immune dysfunction is well described in the literature as well as systemic inflammation that aggravates towards ACLF. Elevated levels of pro- and anti-inflammatory cytokines in these patients mirror this development. However, little is known about the interplay between the different upregulated cytokines and a deeper understanding is necessary to evaluate and improve immunotherapies.

The presented work aims to elucidate the interdependence of chosen cytokines, especially IL-6, IL-22 and IFNγ, in hepatocytes and PBMCs of patients suffering from different stages of liver cirrhosis and ACLF. Our results show that cytokines using the same signalling pathway often influence each other's signalling. In particular, the combination of IL-6 and IL-22 synergistically enhances short-term phosphorylation of Stat1 and Stat3 and supports anti-microbial effects by enhancing LBP RNA expression. However, IL-6 and IFNγ show antagonistic effects regarding TIMP-1 and IRF1 RNA expression. Furthermore, hepatocytes show refractoriness upon repetitive cytokine stimulation which is dependent on the respective cytokine. Though, refractoriness is not based on a general unresponsiveness of Stat phosphorylation itself as it is still inducible by stimulation with another cytokine that used the same Stat signalling molecules as seen for IL-6 and IL-22. Upon cytokine withdrawal, Stat phosphorylation could be reinduced earlier upon repetitive cytokine stimulation compared to hepatocytes that were continuously exposed to the cytokine. Results from multicolour flow cytometry experiments revealed a dysfunctional IL-6-Stat3 pathway in liver cirrhosis patients that aggravates during the course of disease shown by strongly impaired Stat3 phosphorylation, especially in patients with acute decompensation. Additionally, $CD4^+$ and $CD8^+$ T cell subpopulations become refractory upon repetitive cytokine stimulation with IL-6. A preactivation of the Stat3 signalling pathway was predominantly observed in monocytes but also in T cells.

The results show synergistic and antagonistic interdependences between cytokines which are described as upregulated in the context of liver cirrhosis and ACLF.

Continuous stimulation leads to ineffective activation of the IL-6/IL-22-Stat3 signalling axis in hepatocytes and T cells from patients in different states of liver cirrhosis. This might contribute to worsened liver regeneration capacity and increased risk of infection in those patients.

Future experimental approaches should consider the order of administration in combination cytokine therapies as it was shown to be possible to decouple toxicity from efficacy in syngeneic mouse tumour models (IL-2 and IFNα). Functional consequences in PBMCs need to be elaborated. Establishing an animal model that mimics liver cirrhosis and ACLF from patients is a good opportunity to confirm and further investigate the presented findings *in vivo*. It is of further interest how cytokine combinations affect other cells or tissues such as the gastrointestinal barrier function that is described to be strengthened by IL-22.

6.2 Zusammenfassung

Die Leberzirrhose ist der häufigste Grund für Leber-assoziierte Todesfälle. Eine Verschlechterung der Krankheit kann zur Entwicklung eines akut-auf-chronischen Leberversagens (ACLV) führen. Assoziiert mit Leberzirrhose und ACLV sind sowohl immunologische Dysfunktion als auch systemische Inflammation in den Patienten. Diese Symptome verschlechtern sich in Richtung eines ACLV. Zusätzlich sind erhöhte pro- und anti-inflammatorische Zytokinlevel beschrieben, wobei eine direkte Beziehung zwischen der Höhe der Zytokinlevel und dem Krankheitsfortschritt von Leberzirrhose zu ACLV gezeigt werden konnte. Ein besseres Verständnis der Bedeutung der Zytokine in der Krankheitspathogenese ist insbesondere im Hinblick auf ihre therapeutische Nutzbarkeit und ihr Manipulationspotential von großer Bedeutung

In der vorliegenden Arbeit sollen die Wechselwirkungen von ausgewählten Zytokinen, besonders von IL-6, IL-22 und IFNγ, in Hepatozyten und Patienten in verschiedenen Stadien der Leberzirrhose und des ACLV untersucht werden. Die dargestellten Ergebnisse zeigen, dass sich die Zytokine, welche denselben Signalweg bedienen, gegenseitig in ihrem Antwortverhalten beeinflussen. Im Besonderen die Kombination aus IL-6 und IL-22 zeigt einen Synergismus, welcher die kurzzeitige Phosphorylierung von Stat1 und Stat3 verstärkt und die Expression von anti-mikrobieller LBP RNA erhöht. Dahingegen zeigt die Kombination von IL-6 und IFNγ antagonistische Effekte auf die vom jeweils anderen Zytokin induzierte Signalantwort, wenn die Expression von TIMP-1 und IRF1 RNA betrachtet wird. Außerdem konnte in dieser Arbeit gezeigt werden, dass Hepatozyten nach wiederholter Zytokinstimulation und abhängig vom jeweiligen Zytokin refraktär werden. Die verminderte Reaktivität gegenüber einem wiederholten Zytokinstimulus, zum Beispiel IL-6, basiert dabei nicht auf einer generellen Dysfunktion des Stat-Signalwegs selbst, da dieser durch Stimulation mit einem anderen Zytokin, zum Beispiel IL-22, erneut aktiviert werden konnte. Wenn das entsprechende Zytokin dem Medium der Hepatozyten zwischen den Stimulationszeitpunkten entzogen wurde und die Hepatozyten dem Zytokin nicht dauerhaft ausgesetzt wurden, konnte eine schnellere Reaktivierung des Stat-Signalwegs erreicht werden im Vergleich zur dauerhaften Stimulation. Die Ergebnisse der durchflusszytometrischen Analysen zeigen einen gestörten IL-6-Stat3-Signalweg in Patienten mit Leberzirrhose. Diese

Störung verstärkt sich im Verlauf der Erkrankung, was durch stark verminderte Stat3-Phosphorylierung besonders in Patienten mit einer akut dekompensierten Zirrhose gezeigt wurde. Zusätzlich zeigen sich die CD4+- und CD8+-positiven T-Zellpopulationen refraktär bei wiederholter Stimulation mit IL-6. Eine Präakivierung des Stat3-Signalweges wurde deutlich in Monozyten aber auch in T-Zellen von Patienten gezeigt werden.

Die Ergebnisse zeigen synergistische und antagonistische Wechselwirkungen zwischen Zytokinen, die im Kontext einer Leberzirrhose und eines ACLV als hochreguliert beschrieben wurden. Bei dauerhafter Stimulierung wurde eine ineffektive Aktivierung der IL-6/IL-22-Stat3-Signalachse in Hepatozyten und T-Zellen von Patienten in verschiedenen Stadien der Leberzirrhose gezeigt. Dies kann zur verschlechterten Leberregenerationsfähigkeit und dem gesteigerten Infektionsrisiko der Patienten beitragen.

Zukünftige experimentelle Ansätze sollten berücksichtigen, dass die Reihenfolge der Zytokingabe Einfluss auf die Wirkungsweise haben kann. Die Etablierung eines Mausmodells, welches die Leberzirrhose und ACLV darstellen kann bietet eine gute Möglichkeit, die Ergebnisse dieser Arbeit *in vivo* zu bestätigen und weiter zu untersuchen. Da beschrieben ist, dass IL-22 die gastrointestinale Barrierefunktion bewahrt und beeinflusst ist es außerdem von Interesse, in welchem Umfang andere Zelltypen und Gewebe von den hohen Zytokinleveln der Patienten beeinflusst werden.

7 Bibliography

1. Abrams, S.T., et al., *A Novel Assay for Neutrophil Extracellular Trap Formation Independently Predicts Disseminated Intravascular Coagulation and Mortality in Critically Ill Patients.* Am J Respir Crit Care Med, 2019. **200**(7): p. 869-880.
2. Akira, S., S. Uematsu, and O. Takeuchi, *Pathogen recognition and innate immunity.* Cell, 2006. **124**(4): p. 783-801.
3. Alas, S. and B. Bonavida, *Rituximab inactivates signal transducer and activation of transcription 3 (STAT3) activity in B-non-Hodgkin's lymphoma through inhibition of the interleukin 10 autocrine/paracrine loop and results in down-regulation of Bcl-2 and sensitization to cytotoxic drugs.* Cancer Res, 2001. **61**(13): p. 5137-44.
4. Alberts B, J.A., Lewis J, et al. , *Molecular Biology of the Cell*. 4th edition ed. 2002: Garland Science.
5. Albillos, A., M. Lario, and M. Alvarez-Mon, *Cirrhosis-associated immune dysfunction: distinctive features and clinical relevance.* J Hepatol, 2014. **61**(6): p. 1385-96.
6. Andoh, A., et al., *Interleukin-22, a member of the IL-10 subfamily, induces inflammatory responses in colonic subepithelial myofibroblasts.* Gastroenterology, 2005. **129**(3): p. 969-84.
7. Anthony, P.P., et al., *The morphology of cirrhosis. Recommendations on definition, nomenclature, and classification by a working group sponsored by the World Health Organization.* Journal of clinical pathology, 1978. **31**(5): p. 395-414.
8. Arab, J.P., et al., *An Open-Label, Dose-Escalation Study to Assess the Safety and Efficacy of IL-22 Agonist F-652 in Patients With Alcohol-associated Hepatitis.* Hepatology, 2020. **n/a**(n/a).
9. Arroyo, V., et al., *Acute-on-chronic liver failure in cirrhosis.* Nat Rev Dis Primers, 2016. **2**: p. 16041.
10. Asrani, S.K., et al., *Burden of liver diseases in the world.* J Hepatol, 2019. **70**(1): p. 151-171.
11. Aujla, S.J., et al., *IL-22 mediates mucosal host defense against Gram-negative bacterial pneumonia.* Nat Med, 2008. **14**(3): p. 275-81.
12. Babon, J.J., L.N. Varghese, and N.A. Nicola, *Inhibition of IL-6 family cytokines by SOCS3.* Seminars in immunology, 2014. **26**(1): p. 13-19.
13. Baggiolini, M., *Chemokines in pathology and medicine.* J Intern Med, 2001. **250**(2): p. 91-104.
14. Baroni, G.S., et al., *Interferon gamma decreases hepatic stellate cell activation and extracellular matrix deposition in rat liver fibrosis.* Hepatology, 1996. **23**(5): p. 1189-99.
15. Bataller, R. and D.A. Brenner, *Liver fibrosis.* The Journal of Clinical Investigation, 2005. **115**(4): p. 1100-1100.
16. Batra, J., et al., *Matrix metalloproteinase-10 (MMP-10) interaction with tissue inhibitors of metalloproteinases TIMP-1 and TIMP-2: binding studies and crystal structure.* The Journal of biological chemistry, 2012. **287**(19): p. 15935-15946.
17. Beattie, L., et al., *Dynamic imaging of experimental Leishmania donovani-induced hepatic granulomas detects Kupffer cell-restricted antigen presentation to antigen-specific CD8 T cells.* PLoS Pathog, 2010. **6**(3): p. e1000805.

18. Beiras, R., *Chapter 12 - Biotransformation*, in *Marine Pollution*, R. Beiras, Editor. 2018, Elsevier. p. 205-214.
19. Bendall, L.J. and K.F. Bradstock, *G-CSF: From granulopoietic stimulant to bone marrow stem cell mobilizing agent.* Cytokine Growth Factor Rev, 2014. **25**(4): p. 355-67.
20. Bertola, A., et al., *Mouse model of chronic and binge ethanol feeding (the NIAAA model).* Nature protocols, 2013. **8**(3): p. 627-637.
21. Bhat, M.Y., et al., *Comprehensive network map of interferon gamma signaling.* Journal of cell communication and signaling, 2018. **12**(4): p. 745-751.
22. Bleicher, L., et al., *Crystal structure of the IL-22/IL-22R1 complex and its implications for the IL-22 signaling mechanism.* FEBS Lett, 2008. **582**(20): p. 2985-92.
23. Blindenbacher, A., et al., *Interleukin 6 is important for survival after partial hepatectomy in mice.* Hepatology, 2003. **38**(3): p. 674-82.
24. Borregaard, N., *Neutrophils, from marrow to microbes.* Immunity, 2010. **33**(5): p. 657-70.
25. Boyman, O. and J. Sprent, *The role of interleukin-2 during homeostasis and activation of the immune system.* Nature Reviews Immunology, 2012. **12**(3): p. 180-190.
26. Brinkmann, V., et al., *Neutrophil extracellular traps kill bacteria.* Science, 2004. **303**(5663): p. 1532-5.
27. Brunner, T., et al., *Fas (CD95/Apo-1) ligand regulation in T cell homeostasis, cell-mediated cytotoxicity and immune pathology.* Seminars in Immunology, 2003. **15**(3): p. 167-176.
28. Bukowski, J.F., et al., *Adoptive transfer studies demonstrating the antiviral effect of natural killer cells in vivo.* The Journal of experimental medicine, 1985. **161**(1): p. 40-52.
29. Burgdorf, S., et al., *Distinct pathways of antigen uptake and intracellular routing in CD4 and CD8 T cell activation.* Science, 2007. **316**(5824): p. 612-6.
30. Campana, L., et al., *Liver regeneration and inflammation: from fundamental science to clinical applications.* Nature Reviews Molecular Cell Biology, 2021.
31. Cappuccio, A., et al., *Deciphering the combinatorial landscape of immunity.* Elife, 2020. **9**.
32. Caraceni, P., et al., *Long-term albumin administration in decompensated cirrhosis (ANSWER): an open-label randomised trial.* The Lancet, 2018. **391**(10138): p. 2417-2429.
33. Castell, J.V., et al., *Interleukin-6 is the major regulator of acute phase protein synthesis in adult human hepatocytes.* FEBS Lett, 1989. **242**(2): p. 237-9.
34. Cerwenka, A., J.L. Baron, and L.L. Lanier, *Ectopic expression of retinoic acid early inducible-1 gene (RAE-1) permits natural killer cell-mediated rejection of a MHC class I-bearing tumor in vivo.* Proceedings of the National Academy of Sciences of the United States of America, 2001. **98**(20): p. 11521-11526.
35. Chavez-Tapia, N.C., et al., *Granulocyte-colony stimulating factor for acute-on-chronic liver failure: systematic review and meta-analysis.* Ann Hepatol, 2015. **14**(5): p. 631-41.
36. Chen, L., et al., *IL-6 influences the polarization of macrophages and the formation and growth of colorectal tumor.* Oncotarget, 2018. **9**(25): p. 17443-17454.
37. Child, C.G. and J.G. Turcotte, *Surgery and portal hypertension.* Major Probl Clin Surg, 1964. **1**: p. 1-85.

38. Chomarat, P., et al., *IL-6 switches the differentiation of monocytes from dendritic cells to macrophages.* Nature Immunology, 2000. **1**(6): p. 510-514.
39. Christoffersson, G. and M. Phillipson, *The neutrophil: one cell on many missions or many cells with different agendas?* Cell and Tissue Research, 2018. **371**(3): p. 415-423.
40. Chung, Y., et al., *Expression and regulation of IL-22 in the IL-17-producing CD4+ T lymphocytes.* Cell Research, 2006. **16**(11): p. 902-907.
41. Claria, J., V. Arroyo, and R. Moreau, *The Acute-on-Chronic Liver Failure Syndrome, or When the Innate Immune System Goes Astray.* J Immunol, 2016. **197**(10): p. 3755-3761.
42. Claria, J., et al., *Systemic inflammation in decompensated cirrhosis: Characterization and role in acute-on-chronic liver failure.* Hepatology, 2016. **64**(4): p. 1249-64.
43. Collaborators, G.B.D.C.o.D., *Global, regional, and national age-sex-specific mortality for 282 causes of death in 195 countries and territories, 1980-2017: a systematic analysis for the Global Burden of Disease Study 2017.* Lancet (London, England), 2018. **392**(10159): p. 1736-1788.
44. Cosman, D., et al., *ULBPs, novel MHC class I-related molecules, bind to CMV glycoprotein UL16 and stimulate NK cytotoxicity through the NKG2D receptor.* Immunity, 2001. **14**(2): p. 123-33.
45. Costa, D., et al., *Systemic inflammation increases across distinct stages of advanced chronic liver disease and correlates with decompensation and mortality.* Journal of Hepatology, 2021. **74**(4): p. 819-828.
46. Cressman, D.E., et al., *Liver failure and defective hepatocyte regeneration in interleukin-6- deficient mice.* Science, 1996. **274**(5291): p. 1379-1383.
47. Croker, B.A., J. Silke, and M. Gerlic, *Fight or flight: regulation of emergency hematopoiesis by pyroptosis and necroptosis.* Curr Opin Hematol, 2015. **22**(4): p. 293-301.
48. Daniels, M.A., et al., *CD8 binding to MHC class I molecules is influenced by T cell maturation and glycosylation.* Immunity, 2001. **15**(6): p. 1051-61.
49. Dasgupta, A., *Chapter 5 - Liver Enzymes as Alcohol Biomarkers*, in *Alcohol and its Biomarkers*, A. Dasgupta, Editor. 2015, Elsevier: San Diego. p. 121-137.
50. Davies, L.C., et al., *Tissue-resident macrophages.* Nature Immunology, 2013. **14**(10): p. 986-995.
51. Delneste, Y., et al., *Interferon-γ switches monocyte differentiation from dendritic cells to macrophages.* Blood, 2003. **101**(1): p. 143-150.
52. Diefenbach, A., et al., *Rae1 and H60 ligands of the NKG2D receptor stimulate tumour immunity.* Nature, 2001. **413**(6852): p. 165-71.
53. Diehl, S. and M. Rincón, *The two faces of IL-6 on Th1/Th2 differentiation.* Molecular Immunology, 2002. **39**(9): p. 531-536.
54. Dienz, O. and M. Rincon, *The effects of IL-6 on CD4 T cell responses.* Clinical immunology (Orlando, Fla.), 2009. **130**(1): p. 27-33.
55. Drucker, C., et al., *Impact of interleukin-6 classic- and trans-signaling on liver damage and regeneration.* J Autoimmun, 2010. **34**(1): p. 29-37.
56. Duan, X.Z., et al., *Granulocyte-colony stimulating factor therapy improves survival in patients with hepatitis B virus-associated acute-on-chronic liver failure.* World J Gastroenterol, 2013. **19**(7): p. 1104-10.
57. Dudakov, J.A., A.M. Hanash, and M.R.M. van den Brink, *Interleukin-22: immunobiology and pathology.* Annual review of immunology, 2015. **33**: p. 747-785.

58. Dufour, J.-F. and P.-A. Clavien, *Signaling Pathways in Liver Diseases*. 3rd ed. 2015: Wiley Blackwell.
59. Duhen, T., et al., *Production of interleukin 22 but not interleukin 17 by a subset of human skin-homing memory T cells.* Nat Immunol, 2009. **10**(8): p. 857-63.
60. Dustin, M.L., *The immunological synapse.* Cancer immunology research, 2014. **2**(11): p. 1023-1033.
61. Egea, L., Y. Hirata, and M.F. Kagnoff, *GM-CSF: a role in immune and inflammatory reactions in the intestine.* Expert review of gastroenterology & hepatology, 2010. **4**(6): p. 723-731.
62. Ellett, J.D., et al., *Murine Kupffer Cells Are Protective in Total Hepatic Ischemia/Reperfusion Injury with Bowel Congestion through IL-10.* The Journal of Immunology, 2010. **184**(10): p. 5849.
63. Embgenbroich, M. and S. Burgdorf, *Current Concepts of Antigen Cross-Presentation.* Frontiers in Immunology, 2018. **9**(1643).
64. Engel, P., et al., *CD Nomenclature 2015: Human Leukocyte Differentiation Antigen Workshops as a Driving Force in Immunology.* The Journal of Immunology, 2015. **195**(10): p. 4555.
65. Engelmann, C., et al., *Granulocyte-Colony Stimulating Factor (G-CSF) to treat acute-on-chronic liver failure, a multicenter randomized trial (GRAFT study).* J Hepatol, 2021.
66. Erhardt, A., et al., *Treatment of chronic hepatitis delta with pegylated interferon-alpha2b.* Liver Int, 2006. **26**(7): p. 805-10.
67. Fazel Modares, N., et al., *IL-6 Trans-signaling Controls Liver Regeneration After Partial Hepatectomy.* Hepatology, 2019. **70**(6): p. 2075-2091.
68. Feng, D., et al., *Interleukin-22 promotes proliferation of liver stem/progenitor cells in mice and patients with chronic hepatitis B virus infection.* Gastroenterology, 2012. **143**(1): p. 188-98.e7.
69. Fernández, J., et al., *Management of bacterial and fungal infections in cirrhosis: The MDRO challenge.* Journal of Hepatology, 2021. **75**: p. S101-S117.
70. François-Newton, V., et al., *USP18-based negative feedback control is induced by type I and type III interferons and specifically inactivates interferon α response.* PLoS One, 2011. **6**(7): p. e22200.
71. Frank, M.M. and L.F. Fries, *The role of complement in inflammation and phagocytosis.* Immunol Today, 1991. **12**(9): p. 322-6.
72. Fuchs, T.A., et al., *Novel cell death program leads to neutrophil extracellular traps.* The Journal of cell biology, 2007. **176**(2): p. 231-241.
73. Fuchs, T.A., et al., *Extracellular DNA traps promote thrombosis.* Proc Natl Acad Sci U S A, 2010. **107**(36): p. 15880-5.
74. Gabay, C., et al., *Tocilizumab monotherapy versus adalimumab monotherapy for treatment of rheumatoid arthritis (ADACTA): a randomised, double-blind, controlled phase 4 trial.* Lancet, 2013. **381**(9877): p. 1541-50.
75. Gagnon, J., et al., *IL-6, in Synergy with IL-7 or IL-15, Stimulates TCR-Independent Proliferation and Functional Differentiation of CD8⁺ T Lymphocytes.* The Journal of Immunology, 2008. **180**(12): p. 7958.
76. Gaïni, S., et al., *Procalcitonin, lipopolysaccharide-binding protein, interleukin-6 and C-reactive protein in community-acquired infections and sepsis: a prospective study.* Critical Care, 2006. **10**(2): p. R53.
77. Gao, B., *Cytokines, STATs and liver disease.* Cell Mol Immunol, 2005. **2**(2): p. 92-100.

78. Gao, B., W.I. Jeong, and Z. Tian, *Liver: An organ with predominant innate immunity.* Hepatology, 2008. **47**(2): p. 729-736.
79. Garg, V., et al., *Granulocyte colony-stimulating factor mobilizes CD34(+) cells and improves survival of patients with acute-on-chronic liver failure.* Gastroenterology, 2012. **142**(3): p. 505-512.e1.
80. Gaudino, S.J. and P. Kumar, *Cross-Talk Between Antigen Presenting Cells and T Cells Impacts Intestinal Homeostasis, Bacterial Infections, and Tumorigenesis.* Frontiers in immunology, 2019. **10**: p. 360-360.
81. Gauldie, J., et al., *Interferon beta 2/B-cell stimulatory factor type 2 shares identity with monocyte-derived hepatocyte-stimulating factor and regulates the major acute phase protein response in liver cells.* Proceedings of the National Academy of Sciences, 1987. **84**(20): p. 7251.
82. Gewiese-Rabsch, J., et al., *Role of IL-6 trans-signaling in CCl4 induced liver damage.* Biochimica et Biophysica Acta (BBA) - Molecular Basis of Disease, 2010. **1802**(11): p. 1054-1061.
83. Gibbert, K., et al., *IFN-alpha subtypes: distinct biological activities in anti-viral therapy.* Br J Pharmacol, 2013. **168**(5): p. 1048-58.
84. Gilgenkrantz, H. and A. Collin de l'Hortet, *Understanding Liver Regeneration: From Mechanisms to Regenerative Medicine.* The American Journal of Pathology, 2018. **188**(6): p. 1316-1327.
85. Grabowski, J., et al., *Hepatitis D virus-specific cytokine responses in patients with chronic hepatitis delta before and during interferon alfa-treatment.* Liver Int, 2011. **31**(9): p. 1395-405.
86. Guglani, L. and S.A. Khader, *Th17 cytokines in mucosal immunity and inflammation.* Current Opinion in HIV and AIDS, 2010. **5**(2).
87. Guidelines, E., *EASL Clinical Practice Guidelines for the management of patients with decompensated cirrhosis.* Journal of Hepatology, 2018. **69**(2): p. 406-460.
88. Gunsar, F., *Treatment of delta hepatitis.* Expert Rev Anti Infect Ther, 2013. **11**(5): p. 489-98.
89. Heinrich, P.C., J.V. Castell, and T. Andus, *Interleukin-6 and the acute phase response.* The Biochemical journal, 1990. **265**(3): p. 621-636.
90. Hernández-Gea, V., et al., *Preemptive-TIPS Improves Outcome in High-Risk Variceal Bleeding: An Observational Study.* Hepatology, 2019. **69**(1): p. 282-293.
91. Hibi, M., K. Nakajima, and T. Hirano, *IL-6 cytokine family and signal transduction: a model of the cytokine system.* J Mol Med (Berl), 1996. **74**(1): p. 1-12.
92. Hidalgo, A., et al., *The Neutrophil Life Cycle.* Trends Immunol, 2019. **40**(7): p. 584-597.
93. Hirano, T., et al., *Complementary DNA for a novel human interleukin (BSF-2) that induces B lymphocytes to produce immunoglobulin.* Nature, 1986. **324**(6092): p. 73-6.
94. Hong, J., et al., *Recombinant soluble gp130 protein reduces DEN-induced primary hepatocellular carcinoma in mice.* Scientific Reports, 2016. **6**(1): p. 24397.
95. Horras, C.J., C.L. Lamb, and K.A. Mitchell, *Regulation of hepatocyte fate by interferon-γ.* Cytokine & growth factor reviews, 2011. **22**(1): p. 35-43.
96. Hu, X., S.D. Chakravarty, and L.B. Ivashkiv, *Regulation of interferon and Toll-like receptor signaling during macrophage activation by opposing feedforward*

and feedback inhibition mechanisms. Immunological reviews, 2008. **226**: p. 41-56.
97. Huppa, J.B. and M.M. Davis, *T-cell-antigen recognition and the immunological synapse.* Nature Reviews Immunology, 2003. **3**(12): p. 973-983.
98. Isaacs, A. and J. Lindenmann, *Virus interference. I. The interferon.* Proc R Soc Lond B Biol Sci, 1957. **147**(927): p. 258-67.
99. Iwasaki, A. and R. Medzhitov, *Control of adaptive immunity by the innate immune system.* Nature immunology, 2015. **16**(4): p. 343-353.
100. James, L.P., et al., *Interleukin 6 and hepatocyte regeneration in acetaminophen toxicity in the mouse.* Biochem Biophys Res Commun, 2003. **309**(4): p. 857-63.
101. Jenne, C.N. and P. Kubes, *Immune surveillance by the liver.* Nat Immunol, 2013. **14**(10): p. 996-1006.
102. Joffre, O.P., et al., *Cross-presentation by dendritic cells.* Nat Rev Immunol, 2012. **12**(8): p. 557-69.
103. Jones, B.C., N.J. Logsdon, and M.R. Walter, *Structure of IL-22 bound to its high-affinity IL-22R1 chain.* Structure (London, England : 1993), 2008. **16**(9): p. 1333-1344.
104. Kandasamy, K., et al., *NetPath: a public resource of curated signal transduction pathways.* Genome biology, 2010. **11**(1): p. R3-R3.
105. Kang, K., et al., *IFN-γ selectively suppresses a subset of TLR4-activated genes and enhancers to potentiate macrophage activation.* Nature Communications, 2019. **10**(1): p. 3320.
106. Kang, S., et al., *Targeting Interleukin-6 Signaling in Clinic.* Immunity, 2019. **50**(4): p. 1007-1023.
107. Kano, A., et al., *IRF-1 is an essential mediator in IFN-gamma-induced cell cycle arrest and apoptosis of primary cultured hepatocytes.* Biochem Biophys Res Commun, 1999. **257**(3): p. 672-7.
108. Kay, A.B., *Paul Ehrlich and the Early History of Granulocytes.* Microbiol Spectr, 2016. **4**(4).
109. Keir, M., et al., *The role of IL-22 in intestinal health and disease.* The Journal of experimental medicine, 2020. **217**(3): p. e20192195-e20192195.
110. Ki, S.H., et al., *Interleukin-22 treatment ameliorates alcoholic liver injury in a murine model of chronic-binge ethanol feeding: role of signal transducer and activator of transcription 3.* Hepatology, 2010. **52**(4): p. 1291-300.
111. Kishimoto, T., *IL-6: from its discovery to clinical applications.* International Immunology, 2010. **22**(5): p. 347-352.
112. König, R., L.Y. Huang, and R.N. Germain, *MHC class II interaction with CD4 mediated by a region analogous to the MHC class I binding site for CD8.* Nature, 1992. **356**(6372): p. 796-8.
113. Kopf, M., et al., *Impaired immune and acute-phase responses in interleukin-6-deficient mice.* Nature, 1994. **368**(6469): p. 339-342.
114. Kotenko, S.V., et al., *Identification of the functional interleukin-22 (IL-22) receptor complex: the IL-10R2 chain (IL-10Rbeta) is a common chain of both the IL-10 and IL-22 (IL-10-related T cell-derived inducible factor, IL-TIF) receptor complexes.* J Biol Chem, 2001. **276**(4): p. 2725-32.
115. Kroy, D.C., et al., *Lack of interleukin-6/glycoprotein 130/signal transducers and activators of transcription-3 signaling in hepatocytes predisposes to liver steatosis and injury in mice.* Hepatology, 2010. **51**(2): p. 463-73.
116. Kubes, P. and C. Jenne, *Immune Responses in the Liver.* Annual Review of Immunology, 2018. **36**(1): p. 247-277.

117. Kumar, A., et al., *Natural Killer T Cells: An Ecological Evolutionary Developmental Biology Perspective.* Frontiers in Immunology, 2017. **8**(1858).
118. Laleman, W., et al., *Systemic Inflammation and Acute-on-Chronic Liver Failure: Too Much, Not Enough.* Can J Gastroenterol Hepatol, 2018. **2018**: p. 1027152.
119. Lange, C.M. and R. Moreau, *Immunodysfunction in Acute-on-Chronic Liver Failure.* Visc Med, 2018. **34**(4): p. 276-282.
120. LeBien, T.W. and T.F. Tedder, *B lymphocytes: how they develop and function.* Blood, 2008. **112**(5): p. 1570-1580.
121. Lejeune, D., et al., *Interleukin-22 (IL-22) Activates the JAK/STAT, ERK, JNK, and p38 MAP Kinase Pathways in a Rat Hepatoma Cell Line: PATHWAYS THAT ARE SHARED WITH AND DISTINCT FROM IL-10*.* Journal of Biological Chemistry, 2002. **277**(37): p. 33676-33682.
122. Leroy, V., et al., *Circulating matrix metalloproteinases 1, 2, 9 and their inhibitors TIMP-1 and TIMP-2 as serum markers of liver fibrosis in patients with chronic hepatitis C: comparison with PIIINP and hyaluronic acid.* Am J Gastroenterol, 2004. **99**(2): p. 271-9.
123. Liang, S.C., et al., *IL-22 induces an acute-phase response.* J Immunol, 2010. **185**(9): p. 5531-8.
124. Lo, B.C., et al., *IL-22 Preserves Gut Epithelial Integrity and Promotes Disease Remission during Chronic Salmonella Infection.* The Journal of Immunology, 2019. **202**(3): p. 956.
125. Logsdon, N.J., et al., *The IL-10R2 binding hot spot on IL-22 is located on the N-terminal helix and is dependent on N-linked glycosylation.* J Mol Biol, 2004. **342**(2): p. 503-14.
126. Long, E.O. and S. Rajagopalan, *Stress signals activate natural killer cells.* The Journal of experimental medicine, 2002. **196**(11): p. 1399-1402.
127. Lu, W.-Y., et al., *Hepatic progenitor cells of biliary origin with liver repopulation capacity.* Nature Cell Biology, 2015. **17**(8): p. 971-983.
128. Madonna, S., et al., *Suppressor of cytokine signaling 1 inhibits IFN-gamma inflammatory signaling in human keratinocytes by sustaining ERK1/2 activation.* Faseb j, 2008. **22**(9): p. 3287-97.
129. Maecker, H.T., J.P. McCoy, and R. Nussenblatt, *Standardizing immunophenotyping for the Human Immunology Project.* Nature Reviews Immunology, 2012. **12**(3): p. 191-200.
130. Mahnke, Y.D., et al., *The who's who of T-cell differentiation: human memory T-cell subsets.* Eur J Immunol, 2013. **43**(11): p. 2797-809.
131. Manns, M.E.G.a.J.M.V.a.M.P., *Liver Immunology*. 2014: Springer International Publishing.
132. Marasco, E., et al., *B-cell activation with CD40L or CpG measures the function of B-cell subsets and identifies specific defects in immunodeficient patients.* Eur J Immunol, 2017. **47**(1): p. 131-143.
133. Martin-Mateos, R., M. Alvarez-Mon, and A. Albillos, *Dysfunctional Immune Response in Acute-on-Chronic Liver Failure: It Takes Two to Tango.* Frontiers in immunology, 2019. **10**: p. 973-973.
134. Mauer, J., et al., *Signaling by IL-6 promotes alternative activation of macrophages to limit endotoxemia and obesity-associated resistance to insulin.* Nat Immunol, 2014. **15**(5): p. 423-30.
135. Mayadas, T.N., X. Cullere, and C.A. Lowell, *The multifaceted functions of neutrophils.* Annual review of pathology, 2014. **9**: p. 181-218.

136. McCullough, C.T., B.J. Tura, and D.J. Harrison, *Growth factor attenuation of IFNγ-mediated hepatocyte apoptosis requires p21waf−1.* International Journal of Experimental Pathology, 2006. **87**(4): p. 275-281.
137. McNab, F., et al., *Type I interferons in infectious disease.* Nature Reviews Immunology, 2015. **15**(2): p. 87-103.
138. Medeiros, T., et al., *Liver fibrosis improvement in chronic hepatitis C after direct acting-antivirals is accompanied by reduced profibrogenic biomarkers-a role for MMP-9/TIMP-1.* Dig Liver Dis, 2020. **52**(10): p. 1170-1177.
139. Michalopoulos, G.K., *Hepatostat: Liver regeneration and normal liver tissue maintenance.* Hepatology, 2017. **65**(4): p. 1384-1392.
140. Michalopoulos, G.K. and B. Bhushan, *Liver regeneration: biological and pathological mechanisms and implications.* Nature Reviews Gastroenterology & Hepatology, 2021. **18**(1): p. 40-55.
141. Mitra, A., S.K. Raychaudhuri, and S.P. Raychaudhuri, *IL-22 induced cell proliferation is regulated by PI3K/Akt/mTOR signaling cascade.* Cytokine, 2012. **60**(1): p. 38-42.
142. Miyake, K. and H. Karasuyama, *Emerging roles of basophils in allergic inflammation.* Allergology International, 2017. **66**(3): p. 382-391.
143. Mokdad, A.A., et al., *Liver cirrhosis mortality in 187 countries between 1980 and 2010: a systematic analysis.* BMC Medicine, 2014. **12**(1): p. 145.
144. Moreau, R., et al., *Acute-on-chronic liver failure is a distinct syndrome that develops in patients with acute decompensation of cirrhosis.* Gastroenterology, 2013. **144**(7): p. 1426-37, 1437 e1-9.
145. Mosmann, T.R., et al., *Two types of murine helper T cell clone. I. Definition according to profiles of lymphokine activities and secreted proteins.* J Immunol, 1986. **136**(7): p. 2348-57.
146. Muir, A.J., P.B. Sylvestre, and D.C. Rockey, *Interferon gamma-1b for the treatment of fibrosis in chronic hepatitis C infection.* Journal of Viral Hepatitis, 2006. **13**(5): p. 322-328.
147. Müller, U., et al., *The innate immune system of mammals and insects.* Contrib Microbiol, 2008. **15**: p. 21-44.
148. Paget, C., et al., *Interleukin-22 is produced by invariant natural killer T lymphocytes during influenza A virus infection: potential role in protection against lung epithelial damages.* J Biol Chem, 2012. **287**(12): p. 8816-29.
149. Pan, C.-x., et al., *Role of interleukin-22 in liver diseases.* Inflammation research : official journal of the European Histamine Research Society ... [et al.], 2014. **63**(7): p. 519-525.
150. Park, J., et al., *Elevated level of SUMOylated IRF-1 in tumor cells interferes with IRF-1-mediated apoptosis.* Proc Natl Acad Sci U S A, 2007. **104**(43): p. 17028-33.
151. Parker, B.S., J. Rautela, and P.J. Hertzog, *Antitumour actions of interferons: implications for cancer therapy.* Nature Reviews Cancer, 2016. **16**(3): p. 131-144.
152. Pellegrini, M., et al., *IL-7 engages multiple mechanisms to overcome chronic viral infection and limit organ pathology.* Cell, 2011. **144**(4): p. 601-13.
153. Pestka, S., C.D. Krause, and M.R. Walter, *Interferons, interferon-like cytokines, and their receptors.* Immunol Rev, 2004. **202**: p. 8-32.
154. Peters, M., et al., *Combined interleukin 6 and soluble interleukin 6 receptor accelerates murine liver regeneration.* Gastroenterology, 2000. **119**(6): p. 1663-71.

155. Pillay, J., et al., *In vivo labeling with 2H2O reveals a human neutrophil lifespan of 5.4 days.* Blood, 2010. **116**(4): p. 625-7.
156. Platanias, L.C., *Mechanisms of type-I- and type-II-interferon-mediated signalling.* Nat Rev Immunol, 2005. **5**(5): p. 375-86.
157. Pradhan, A.D., et al., *C-Reactive Protein, Interleukin 6, and Risk of Developing Type 2 Diabetes Mellitus.* JAMA, 2001. **286**(3): p. 327-334.
158. Price, D.A., et al., *Cytotoxic T lymphocytes, chemokines and antiviral immunity.* Immunol Today, 1999. **20**(5): p. 212-6.
159. Puel, A. and J.-L. Casanova, *The nature of human IL-6.* Journal of Experimental Medicine, 2019. **216**(9): p. 1969-1971.
160. Qin, B., et al., *IL-6 Inhibits Starvation-induced Autophagy via the STAT3/Bcl-2 Signaling Pathway.* Scientific Reports, 2015. **5**(1): p. 15701.
161. Qing, Y. and G.R. Stark, *Alternative activation of STAT1 and STAT3 in response to interferon-gamma.* J Biol Chem, 2004. **279**(40): p. 41679-85.
162. Radaeva, S., et al., *Interleukin 22 (IL-22) plays a protective role in T cell-mediated murine hepatitis: IL-22 is a survival factor for hepatocytes via STAT3 activation.* Hepatology, 2004. **39**(5): p. 1332-42.
163. Randall, G., et al., *Silencing of USP18 potentiates the antiviral activity of interferon against hepatitis C virus infection.* Gastroenterology, 2006. **131**(5): p. 1584-91.
164. Read, S.A., et al., *The Mechanism of Interferon Refractoriness During Hepatitis C Virus Infection and Its Reversal with a Peroxisome Proliferator-Activated Receptor α Agonist.* Journal of interferon & cytokine research : the official journal of the International Society for Interferon and Cytokine Research, 2015. **35**(6): p. 488-497.
165. Ren, X., B. Hu, and L.M. Colletti, *IL-22 is involved in liver regeneration after hepatectomy.* American journal of physiology. Gastrointestinal and liver physiology, 2010. **298**(1): p. G74-G80.
166. Richards, M.K., et al., *Pivotal role of granulocyte colony-stimulating factor in the development of progenitors in the common myeloid pathway.* Blood, 2003. **102**(10): p. 3562-8.
167. Robinson, M.W., C. Harmon, and C. O'Farrelly, *Liver immunology and its role in inflammation and homeostasis.* Cellular & Molecular Immunology, 2016. **13**(3): p. 267-276.
168. Roche, P.A. and K. Furuta, *The ins and outs of MHC class II-mediated antigen processing and presentation.* Nature reviews. Immunology, 2015. **15**(4): p. 203-216.
169. Rockey, D.C. and J.J. Chung, *Interferon gamma inhibits lipocyte activation and extracellular matrix mRNA expression during experimental liver injury: implications for treatment of hepatic fibrosis.* J Investig Med, 1994. **42**(4): p. 660-70.
170. Romeo, G., et al., *IRF-1 as a negative regulator of cell proliferation.* J Interferon Cytokine Res, 2002. **22**(1): p. 39-47.
171. Rose-John, S. and M.F. Neurath, *IL-6 "trans"-Signaling: The Heat Is On.* Immunity, 2004. **20**(1): p. 2-4.
172. Rothschilds, A., et al., *Order of administration of combination cytokine therapies can decouple toxicity from efficacy in syngeneic mouse tumor models.* OncoImmunology, 2019. **8**(5): p. e1558678.
173. Rueschenbaum, S., et al., *Translation of IRF-1 Restricts Hepatic Interleukin-7 Production to Types I and II Interferons: Implications for Hepatic Immunity.* Frontiers in immunology, 2021. **11**: p. 581352-581352.

174. Rueschenbaum, S., et al., *Dysregulated Adaptive Immunity Is an Early Event in Liver Cirrhosis Preceding Acute-on-Chronic Liver Failure.* Front Immunol, 2020. **11**: p. 534731.
175. Rüschenbaum, S., *The role of Interleukin-7 in hepatocellular immunoregulation*. 2018.
176. Sarasin-Filipowicz, M., et al., *Alpha interferon induces long-lasting refractoriness of JAK-STAT signaling in the mouse liver through induction of USP18/UBP43.* Mol Cell Biol, 2009. **29**(17): p. 4841-51.
177. Saravia, J., N.M. Chapman, and H. Chi, *Helper T cell differentiation.* Cellular & Molecular Immunology, 2019. **16**(7): p. 634-643.
178. Sarrazin, C., et al., *[Prophylaxis, diagnosis and therapy of hepatitis-C-virus (HCV) infection: the German guidelines on the management of HCV infection - AWMF-Register-No.: 021/012].* Z Gastroenterol, 2018. **56**(7): p. 756-838.
179. Sato, T., et al., *Inhibition of interferon regulatory factor-1 expression results in predominance of cell growth stimulatory effects of interferon-gamma due to phosphorylation of Stat1 and Stat3.* Blood, 1997. **90**(12): p. 4749-58.
180. Saxton, R.A., et al., *The tissue protective functions of interleukin-22 can be decoupled from pro-inflammatory actions through structure-based design.* Immunity, 2021. **54**(4): p. 660-672.e9.
181. Schmidt-Arras, D. and S. Rose-John, *IL-6 pathway in the liver: From physiopathology to therapy.* Journal of Hepatology, 2016. **64**(6): p. 1403-1415.
182. Schroder, K., et al., *Interferon-γ: an overview of signals, mechanisms and functions.* Journal of Leukocyte Biology, 2004. **75**(2): p. 163-189.
183. Schuchmann, M., *Klinisches Management der Leberzirrhose und ihrer Komplikationen*. 2014: Thieme.
184. Schulze, R.J., et al., *The cell biology of the hepatocyte: A membrane trafficking machine.* J Cell Biol, 2019. **218**(7): p. 2096-2112.
185. Schwarzkopf, K., et al., *IL-22 and IL-22-Binding Protein Are Associated With Development of and Mortality From Acute-on-Chronic Liver Failure.* Hepatol Commun, 2019. **3**(3): p. 392-405.
186. Schwarzkopf, K.M., et al., *Interleukin-22 in acute-on-chronic liver failure: A matter of ineffective levels, receptor dysregulation or defective signalling?* J Hepatol, 2020.
187. Seder, R.A. and W.E. Paul, *Acquisition of lymphokine-producing phenotype by CD4+ T cells.* Annu Rev Immunol, 1994. **12**: p. 635-73.
188. Sepanlou, S.G., et al., *The global, regional, and national burden of cirrhosis by cause in 195 countries and territories, 1990–2017: a systematic analysis for the Global Burden of Disease Study 2017.* The Lancet Gastroenterology & Hepatology, 2020. **5**(3): p. 245-266.
189. Simonetto, D.A., V.H. Shah, and P.S. Kamath, *Improving survival in ACLF: growing evidence for use of G-CSF.* Hepatol Int, 2017. **11**(6): p. 473-475.
190. Sohn, S.J., et al., *A restricted role for TYK2 catalytic activity in human cytokine responses revealed by novel TYK2-selective inhibitors.* Journal of immunology (Baltimore, Md. : 1950), 2013. **191**(5): p. 2205-2216.
191. Solé, C., et al., *Characterization of Inflammatory Response in Acute-on-Chronic Liver Failure and Relationship with Prognosis.* Scientific reports, 2016. **6**: p. 32341-32341.
192. Starr, R., et al., *SOCS-1 binding to tyrosine 441 of IFN-gamma receptor subunit 1 contributes to the attenuation of IFN-gamma signaling in vivo.* J Immunol, 2009. **183**(7): p. 4537-44.

193. Steinman, R.M. and H. Hemmi, *Dendritic cells: translating innate to adaptive immunity.* Curr Top Microbiol Immunol, 2006. **311**: p. 17-58.
194. Stevens, T.L., et al., *Regulation of antibody isotype secretion by subsets of antigen-specific helper T cells.* Nature, 1988. **334**(6179): p. 255-8.
195. Strnad, P., et al., *Liver — guardian, modifier and target of sepsis.* Nature Reviews Gastroenterology & Hepatology, 2017. **14**(1): p. 55-66.
196. Su, Z.Z., et al., *Central role of interferon regulatory factor-1 (IRF-1) in controlling retinoic acid inducible gene-I (RIG-I) expression.* J Cell Physiol, 2007. **213**(2): p. 502-10.
197. Sun, H., et al., *Tissue-resident lymphocytes: from adaptive to innate immunity.* Cellular & Molecular Immunology, 2019. **16**(3): p. 205-215.
198. Sun, R. and B. Gao, *Negative regulation of liver regeneration by innate immunity (natural killer cells/interferon-gamma).* Gastroenterology, 2004. **127**(5): p. 1525-39.
199. Sun, R., et al., *STAT1 contributes to dsRNA inhibition of liver regeneration after partial hepatectomy in mice.* Hepatology, 2006. **44**(4): p. 955-66.
200. Tachibana, S., et al., *Interleukin-6 is required for cell cycle arrest and activation of DNA repair enzymes after partial hepatectomy in mice.* Cell & Bioscience, 2014. **4**(1): p. 6.
201. Taga, T. and T. Kishimoto, *Gp130 and the interleukin-6 family of cytokines.* Annu Rev Immunol, 1997. **15**: p. 797-819.
202. Tamura, F., et al., *FK506 promotes liver regeneration by suppressing natural killer cell activity.* Journal of Gastroenterology and Hepatology, 1998. **13**(7): p. 703-708.
203. Tanaka, T., M. Narazaki, and T. Kishimoto, *IL-6 in inflammation, immunity, and disease.* Cold Spring Harbor perspectives in biology, 2014. **6**(10): p. a016295-a016295.
204. Tanigawa, K., et al., *Augmenter of liver regeneration (ALR) may promote liver regeneration by reducing natural killer (NK) cell activity in human liver diseases.* J Gastroenterol, 2000. **35**(2): p. 112-9.
205. Trebicka, J., et al., *Addressing Profiles of Systemic Inflammation Across the Different Clinical Phenotypes of Acutely Decompensated Cirrhosis.* Front Immunol, 2019. **10**: p. 476.
206. Trefts, E., M. Gannon, and D.H. Wasserman, *The liver.* Current Biology, 2017. **27**(21): p. R1147-R1151.
207. Tschaikowsky, K., et al., *Lipopolysaccharide-Binding Protein for Monitoring of Postoperative Sepsis: Complemental to C-Reactive Protein or Redundant?* PLOS ONE, 2011. **6**(8): p. e23615.
208. Tsuchida, T. and S.L. Friedman, *Mechanisms of hepatic stellate cell activation.* Nature Reviews Gastroenterology & Hepatology, 2017. **14**(7): p. 397-411.
209. Valente, G., et al., *Distribution of interferon-gamma receptor in human tissues.* Eur J Immunol, 1992. **22**(9): p. 2403-12.
210. Valle, M.L., et al., *Inhibition of interleukin-6 trans-signaling prevents inflammation and endothelial barrier disruption in retinal endothelial cells.* Experimental eye research, 2019. **178**: p. 27-36.
211. Villanueva, E., et al., *Netting neutrophils induce endothelial damage, infiltrate tissues, and expose immunostimulatory molecules in systemic lupus erythematosus.* J Immunol, 2011. **187**(1): p. 538-52.
212. Vincent, J.L., et al., *The SOFA (Sepsis-related Organ Failure Assessment) score to describe organ dysfunction/failure. On behalf of the Working Group*

on Sepsis-Related Problems of the European Society of Intensive Care Medicine. Intensive Care Med, 1996. **22**(7): p. 707-10.
213. Vivier, E. and B. Malissen, *Innate and adaptive immunity: specificities and signaling hierarchies revisited.* Nature Immunology, 2005. **6**(1): p. 17-21.
214. Wack, A., E. Terczyńska-Dyla, and R. Hartmann, *Guarding the frontiers: the biology of type III interferons.* Nature Immunology, 2015. **16**(8): p. 802-809.
215. Walker, J.A. and A.N.J. McKenzie, *TH2 cell development and function.* Nature Reviews Immunology, 2018. **18**(2): p. 121-133.
216. Wang, Y.-C., et al., *Predictors of response to pegylated interferon in chronic hepatitis B: a real-world hospital-based analysis.* Scientific Reports, 2016. **6**(1): p. 29605.
217. Wang, Y., et al., *IL-22 Increases Permeability of Intestinal Epithelial Tight Junctions by Enhancing Claudin-2 Expression.* J Immunol, 2017. **199**(9): p. 3316-3325.
218. Weiss, E., et al., *Characterization of Blood Immune Cells in Patients With Decompensated Cirrhosis Including ACLF.* Frontiers in immunology, 2021. **11**: p. 619039-619039.
219. Weiss, R., et al., *Obesity and the metabolic syndrome in children and adolescents.* New England Journal of Medicine, 2004. **350**(23): p. 2362-2374.
220. Werner, M., et al., *All-In-One: Advanced preparation of Human Parenchymal and Non-Parenchymal Liver Cells.* PLOS ONE, 2015. **10**(9): p. e0138655.
221. Whitmire , J.K., J.T. Tan , and J.L. Whitton *Interferon-γ acts directly on CD8+ T cells to increase their abundance during virus infection.* Journal of Experimental Medicine, 2005. **201**(7): p. 1053-1059.
222. Wiegard, C., et al., *Defective T helper response of hepatocyte-stimulated CD4 T cells impairs antiviral CD8 response and viral clearance.* Gastroenterology, 2007. **133**(6): p. 2010-8.
223. Wolk, K., et al., *Cutting edge: immune cells as sources and targets of the IL-10 family members?* J Immunol, 2002. **168**(11): p. 5397-402.
224. Wolk, K., et al., *IL-22 Increases the Innate Immunity of Tissues.* Immunity, 2004. **21**(2): p. 241-254.
225. Wolk, K. and R. Sabat, *Interleukin-22: a novel T- and NK-cell derived cytokine that regulates the biology of tissue cells.* Cytokine Growth Factor Rev, 2006. **17**(5): p. 367-80.
226. Wolk, K., et al., *IL-22 induces lipopolysaccharide-binding protein in hepatocytes: a potential systemic role of IL-22 in Crohn's disease.* J Immunol, 2007. **178**(9): p. 5973-81.
227. Wu, J., et al., *Toll-like receptor-induced innate immune responses in non-parenchymal liver cells are cell type-specific.* Immunology, 2010. **129**(3): p. 363-374.
228. Wunderlich, C.M., et al., *Cutting Edge: Inhibition of IL-6 Trans-Signaling Protects from Malaria-Induced Lethality in Mice.* The Journal of Immunology, 2012. **188**(9): p. 4141.
229. Xiang, X., et al., *Interleukin-22 ameliorates acute-on-chronic liver failure by reprogramming impaired regeneration pathways in mice.* Journal of Hepatology, 2020. **72**(4): p. 736-745.
230. Xiao, W., et al., *TIMP-1-Mediated Chemoresistance via Induction of IL-6 in NSCLC.* Cancers, 2019. **11**(8): p. 1184.
231. Xu, J., et al., *Extracellular histones are major mediators of death in sepsis.* Nat Med, 2009. **15**(11): p. 1318-21.

232. Yamaguchi, K., et al., *Blockade of interleukin-6 signaling enhances hepatic steatosis but improves liver injury in methionine choline-deficient diet-fed mice.* Lab Invest, 2010. **90**(8): p. 1169-78.
233. Yang, H.-R., et al., *A critical role of TRAIL expressed on cotransplanted hepatic stellate cells in prevention of islet allograft rejection.* Microsurgery, 2010. **30**(4): p. 332-337.
234. Yang, R., et al., *IL-6 promotes the differentiation of a subset of naive CD8+ T cells into IL-21-producing B helper CD8+ T cells.* The Journal of experimental medicine, 2016. **213**(11): p. 2281-2291.
235. You, Q., et al., *Mechanism of T cell tolerance induction by murine hepatic Kupffer cells.* Hepatology, 2008. **48**(3): p. 978-90.
236. Young, R.S., B.M. Wiles, and D.W. McGee, *IL-22 Enhances TNF-α- and IL-1-Induced CXCL8 Responses by Intestinal Epithelial Cell Lines.* Inflammation, 2017. **40**(5): p. 1726-1734.
237. Zhang, Y., et al., *A proinflammatory role for interleukin-22 in the immune response to hepatitis B virus.* Gastroenterology, 2011. **141**(5): p. 1897-906.
238. Zhou, Q., et al., *Interferon-α2b Treatment for COVID-19.* Frontiers in Immunology, 2020. **11**(1061).

8 Appendix

8.1 List of Abbreviations

RT	Room temperature
Min	Minutes
h	hours
HCC	Hepatocellular carcinoma
ACLF	Acute-on-chronic liver failure
LC	Liver cirrhosis
HIV	Human immunodeficiency virus
EASL	European association for the study of the liver
P/S	Penicillin / Streptomycin
IL	Interleukin
IFN	Interferon
WST	4-[3-(4-Iodophenyl)-2-(4-nitro-phenyl)-2H-5-tetrazolio]-1,3-benzene sulfonate
PBMC	Peripheral blood mononuclear cell
FCS	Fetal calf serum
A	Ampere
V	Volt
APS	Ammonium persulfate
TEMED	Tetramethylethylenediamine
SDS	Sodium dodecyl sulfat
HRP	Horseradish peroxidase
PFA	Paraformaldehyde
PHH	Primary human hepatocyte
Nm	Nanometer
Mm	Millimeter
µm	Micrometer
g	Gram
l	Liter
PCR	Polymerase chain reaction

rpm	Rounds per minute
IL	Interleukin
IFN	Interferon
CTL	Cytotoxic T cells
CD	Cluster of differentiation
APC	Antigen presenting cell
DC	Dendritic cell
NK cell	Natural killer cell
MHC	Major histocompatibility complex
TCR	T cell receptor
MMP	Matrix Metalloproteinase
Jak	Janus Kinase
Stat	Signal Transducer and Activator of Transcription
RIG-I	Retinoic acid inducible gene I
MDA5	Melanoma differentiation-associated protein 5
ISG15	interferon-stimulated gene 15
SARS-CoV-2	Severe acute respiratory syndrome *coronavirus* type *2*
BSF-2	B cell stimulatory factor 2
HSF	Hepatocyte-stimulating factor
HGF	Hybridoma growth factor
SOCS	Suppressor of cytokine signalling
TIF	T cell-derived inducible factor

8.2 List of Figures

8.3 List of Tables

8.4 Acknowledgements

I like to thank Prof. Dr. Christian Lange for giving me the opportunity to work on this thesis and to intensively study the aspects of liver immunology. I am grateful for all the support during my time at the University Hospital in Essen.

Furthermore, I thank Prof. Dr. Hansen for taking over the task as my second supervisor.

I would like to acknowledge all fruitful discussions, the support and offered expertise given by my direct colleagues Mona Langer and Dr. Sabrina Guckenbiehl. It is always more fun to be not alone at conferences. Also thank you Julia Pietrek, Leonie Weber and Stefan Schefczyk for all opinions, cooperations and of course the shared lunch times.

I thank PD Dr. Ruth Bröring for her support and valued advice during the last years and now towards my defence.

I want to thank all lab members from the Gastroenterology and Hepatology lab at the University Hospital in Essen for all the help, discussions and fun we had together but also the tough times that we survived and that made us stronger.

I want to express my gratitude to Timothy, my family and my friends for their constant support during the last three years. You gave me never ending support during my ups and downs, mental breakdowns and you had understanding for the limited time I could spend with all of you.

8.5 Curriculum vitae

Der Lebenslauf ist in der Online-Version aus Gründen des Datenschutzes nicht enthalten.

8.6 Erklärungen

Hiermit erkläre ich, gem. § 7 Abs. (2) d) + f) der Promotionsordnung der Fakultät für Biologie zur Erlangung des Dr. rer. nat., dass ich die vorliegende Dissertation selbständig verfasst und mich keiner anderen als der angegebenen Hilfsmittel bedient, bei der Abfassung der Dissertation nur die angegeben Hilfsmittel benutzt und alle wörtlich oder inhaltlich übernommenen Stellen als solche gekennzeichnet habe.

Essen, den _____ _____

Stefanie Sichelschmidt

Hiermit erkläre ich, gem. § 7 Abs. (2) e) + g) der Promotionsordnung der Fakultät für Biologie zur Erlangung des Dr. rer. nat., dass ich keine anderen Promotionen bzw. Promotionsversuche in der Vergangenheit durchgeführt habe und dass diese Arbeit von keiner anderen Fakultät/Fachbereich abgelehnt worden ist.

Essen, den _____ _____

Stefanie Sichelschmidt

Hiermit erkläre ich, gem. § 6 Abs. (2) g) der Promotionsordnung der Fakultät für Biologie zur Erlangung der Dr. rer. nat., dass ich das Arbeitsgebiet, dem das Thema „**Impact of combined cytokine stimulation on liver cells and immune cells of liver cirrhosis and acute-on-chronic liver failure (ACLF) patients“** zuzuordnen ist, in Forschung und Lehre vertrete und den Antrag von **Stefanie Sichelschmidt** befürworte und die Betreuung auch im Falle eines Weggangs, wenn nicht wichtige Gründe dem entgegenstehen, weiterführen werde.

Essen, den _____ _____

Prof. Dr. med. Christian M. Lange

DuEPublico

Duisburg-Essen Publications online

UNIVERSITÄT DUISBURG ESSEN

Offen im Denken

ub | universitäts bibliothek

Diese Dissertation wird via DuEPublico, dem Dokumenten- und Publikationsserver der Universität Duisburg-Essen, zur Verfügung gestellt und liegt auch als Print-Version vor.

DOI: 10.17185/duepublico/74999
URN: urn:nbn:de:hbz:465-20231024-143420-2

Alle Rechte vorbehalten.